Spatial theories and experiments on the evolution of cooperation

Théories et expériences spatiales sur l'evolution de la coopération

Edward Wong Tekwa

Department of Biology, McGill University, Montreal, Canada

December 2015

A thesis submitted to McGill University in partial fulfillment of the requirements of the degree of Doctor of Philosophy

Table of contents

Abstract

From simple bacteria to complex organisms, cooperation binds together cells to form greater aggregates, which represent some of the most important and fascinating biological phenomena, such as biofilms and colonies. At the heart of these phenomena is the rise of spatial clustering, which has been implicated to promote and maintain cooperation. I first synthesize how different theories model space through the spatial ecological metrics of local densities and clustering coefficients. Based on these metrics, I introduce a simple spatial public-good model, where cooperation benefits the greater population and leads to complex pattern formation. Mathematical analyses and individual-based simulations produce the seemingly paradoxical result: cooperator clustering decreases cooperator frequency and overall population density. This arises from the models' premise that cooperation only dampens competition, such that cooperators are still competing with one another. The model and predictions are used to analyze the evolution of siderophore production in *Pseudomonas aeruginosa*. In a simple microhabitat device, cooperators and defectors are tracked, and their spatial patterns suggest that at a very small scale, clustering explains much of the variation in eco-evolutionary outcomes. Moreover, the experiment confirms that cooperator clustering decreases cooperator frequency and population density. Both theoretical and empirical results show that strong selection – due to the large phenotypic difference between cooperators and defectors – and demographic dynamics lead to complex clustering patterns and effects. The research contributes novel spatial metrics, theories, and experimental tools to study the evolution of cooperation and its impact on the greater population.

Présente tant chez les simples bactéries que chez des organismes complexes, la coopération lie les cellules pour former de plus grands agrégats. Ceux-ci, observables exemple chez un biofilm ou une colonie, font partie des phénomènes biologiques les plus importants et les plus fascinants. Au cœur de ces phénomènes est l'augmentation du regroupement spatial, qui est impliqué pour la promotion et le maintien de la coopération. J'ai d'abord synthétisé comment différentes théories modélisent l'espace à travers les mesures écologiques spatiales de densités locales et les coefficients de *clustering*. Basé sur ces mesures, je présente un modèle spacial simple de bien commun, où la coopération profite à la population au sens large et conduit à la formation de motifs complexes. Les analyses mathématiques et les simulations basées sur l'individu produisent un résultat apparemment paradoxal: le regroupement coopérateur diminue la fréquence des coopérateurs et la densité de la population globale. Ceci découle de la prémisse du modèle selon laquelle la coopération diminue la compétition, c'est-à-dire que les coopérateurs soient toujours en compétition les uns avec les autres. Le modèle et les prévisions sont utilisés pour analyser l'évolution de la production de sidérophores chez *Pseudomonas aeruginosa*. Dans un dispositif de microhabitat simple, les coopérateurs et les défecteurs sont monitorés et leurs configurations spatiales suggèrent que sur une très petite échelle, le *clustering* explique une grande partie de la variation éco-évolutive des résultats. En outre, l'expérience confirme que le regroupement des coopérateurs diminue la fréquence des coopérateurs et la densité de la population. Les deux résultats théoriques et empiriques montrent que la forte sélection - en raison de la grande différence phénotypique entre les coopérateurs et les défecteurs - et la dynamique démographique conduit à des motifs et effets de *clustering* complexes. Cette

recherche fournit de nouvelles métriques spatiales, théories et outils expérimentaux pour étudier l'évolution de la coopération et de son impact sur une population.

Acknowledgements

I would like to thank my PhD supervisors Andrew Gonzalez and Michel Loreau. Coming from a non-traditional academic background myself, we kept things non-traditional as ecologists studying the evolution of cooperation. Andy has been an inspirational role model and a dedicated mentor who believed in me seemingly unconditionally. Michel and I have had many deep discussions ranging from the fundamentals of biology to the evolution of the universe, and he was pivotal in shaping my scientific endeavor. From the beginning, both Andy and Michel have encouraged me to pursue new ideas, but were always there to guide me back on track when ideas turned too fantastic. I feel incredibly fortunate to be able to count on them for support – they created a unique environment where I can dare to dream, and I cannot imagine having conducted my PhD research anywhere else. Members of both labs created a stimulating intellectual and social environment, for which I am grateful.

Dao Nguyen is part of my advisory committee, and has unofficially adopted me to be part of her lab. All experiments were performed at her lab. Her expertise in *Pseudomonas aeruginosa* and broad interests in evolution and ecology proved crucial in my thesis completion. At the Nguyen lab, Geoff McKay helped enormously with preparing bacteria strains and providing experimental advice. Simone Périnet helped with the translation of the thesis' French abstract. Rex Xia and Jody Wong were undergraduate students at the lab who conducted preliminary experiments relevant to my research. Members of the Nguyen lab over the years were extremely accommodating and provided valuable feedback on my experiments.

My committee members, Fred Guichard and Claire de Mazancourt have been excellent mentors. Fred and his student Eric Pedersen introduced me to the spatial ecology literature, which heavily influenced my thesis. Claire provided insightful comments and pointed out some mathematical errors as I developed my theories. Troy Day gave valuable comments leading to a fuller treatment of the mathematical derivations and analyses throughout the thesis.

David Juncker generously provided lab space and advised on the design and operation of the microfluidic experimental device. Matthieu Nannini produced the silicon mold for the device. I thank the National Institute for Mathematical and Biological Synthesis (NIMBioS) in Knoxville, TN for supporting me in a summer graduate course in statistics in 2013. Leticia Aviles and Michael Doebeli provided lab space during my visit at the University of British Columbia in 2012, and I thank them for insightful discussions. I am in debt to Ross Black and Robin O'Quinn at Eastern Washington University for being encouraging mentors during my initial foray into biology.

I want to thank Andrea Portt for being an inspiring role model, for helping me with writing and microbiology, and for pointing out possible social and medical links in my research. I am lucky to be in an incredible graduate student cohort at McGill, filled with friends who are exceedingly intelligent, charitable, positive, and fun. They are important parts of my formative scientific years, and I will continue to count on them as friends and colleagues.

My PhD research was supported by the Fonds Québécois de la Recherche sur la Nature et les Technologies and the Québec Centre for Biodiversity Science.

Preface & contribution of authors

It started out of a personal curiosity about why humans cooperate. This curiosity first took root when I became fascinated with Hamilton's formulation of inclusive fitness (*1*), or how one can partially count the benefit bestowed on others as a part of one's own fitness. With little training in biology, I became engrossed in reformulating how cooperation can evolve, for my own understanding. I quit my job as an engineer and began my formal academic career at McGill. Through unexpected paths, Andy, Michel and I forged a novel research program involving theories and experiments.

I do not pretend to be more familiar with cooperation in my study organisms (bacteria, algebra, simulated beings) than in humans. Humans are after all my first interest. It is easy to erroneously anthropomorphize cooperation in non-human organisms, and so it is lucky that my model organisms are so far removed from us. However, the advantage of thinking about humans and bacteria at once is that I strive for models that can describe both, with generality and simplicity as my guiding principles.

It is difficult for a scientist to speak of personal motivations, perhaps out of fear that it may cloud objectivity. But I will allow myself a small relapse here to express my hidden, unscientific motivations for studying the evolution of cooperation. I believe that cooperation is the key to major evolutionary transitions (*2*) – but not only biotic transitions. The universe created a cloud of matter and energy, and from the beginning new entities continually form and dissipate into other entities. The influence of natural selection on the abundances of entities depends on the fact that they are once created, but do not depend on a continual biotic replication process. If all things were

immutably created once by a sleepy god, natural selection would still act to select for those things which die more slowly than others, without any need for growth.

But more interestingly, entities seem capable of replication, and not necessarily by descent – the number of galaxies and planets grow because of the physics of condensation everywhere in the universe up to now. In the shorter time frame, biotic replications are capable of extraordinarily explosive growths. But these individual level growths presuppose that such entities were once created. Generally, the most common ingredient leading to the creation of entities is the condensation of matter and energy in space. To form stable entities capable of replication and reproduction (which includes the quietly creative factor of mutation), basic units such as amino acids and cells come together. And to be evolutionarily successful as new entities, the basic units must cooperate to some degree. Atoms in molecules, globular clusters in galaxies, and cells in aggregates and multicellular organisms must cooperate within their boundaries in order to form the entities that we now observe with our naked eyes.

My studies on how to model space in the evolution of cooperation, how to apply such a theory to bacteria public-good cooperation, and how such experiments inform and improve the theory, form a small contribution to explaining a creative ingredient in the evolution of the universe. In short, I want to understand creation. More personally, I am interested in how the creative force of cooperation may explain where I come from. Hamilton wrote, "I am fundamentally mixed, male with female, parent with offspring, warring segments of chromosomes that interlocked in strife"(*3*). Replacing "male with female" with "mammalian and bacterial" works too. For me, it is existentially imperative to learn how simple bacteria and humans may share similar cooperative strategies and be subject to similar evolutionary forces, for such is a theory that can

transcend the tree of life. It is part of the modern spiritual epic that connects us to distant organisms, which not only resemble our distant ancestors, but also make up a big part of our own bodies today.

The thesis consists of four journal-styled manuscripts, of which I am the first author. Michel Loreau, Andrew Gonzalez and I conceived all studies in the thesis. I wrote the first draft, and Michel and Andy contributed to revisions. Dao Nguyen contributed to the experimental design, provided facilities, and contributed significantly to the revisions of Chapter 3 and 4. David Juncker contributed to the experimental design, provided facilities, and contributed significantly to the revision of Chapter 3.

All experimental and theoretical works in this thesis are of original scholarship, and are distinct contributions to knowledge.

Introduction

The evolution of cooperation evokes primal imageries: boundary, nepotism, discrimination, theft, war and peace. Across the tree of life, from simple bacteria to ants and humans, cooperation binds together cells to form greater aggregates, which represent some of the most important and fascinating biological phenomena (*4*, *5*) such as biofilms and colonies. Cooperation is an evolutionary dilemma, which has been retold as the Prisoner's Dilemma (*6*), the tragedy of the common (*7*), and the public goods dilemma (*8*, *9*). In all these tales, even though cooperation would benefit all, defection is the null expectation. These tales also imbue the sense that cooperation between individuals involves changes at a higher level – for the good of all prisoners, the common, or the public. Thus, the evolution of cooperation has far reaching consequences in terms of individual characters, spatial patterns, and population demography.

Both by its nature and by the way it was discovered, cooperation continues to inspire passion and controversies. From the beginning, while Darwin emphasized the role of competition in evolution by natural selection in 1859 (*10*), Kropotkin suggested that cooperation plays an equal part (1902) (*11*, *12*). When Hamilton formulated inclusive fitness in 1964 (*13*), it was in objection to the indiscriminate ways in which biologists of his day evoked group selection (*14*), or selection for the good of populations, species, or other entities higher than the individual. Evolutionary game theory joined the foray and brought in the idea of rational decisions in the 70's (*6*, *15*). Recently, multilevel selection (*16*, *17*) has been embraced by many biologists, at least conceptually, to explain how natural selection can simultaneously act on genes,

organisms, groups and higher organizations, albeit with decreasing likelihood as the unit becomes bigger. At the same time, disagreements abound as to how to model the evolution of cooperation (*18*, *19*). The topic is particularly controversial now, partly because different schools have risen to prominence with seemingly convergent discoveries. At worst, their conceptual differences can hamper empirical studies and inhibit meaningful progress. But the flux in ideas and convergent discoveries may also be signs that real progress can be made in multiple lines of inquiries, if such a proliferation can periodically be synthesized.

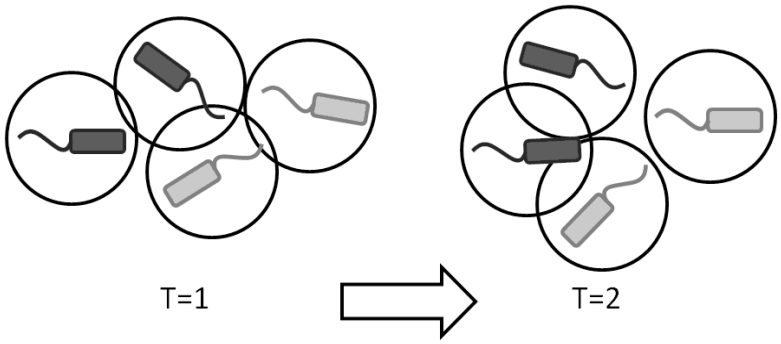

Figure 1. Spatial association or clustering can occur within morph and between morphs (represented by the two shades, which can be cooperators and defectors), with interaction potentials determined by distance. For example, individuals may only interact if they are within each others' interaction scales, as represented by circles around them. Clustering can change from time T=1 to T=2.

Amidst the diverse theoretical investigations, there is a consensus that space plays an important role in promoting cooperation. Early spatial game simulations showed that cooperators involved in the Prisoner's Dilemma persist, in contrast to non-spatial results (*20*). Subsequent works identified that the spatial association or clustering between cooperators (Figure 1) generally promote cooperation within the population (*13*, *21–26*). This can be achieved through various mechanisms, including limited movement (*27*), chemotaxis or directed movement (*28*), and spatial constraints in patchy habitats (*29*), among others. The latest developments of spatial theories of

cooperation can be found in the classical synthesis of genetic structure and selection in subdivided populations (*22*), in the statistical mechanical approximation of evolution in probabilistic cellular automata simulations (*30*), and in evolutionary games in structured populations (*26*).

Curiously, space is modeled using similar ingredients across different schools of thought. To give a taste without going into details, the well-known metrics of structure coefficient (*24*), spatial variance (*21*), contextual covariance (*31*), relatedness (*13*), and inbreeding coefficient or *F* statistics (*32*) can all be derived from basic spatial ingredients called pair densities (*33*) or probabilities of identity (*34*), as I will show. These ingredients can be condensed into the more demographically flexible metrics of local densities – spatial correlation metrics, or spatial moments, that were developed to describe plant interactions (*35*). The primary objective of my thesis is to bring to light the foundational roles that local densities can play in furthering the science of cooperation, but which have thus far remained relatively obscure mathematics.

In order to accomplish the primary objective, both theoretical and empirical problems are addressed. Local densities need to be connected to established metrics in the evolution of cooperation theories, in order to demonstrate generality (Chapter 1). In addition, the value of local densities would only become apparent if they can lead to new biological insights.

An outstanding problem in cooperation is that we lack a basic, demographically explicit model of spatial public goods that is fully defined from first principles of individual behaviours. Public goods are a major class of cooperation that benefits the population at large (*9*), but most evolutionary models impose an upper population limit (*36–38*). To explore public good more realistically, local densities are essential

modeling ingredients, because they allow for the emergence of complex clustering patterns and the analysis of direct eco-evolutionary effects due to specific aspects of clustering (Chapter 2).

A new type of microbial experiments has made it possible to rigorously test spatial theories on the evolution of cooperation. These are microfluidic devices (*39*, *40*), where small habitat features can be imposed on engineered cooperator and defector microbial strains in evolutionary competition. The bacteria *Pseudomonas aeruginosa* have emerged as a major experimental organism both in medical research (*29*) and fundamental research on cooperation (*41*). *P. aeruginosa* inhabit diverse habitats in nature, but can also colonize the respiratory tract and bloodstream in cystic fibrosis patients. In the wild, most of these bacteria secrete a diffusive public good called siderophores, which are iron-chelating agents essential for growth (*42*). The demographic consequences of evolution in this public good can impact the patchy (i.e. high edge-to-area ratio (*43*)) respiratory tract of the human host, which *P. aeruginosa* colonizes (*44*, *45*). While siderophore cooperation has been explored in traditional test tube experiments (*46*, *47*), it has not been studied in a setting where spatial pattern emerges. By designing a novel and simple microhabitat device (MHD) with a systematic treatment in patchiness, we can explore how patchiness, an important and passive driver of spatial ecological patterns (*43*, *48*), influences the evolution and co-existence of cooperators in competition with defectors (Chapter 3).

Some theoretical and empirical challenges remain in applying local densities, not only in the context of cooperation, but also in general spatial ecology. The relevance of local densities relies on using the appropriate interaction scale, but scale remains an open theoretical problem (*35*), and has not been inferred from the spatiotemporal data

of real organisms in studies of cooperation. This is an organism-specific problem that can only be addressed empirically, and until now, we lacked the appropriate data. The novel MHD (Chapter 3), coupled with confocal miscroscopy, can generate spatiotemporal data at individual-level resolution. This allows us to test whether we can infer the scale at which cooperation and competition occurs in *P. aeruginosa* (Chapter 4), and whether the spatial patterns, quantified by local densities, lead to the eco-evolutionary effects predicted by the spatial public-goods model (Chapter 2).

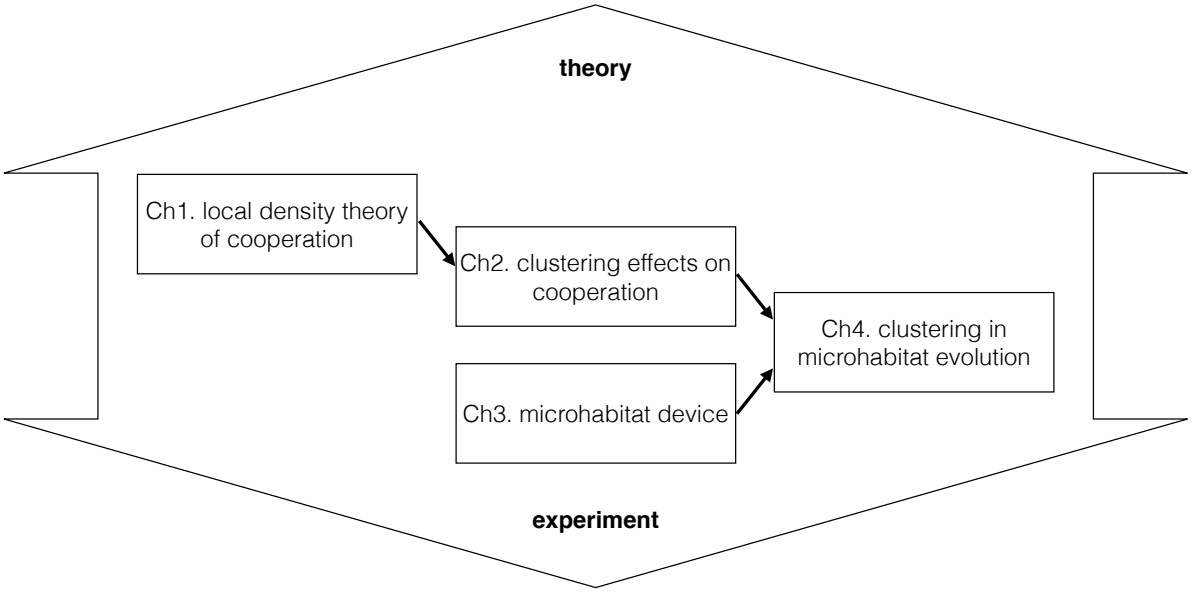

Figure 2. Logical connections of thesis chapters and where the chapters stand in the theory-experiment spectrum.

The titles of the four chapters are:

Chapter 1. Local densities connect spatial ecology to game, multilevel selection and inclusive fitness theories of cooperation

Chapter 2. The influence of spatial clustering on the evolution of cooperation

Chapter 3. Patchiness in a microhabitat chip affects evolutionary dynamics of bacterial cooperation

Chapter 4. Small-scale clustering mediates the evolution of cooperation in a pathogenic bacterium

The logic of the thesis is illustrated in Figure 2. In Chapter 1, I develop local densities as central metrics for modeling spatial effects in the evolution of cooperation theories. Using these concepts, Chapter 2 explores how a demographically explicit model of cooperation leads to novel clustering patterns and eco-evolutionary effects. In particular, through mathematical analyses and individual-based simulations, I find that cooperator clustering counterintuitively decreases cooperator frequency and population density. In Chapter 3, I set up a novel experimental device that is capable of testing habitat patchiness effects, at 100-μm scales, on the evolution and maintenance of cooperation. I find that patchiness does not change the fact that defectors dominate, but contributes to coexistence. The experiment also generates high-resolution spatiotemporal data of fluorescent cooperators and defectors, which I further analyse in Chapter 4. The major results are that clustering metrics, derived from local densities, explain almost 80% of eco-evolutionary outcomes in the experiments, and that the most important spatial heterogeneities are captured at <5 μm, and not at the patchiness treatment scale (a bacterium is ~2 μm). Moreover, the data confirm that cooperator clustering decreases both cooperator frequency and population density. As to how these apparently surprising results can be reconciled with the existing literature, where clustering is generally believed to promote the evolution of cooperation (*13*, *20–22*, *24*, *26*, *30*), I hope that Chapter 2 and 4 will provide the answers. Briefly, the new results arise from strong selection, coupled demographic dynamics, and the interplay between cooperation and competition.

This thesis was envisioned as an organic whole that traverses from theory to experiment and back to theory, and not simply as a composition of individually self-sufficient chapters. In the following sections, I introduce each chapter with a prelude, in which I provide context to how and why the work was conceived, and where it sits in relation to the other chapters.

Chapter 1. Local densities connect spatial ecology to game, multilevel selection and inclusive fitness theories of cooperation

Edward W. Tekwa, Andrew Gonzalez, Michel Loreau

Journal of Theoretical Biology 380 (2015) 414-425

1.1. Prelude

The first version of this manuscript was conceived during my first year at McGill, but its seed was planted even earlier. Two years before I began my PhD, I casually stumbled upon the concept of inclusive fitness in a psychology book (*49*) which talked about how humans and animals made decisions. It set the tone of my early thoughts about cooperation – individuals behave in a calculated way to maximize their chances of achieving some goal. In nature, that goal is some form of fitness. It is a fascinating idea, that individuals have some objective goal, and that helping others may be a means and not the goal itself. Roughly, inclusive fitness theory states that the goal of any behaviour is to maximize the fitness of the genes controlling a particular behaviour (*13*). This imbues a sense of purpose to cooperation, which is a highly influential and philosophically important perspective (*50*). More technically, the inclusive fitness perspective emphasizes the possibility that cooperators may cooperate discriminately, perhaps according to kinship, so as to increase the success of cooperation.

However, the goal-seeking perspective is not the only way to think about cooperation. During my first year at McGill, I was introduced to the spatial moment literature (*35*). Back then, I tried to channel every new thing I learned into explaining the evolution of cooperation, and so I began comparing the central metric in inclusive

fitness theory – relatedness – with spatial moments, or the spatial distribution of individuals, summarized as local densities. The spatial perspective posits that individuals have to be physically close by in order to interact. With the exception of human telecommunication, thinking of cooperation as a locally restricted process seems astute and self-evident. It also does not suppose that any fitness quantity is being maximized – a controversial idea (*51*, *52*). Instead of imposing an overarching narrative, modeling cooperative interactions in space relies on simple assumptions about individual behaviours – what can be considered as first principles (*53*). It is a boring method because it does not identify a single measure of evolutionary success; here we are only concerned with the quantification of spatial and non-spatial mechanisms of selection. In a field as controversial as the evolution of cooperation (*18*, *19*), it may pay to be boring.

The spatial perspective helps delineate spatial versus non-spatial cooperation. Evolutionary game theory, in the form of reciprocity (*6*, *15*), traditionally concentrates on non-spatial cooperation – individuals have no choice as to whom they encounter, but they can choose what to do with their partners. This is rather similar to inclusive fitness theory, where kinship is one way for individuals to decide what to do. But of course individuals can choose to move close to kin, so there can be a spatial component. In contrast, multilevel selection theories (*54*), in particular group models (*21*), are mostly spatial. But then, groups or levels may form out of individuals' intent to move together. Moreover, there has been a recent bloom in spatial game theories (*24*, *26*). So while it seems that there is more than one way to model cooperation, there is a general convergence in the sense that all perspectives are now expanding to model multiple

mechanisms. It turns out that one can construct the spatial component of all these theories using local densities.

So why present another perspective, when there are already quite a few that seems potentially all-encompassing? Firstly, spatial effects are critical for cooperation in all organisms, including microbes and humans. Space is not the only important factor for the evolution of cooperation, but that is all the more reason to delineate spatial from non-spatial effects. Secondly, different theories are already gravitating towards the technical method of using local densities or their analogues; we simply have to highlight and elevate the conceptual roles these technical metrics can play. Thirdly, explaining cooperation from a spatial ecological point of view is a basic modeling approach anchored in first principles of how individuals interact (*55*); any overarching perspective or analysis can be imposed on the model after with potential conceptual gain. But I must emphasize that the perspective I take is only one alternative with its own advantages and disadvantages. I will defer these points to the main text.

This first chapter can be described as the culmination of my obsession with methodology, which early on my committee accused me of having instead of taking an interest in biology. An obsession with becoming genuinely interested in biology occupied me since then, and seeing that this chapter took its final form after years of fiddling, I hope biology infiltrated here also. But the main objective here is personal – to understand the theories on the evolution of cooperation for myself. And anyway, I believe that before one can study biology, one must have a method of getting to biologically interesting questions. I hope to have come up with some useful and novel insights on how different theories are connected by spatial metrics, which also help distinguish the classes of mechanisms that influence the evolution of cooperation.

The identification of local densities as central metrics, and the mathematical connections established with more traditional metrics in this chapter pave the way to finding novel spatial effects in Chapter 2, and to confirming these effects experimentally in Chapter 4.

1.2. Abstract

Cooperation plays a crucial role in many aspects of biology. We use the spatial ecological metrics of local densities to measure and model cooperative interactions. While local densities can be found as technical details in current theories, we aim to establish them as central to an approach that describes spatial effects in the evolution of cooperation. A resulting local interaction model neatly partitions various spatial and non-spatial selection mechanisms. Furthermore, local densities are shown to be fundamental for important metrics of game theory, multilevel selection theory and inclusive fitness theory. The corresponding metrics include structure coefficients, spatial variance, contextual covariance, relatedness, and inbreeding coefficient or *F*-statistics. Local densities serve as the basis of an emergent spatial theory that draws from and brings unity to multiple theories of cooperation.

Keywords: evolution of cooperation, local density, relatedness, contextual analysis, Price's equation

1.3. Introduction

Cooperation is thought to play a crucial role in biological phenomena, including the rise of bacterial biofilms, eukaryotic cells, multicellular organisms, and societies (*2*, *54*). In the theories on the evolution of cooperation, as in many other complex subjects, there does not exist a universal theory that best explains all observed behaviours. Some non-spatial explanations include reciprocity (*6*) and discrimination (*56*). Several theories invoke a role for space. Although space is certainly not the only important factor in the evolution of cooperation (*25*, *32*, *57*, *58*), it is one of the most important (*26*, *30*, *59*, *60*).

Space is represented in different ways and described by a variety of metrics. These include structure coefficient (*24*), spatial variance (*21*), contextual covariance (*31*), relatedness (*13*), and inbreeding coefficient or *F* statistics (*32*), among others. But these metrics are not all purely spatial. It is thus important to identify a common language with which to measure and discuss spatial effects on cooperation, in order to discern when space really plays a role.

A recurrent discovery is that the evolutionary dynamics of cooperation in space can be modelled using pair densities (*26*), or alternatively using the probabilities of identity between individuals (*34*). These are then used to derive one of the five metrics we cite above. The discussions surrounding these terminologies remain encumbered by the highly technical mathematics and assumptions needed to mechanistically derive them, which include spatial moment approximation (*35*), pair approximation (*33*), and quasi-equilibrium approximation (*26*). If we are willing to take pair densities or probabilities of identity as quantities that can be measured and not necessarily

mechanistically derived, then we may be able to open up the discussion of space and cooperation to empirical application. For this purpose, we will turn to the related and empirically applied metrics – local densities – which originate in neighbourhood models of plant interaction in spatial ecology (*61*, *62*).

The purpose of this article is to present a coherent and comprehensive theoretical support for using a set of local densities as the central metrics in deciphering the spatial components of eco-evolutionary cooperation dynamics. First, we define local densities (Section 2.1) in precise terms, such that they can be empirically applied and incorporated into a dynamic model (Section 2.2). We then show that such a local interaction model can neatly distinguish the spatial and non-spatial selection mechanisms for cooperation (Section 2.3). By mathematically relating local densities to the current major paradigms, we can analyze when kin selection (*13*), group or multi-level selection (*21*), and reciprocity (*6*) refer to spatial, non-spatial, or partly spatial phenomena (Section 3).

There is an excellent theoretical synthesis on the various ways in which current major paradigms model space, and it is the immediate predecessor of our paper (*30*). Nevertheless, the previous synthesis used a more restrictive definition of local densities, which are used as pair densities in graphs with a predefined number of nodes. Our main task is thus to identify and establish a spatial metric that can be generally applied in both evolutionary and ecological contexts, in continuous or discrete space and graphs. Some additional novelties in our synthesis include: relating ecologically and game-theoretically motivated spatial models to the traditional concept of selection through Price's equation (*63*); incorporating recent spatial evolutionary game developments (*24*); and relating spatial metrics to multilevel selection analyses (*54*). Along the way,

more familiar derivations are included to facilitate the transitions from one novel idea to the next, and to be inclusive, such that theoretical experts, empirical researchers, and any interested biologist can appreciate the generality and limitations of our model.

Our work does not adhere to a particular method of computing evolutionary fitness (see Tarnita and Taylor, 2014), or elucidate how spatial patterns arise (see Hamilton, 1964; Levin and Pacala, 1997; Matsuda et al., 1992). The local interaction model is not a complete synthesis; rather, it introduces a more general concept of local densities and strengthens the foundations of an ongoing spatial synthesis to include both traditional selection concepts and new dynamic theories.

1.4. Local interaction model

We begin with the concept of local density, which measures and models spatial interactions between individuals. Then we construct the general dynamic equations for the evolution of cooperation by adding terms for intrinsic growth rates and payoff functions. We conclude the section with an analysis of spatial and non-spatial selection mechanisms.

1.4.1. Local densities

We first introduce local densities as metrics that describes encounters, or interaction potentials in space, then we incorporate changes in local densities. These metrics were developed in the neighbourhood models of plant interactions (*35*, *61*, *65*), and are directly related to the pair densities (*33*) often used in cooperation theories (*26*). We will carefully generalize these metrics for interacting individuals beyond plants. See Table 1.1 for symbol definitions.

Let us define a morph as a discrete trait or character that is heritable through survival or reproduction. We will call carriers of these discrete characters individuals. This definition of an individual is most applicable to haploid organisms, but can also be applied to individual genes, and to higher organisms if we adopt the phenotypic gambit (where the character inheritance of non-haploid organisms is assumed to approximate haploid inheritance – see Grafen (1984)). For each focal individual u across the entire population, we can measure the local density x_{uj} of morph j. Such local density is the number of morph j individuals weighted as a function of their distance from the focal

individual. The local density of morph j around each individual u at location y_u in space is then:

$$x_{uj} = \sum_{v}^{\text{all } j \text{ indiv}} \phi_{uj}\left(y_v - y_u\right) \tag{1.1}$$

The key to local density is the interaction kernel, i.e. the weighting function ϕ_{uj}. The interaction kernel is a probability density function, specifying the probability that a focal individual u interacts with a morph j partner v a distance $y_v - y_u$ apart. As a probability density function, ϕ_{uj} is positive and integrates to one over all possible distances. The shape of the interaction kernel implicitly models the intermediary spatial processes that affect fitness (fitness is defined later in Eq. 1.3). Such processes may include the transmission of public goods (e.g. metabolites), information (e.g. warning calls), toxins, or at the simplest, physical boundaries or territories of individuals in contact-based interactions. Two symmetric interaction kernels, applicable in both continuous and discrete space, are illustrated in Fig. 1.1. We simplify the modeling problem by assuming that all individuals u of morph i experience their biotic environment through the same interaction kernel, ϕ_{ij}.

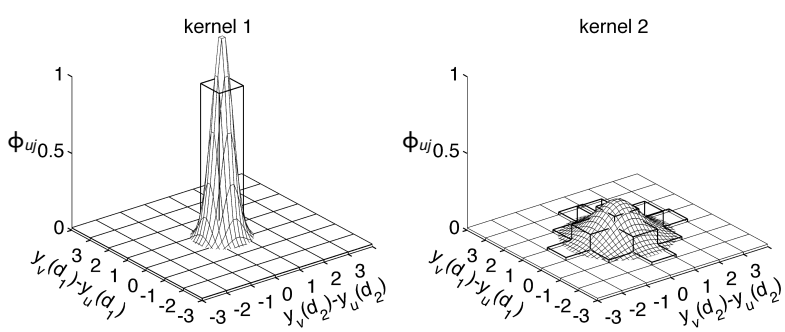

Figure 1.1. A localized interaction kernel 1 versus a diffuse local interaction kernel 2. The smooth Gaussian mesh plots represent continuous-space kernels, while the bar plots represent discretized space approximation kernels, where spatial locations are defined at a lower resolution. y_u is the position of the focal individual (in dimensions d_1 and d_2), y_v is any position that may be occupied by other individuals, and ϕ_{uj} is the kernel weighting for the Euclidean distance y_v - y_u from the focal individual.

Table 1.1. Symbol definitions.

Symbol	Definition	Symbol	Definition
a_{ij}	payoff to i when interacting with j	q	potential neighbour location
A_m	size of patch m	Q_b	probability of identity between group
$b_{u\to v}$	benefit u gives to v	Q_w	probability of identity within group
$b_{i\to}$	benefit that i gives to any partner	r_i	intrinsic growth (or death) rate of i
β	basic intrinsic growth rate	R_j	relatedness of morph j neighbours to morph 1
β_x	selection coefficient for x level character	R_{ij}	relatedness of morph j to morph i
c_{uv}	plastic cost to u due to presence of v	S	number of morphs
c_i	non-plastic cost to i	t	time
C	within-morph clustering coefficient	u, v	indices for individual
C_{ij}	clustering coefficient of j around i	w_u	fitness of individual u (birth-death)
$cov_{ij}(q)$	spatial covariance between i and j at distance q	x_{uj}	local density of morph j around u
$Cov_{ij}(q)$	spatial covariance between i and j at distance q	x_{ij}	local density of morph j around morph i
f_i	payoff function for morph i	X	global population density (of all morphs)
F_{ST}	inbreeding coefficient	X_i	global density of i (1st moment)
g	between-patch dispersal probability	X_{ij}	average local density of j around i neighbourhood
h	cell area	$X_{i\bullet}$	total average local densities of all morphs around i
ϕ_{uj}	interaction kernel of morph j around u	y	focal location
ϕ_{ij}	interaction kernel of morph j around morph i	y_u	location of individual u
i, j, k, l	indices for morph type	Y	maximum local population density
n	number of patches	z	average character of population
N_i	morph i population size	z_u	character of individual u
N_d	deme population size	Z_u	character of individual u's group
N	total population size	σ	structure coefficient
p	frequency of morph 1	σ^2	spatial variance
p_i	frequency of morph i	Ω	habitat space
ρ	probability of interacting again		

The expected value of x_{uj} over all individual u belonging to morph i, $X_{ij} = E[x_{uj}]$, is the average local density of morph j around morph i. X_{ij} can also be interpreted as morph i's encounter potential of morph j at a given time. We postulate that average

local densities are the biotic neighbourhood variables affecting fitness. As the interaction kernel ϕ_{ij} becomes less localized (approaching a uniform function in space), the local density X_{ij} approaches the global density X_j, because then every neighbour is counted equally regardless of distance. The global density X_j is, by definition, the total number of individuals belonging to a morph per unit area globally, devoid of spatial information.

The average local density X_{ij} can deviate from the global density X_j, capturing the effect of clustering or segregation. The clustering between individuals of the same morph and the segregation from other morphs are spatial mechanisms that can favour cooperation, as we will see later.

Local densities, in the continuous-space version (see 1.7.9. Appendix I), are in the spatial moment literature functions of the second moment of the population distribution (*67*). The first moment is the global density. Thus, local density encapsulates the variance of the population distribution, and is analogous to local stochasticity in the structured population genetics literature (*22*). We identify local densities, applicable in both continuous and discrete space, as the most general version of closely related concepts, such as pair densities or the environs (*33*), and probabilities of identity (*34*). Pair densities $q_{i/j}$ are defined on graphs or lattices where each node can contain at most one individual, and express the probabilities that a randomly chosen neighbouring node of a morph i individual is of morph j. Thus, $q_{i/j}$ is simply X_{ij} when local densities are normalized by a predefined density ceiling (which is 1 in scenarios where pair densities apply). Probabilities of identity Q_x can be written as $q_{i/i}$, but are measured at a spatial scale denoted by x (such as within-deme and between-demes) and concern only the probabilities that two individuals are of the same morph i. Thus, local densities are

more general: they allow us to use interaction kernels that may be diffused beyond immediate neighbours, and they capture morph-specific clustering relationships. In Section 3, we will revisit how these correspondences help us translate existing theories into the local interaction model.

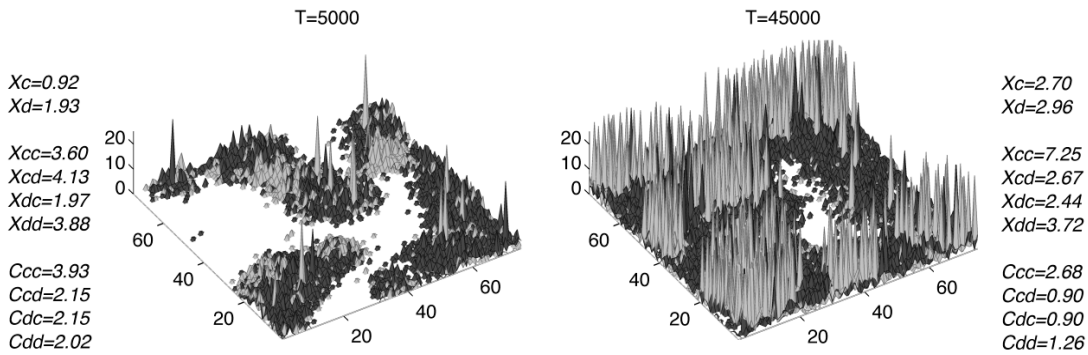

Figure 1.2. An example of cooperator (subscript c) and defector (subscript d) spatial distributions, illustrated as local peaks in light and dark at two time points. Between time T=5000 and T=45000, global population densities (Xc and Xd), average local densities (Xcc, Xcd, Xdc, Xdd), and clustering coefficients (Ccc, Ccd, Cdc, Cdd) change. The individual-based simulation is based on the production and consumption of an underlying diffusible public good on a 75x75 spatial grid. Both individuals and public good move in density-dependent fashions, leading to cluster formations (see 1.7.1. Appendix A). Local densities and clustering coefficients were computed using kernel 2 in Figure 1.1.

Over many generations, the spatial distribution of individuals changes due to birth, death, natal dispersal and migratory movement. In Fig. 1.2, we illustrate how such spatial dynamics affect local densities in a hypothetical system of cooperators and defectors (see 1.7.1. Appendix A). Birth, limited natal dispersal, and chemotactic movement (tendency to come together) increase spatial clustering, whereas death leads to thinning and random movement decreases clustering. We can relate average local densities to global densities through the clustering coefficient C_{ij} (defined at t to emphasize possible time dependence):

$$X_{ij}(t) = C_{ij}(t) X_j(t) \tag{1.2}$$

X_{ij} should be positively correlated to X_j – if there are more individuals of morph j, they will probably be encountered more often by any morph i even without spatial structure. By taking out this default correlation, clustering coefficients (i.e. normalized local densities) reveal clustering levels beyond mean-field expectations. When the clustering coefficient C_{ij} is greater than one, morph j tends to cluster around morph i individuals more than would be expected if individuals were distributed randomly. Note that $X_{ij}X_i=X_{ji}X_j$, because the average number of ij pairs from either the i or j perspective is the same. By substitution, $C_{ij}X_jX_j=C_{ji}X_iX_j$, thus $C_{ij}=C_{ji}$. Clustering coefficients are convenient ratios with which to interpret within-morph and between-morph clustering patterns. Even though local densities and clustering coefficients can change over the course of evolution (Fig. 1.2), for most of our discussion we will use them as values from the population's evolutionary equilibrium where evolutionary success, such as stability, is often calculated.

1.4.2. General dynamic equation and payoff function

In the general dynamic equations that describe how a cooperative population evolves, the response variable of interest is the per capita growth rate, i.e., the per capita rate of change in the global density of each morph, which we define as fitness. But we emphasize the dynamics of fitness, because the biotic environment – the local densities – changes through the course of evolution. We thus relate per capita growth rates of S number of morphs to average local densities in the following form (see 1.7.9. Appendix I for derivation):

$$\frac{dX_i}{X_i dt}(t) = r_i + f_i\left(X_{i1}(t), X_{i2}(t), \ldots, X_{iS}(t)\right) \quad (1.3)$$

Eq.1.3 is the local interaction model, which states that the per capita growth rate depends on a constant r_i, the intrinsic growth rate, and a function f_i containing local densities. r_i is called the intrinsic growth rate because it does not depend on densities. f_i can be called the payoff function (*68*), which can be non-linear – although in this case densities of triplets and above may also play direct roles (*65*). Such a density-based model by itself does not assume a finite population size, but does account for the discreteness of individuals (*35*, *69*), a character that is important in realistic spatial models. The model concentrates on the effect of selection, in contrast to finite-population models where mutation and drift are important (*64*). To explicitly incorporate drift, one can work with a stochastic version of Eq. 1.3. The main advantage of Eq. 1.3 is that it allows for a simple mathematical treatment of spatial demographic dynamics without necessarily assuming a model-imposed (rather than emergent) population ceiling or a movement/dispersal pattern restricted by simulation update rules. The parameters can therefore be easily estimated either from time series or independently. As a differential equation, Eq. 1.3 also represents a concise mathematical form that can approximate the dynamics of other model systems, and will facilitate the identification of common terms across different theories. It is important to note that Eq. 1.3 does not necessarily constitute a closed set of equations, as triplet densities and higher spatial moments affect the dynamics of local densities (see Appendix I); however, Eq. 1.3 allows us to articulate local densities as important variables for eco-evolutionary dynamics.

From global densities, we get the frequency, or relative proportion, of each morph, $p_i = X_i/X$, where X is the total population density. Further, in a 2-morph population, if morph 1 is assigned a character value of 1, and morph 2 a character value of 0, then p_1 (written as p when it is clear) is just the average morph character z of the population. Traditionally, z is understood as the evolutionary state. dz/dt (or equivalently dp/dt) is the change in morph character, i.e., the evolutionary change.

There are several features of the payoff function that are crucial to cooperation. If the payoff function f_i is an increasing function of X_{ij}, then morph j provides a net benefit to morph i. f_i can be nonlinear, as there can be regimes where cooperation dominates, and others where competition dominates. This idea has been developed in population ecology as the Allee effect (*70*, *71*). Nonlinearity allows us to account for the fact that individuals simultaneously possess multiple cooperative and competitive traits or characters that are amplified at different environmental states. Further, if $f_1 \neq f_2$, then morph 1 and 2 are said to have asymmetric payoff functions. That is, different morphs may be affected differently by the same biotic environment.

In summary, our model incorporates three components for the evolution of cooperation: intrinsic growth rates (r_i), payoff functions (f_i), and local densities (x_{ij}). Next, through a simpler analytical model, we analyze what these components mean in the Darwinian language of selection.

1.4.3. Selection for cooperation

The three components introduced above can be funneled into general classes of selection mechanisms. We need to transform the equations for morph density change

(Eq. 1.3) into ones for morph character change. Price's (1970, 1972) equation is one way of performing such a transformation, which has the advantage of being central to multilevel selection analysis, as we will see. Here we use a continuous-time version, which is just an application of the chain rule from calculus (*73*, *74*), to analyze the change in the average individual character of a population $dz(t)/dt$ at a given time t. The equation is:

$$\frac{dz(t)}{dt} = \mathrm{cov}\left(w_u, z_u\right) \tag{1.4}$$

where w_u is the fitness of an individual u, and z_u is the character value of that individual. On average, w_u is just the per capita growth rate of the individual's morph given the set of average local densities experienced at time t (Eq. 1.3).

In the following analytical example, we consider two morphs that have different intrinsic growth rates. In addition, morph 1 provides help, from which the two morphs benefit differently. This evolutionary scenario may be expected of a cooperative trait (possessed by morph 1) – the production of a costly local public good. Here we ignore the effect of competition and payoff function non-linearity. The fitness of morph i can then be simplified to the following equation:

$$\frac{dX_i}{X_i dt}(t) = r_i + a_{i1} X_{i1}(t) \tag{1.5}$$

A positive a_{i1} indicates helping by morph 1. But Eq. 1.5 expresses the fitness of a morph and not of an individual. To obtain w_u, let us define the fitness of an individual u in term of character value z_u; let $z_u = 1$ be the character value of an individual of morph 1, and $z_u = 0$ be the character value of an individual of morph 2. We can then write an individual u's intrinsic growth rate as $r_u(z) = r_2 + (r_1 - r_2)z_u$, and payoff function as

$a_{u1}(z) = a_{21} + (a_{11} - a_{21})z_u$. From here, we can write down the fitness of an individual u, which depends on its morph and on its local density x_{u1} at time t:

(1.6) $$w_u = r_2 + (r_1 - r_2)z_u + (a_{21} + (a_{11} - a_{21})z_u)x_{u1}$$

Note that for z_u=1, Eq. 1.6 gives the fitness of morph 1 ($r_1+a_{11}x_{11}$); and for z_u=0, Eq. 1.6 gives the fitness of morph 2 ($r_2+a_{21}x_{21}$). By substituting Eq. 1.6 into the covariance Eq. 1.4, we obtain the change in the population's average character:

(1.7) $$\begin{aligned}\frac{dz(t)}{dt} &= \operatorname{cov}\left(r_2 + \left(r_1 - r_2\right)z_u + \left(a_{21} + \left(a_{11} - a_{21}\right)z_u\right)x_{u1}, z_u\right) \\ &= \overbrace{\left(r_1 - r_2\right)\operatorname{var}\left(z_u\right)}^{[1]} + \overbrace{a_{21}\operatorname{cov}\left(x_{u1}, z_u\right)}^{[2]} + \overbrace{\left(a_{11} - a_{21}\right)\operatorname{cov}\left(z_u x_{u1}, z_u\right)}^{[3]}\end{aligned}$$

This equation identifies 3 distinct selective forces at a given time, each of which consists of a selection coefficient and a variance or covariance term – a potential for selection. Term [1] points to the non-spatial selection due to the intrinsic growth difference between morphs 1 and 2, which is amplified by the character variance in the population. Term [2] accounts for the selection for cooperation due to purely spatial effects. That is, the basic amount of benefit that both morphs obtain from encounters with morph 1 (a_{21}) contributes to the disproportionate increase in morph 1, if morph 1 individuals tend to cluster (high x_{u1} for u belonging to morph1) and segregate from morph 2 (low x_{u1} for u belonging to morph 2). Term [3] accounts for the non-spatial selection for cooperation due to payoff function asymmetry. Since $\operatorname{cov}(zx_{u1},z) > 0$ by the definition of covariance, the selection term [3] is positive as long as morph 1 benefits more from interaction with the helper (morph 1) than morph 2 does.

We have thus demonstrated that the evolution of cooperation acts through selection on one or more of the following mechanisms: intrinsic growth, space, and

payoff function asymmetry. More mechanisms subject to selection can be easily identified by analyzing a more complex payoff function. For instance, if we consider effects that result from interactions between morphs, then the between-morph local density x_{12} would become part of the spatial selection potentials. In connecting local densities to the language of selection, Eq. 1.7 constitutes a novel technical contribution.

1.5. Relations to other evolutionary theories

We will now establish the formal correspondence between local densities and metrics in evolutionary game theory, multilevel selection theory, and inclusive fitness theory.

1.5.1. Evolutionary game theory

Game theory has been employed to understand cooperation, first in human society (*75*), and later in the evolution of other organisms (Maynard Smith & Price 1973). We will develop the basic game formalism and focus on the classical Prisoner's Dilemma as an example. Then, we will discuss two mechanisms that game theory has proposed to explain the evolution of cooperation, i.e. non-spatial reciprocity and spatial reciprocity, and interpret them in terms of payoff function and local densities.

In a round of game, an individual (actor) interacts with another individual (partner) according to the partner's global morph frequency, gaining or losing fitness according to a payoff matrix with constant interaction coefficients. For a 2-player game, the payoff matrix A is:

$$A = \begin{array}{cc} & \textit{partner} \\ & \begin{array}{cc} 1 & 2 \end{array} \\ \textit{actor} \begin{array}{c} 1 \\ 2 \end{array} & \begin{bmatrix} a_{11} & a_{12} \\ a_{21} & a_{22} \end{bmatrix} \end{array} \tag{1.8}$$

One simple condition commonly used for the evolutionary stability of morph 1 is the strict Nash condition (*76*): $a_{11} > a_{21}$. Even though other payoff terms contribute to determine precise evolutionary trajectories, we will begin with the strict Nash condition.

The Prisoner's Dilemma is the case where morph 1 is the cooperator, morph 2 is the defector, and $a_{21} > a_{11} > a_{22} > a_{12}$. The game prevents the strict Nash condition for morph 1. This is the toughest game for cooperation because cooperators are exploited by defectors, even though the best outcome for the population is for all to cooperate.

We can derive the non-spatial game equation as a special case of the local interaction model. The three traditional game assumptions, interpreted through our model, are: (1) the payoff functions are linear functions of relative morph densities (or frequencies), (2) the total population size does not matter (no demographic feedback), and (3) intrinsic growth rates are identical between morphs. It can be readily shown that the payoffs a_{ij} in game theory are the coefficients of linear payoff functions in the local interaction model (1.7.2. Appendix B). It follows that the Prisoner's Dilemma must involve payoff function asymmetries ($a_{21} \neq a_{11}$, $a_{22} \neq a_{12}$). For other important types of cooperative games such as the Snowdrift Game and pseudo-reciprocity (*77*), the underlying payoff orders are different but still retain the basic feature that they can be expressed as payoff function asymmetries. While these games are perhaps theoretically less curious because no augmenting terms are needed for cooperation to evolve, they are more common in nature (Connor 2010).

Non-spatial reciprocity can solve the Prisoner's Dilemma. Trivers (1971) postulated that if individuals change their behaviour, or reciprocate, depending on the history of their interactions in repeated games, they can change the game payoffs such that cooperators are favoured. For example, the famous tit-for-tat strategy of cooperators (morph 1) versus defectors (morph 2) in a non-spatial iterated Prisoner's Dilemma game (*15*) is one that modifies payoffs (*79*) as:

$$A = \begin{bmatrix} \frac{a_{11}}{1-\rho} & a_{12} + \frac{\rho a_{22}}{1-\rho} \\ a_{21} + \frac{\rho a_{22}}{1-\rho} & \frac{a_2}{1-\rho} \end{bmatrix} \quad (1.9)$$

ρ is the probability that an individual continues interacting with a particular partner, and a_{ij} are the payoffs if there were no repetition of the game. There exists a ρ such that the cooperative strategy in a Prisoner's Dilemma is a strict Nash equilibrium (would be selected for), i.e. $a_{11}/(1-\rho) > a_{21} + \rho a_{22}/(1-\rho)$. For the same reason that game can incorporate nonspatial reciprocity - and the implied association through discrimination - by modifying payoffs, the local interaction model does the same through payoff functions. This leaves local densities to capture purely spatial effects.

The second solution to the Prisoner's Dilemma incorporates space into game theory (*20*), resulting in spatial reciprocity (*80*). The intuition is the same as what we gained from our model: clustering between cooperators can allow cooperation to evolve. Today, many spatial games are built from simulations on a lattice or graph, with a total population size that either does (*30*) or does not change (*24*). We will first introduce a novel formulation of spatial game that adheres more closely to the tradition of game and reciprocity theories. Then we will highlight the connections between existing spatial game formulations and local densities.

We begin with a bilinear version of the local interaction model, the spatial Lotka-Volterra model (*33*), which is (1.7.2. Appendix B):

$$\frac{dX_i}{X_i dt} = r_i + \sum_{j=1}^{2} a_{ij} X_{ij} \quad (1.10)$$

By assuming no intrinsic growth difference we can arrive at a spatial game formulation that is analogous to the non-spatial game (see 1.7.2. Appendix B). In term of clustering coefficients, the modified 2-player payoff matrix becomes:

$$A = \begin{bmatrix} C_{11}(t)a_{11} & C_{12}(t)a_{12} \\ C_{21}(t)a_{21} & C_{22}(t)a_{22} \end{bmatrix} \quad (1.11)$$

C_{ij} is the time-dependent clustering coefficient between morph i and morph j as introduced before (and $C_{12}=C_{21}$). When the coefficient is larger than one, there is clustering, which amplifies the interaction between the morphs i and j. By analogy to non-spatial reciprocity, if the clustering coefficients are constants, there exists augmenting terms, C_{11} and C_{12}, such that the cooperative strategy in a Prisoner's Dilemma is analogous to a strict Nash equilibrium (would be selected for), i.e., $C_{11}a_{11}>C_{21}a_{21}$. In general, however, clustering coefficients may be time-dependent, in which case the selection condition may differ.

A more prevalent type of cooperation in nature, by-product mutualism (*78*), is often implicitly associated with a spatial component – morph 2 intentionally approaches morph 1 to increase the benefit received (a_{21}) while also providing help (i.e. a positive a_{12}). By-product mutualism is in fact a type of spatial game, where C_{21} in particular is raised above 1. Again, it is instructive to view the spatial effect as augmenting the underlying payoffs (i.e. the term $C_{21}a_{21}$).

In current game models that incorporate space explicitly and assume constant and finite population size, nodes are always occupied by an individual of one morph or another (*23*, *81*). The appropriate selection condition for such a game in the limits of low mutation rate and weak selection is when the fixation probability of morph 1 is greater than that of morph 2 (*24*). The effect of the graph can be summarized through a

single structure coefficient σ (*24*, *26*, *82*). This coefficient enters the selection condition as:

(1.12) $$\sigma a_{11} + a_{12} > a_{21} + \sigma a_{22}$$

While the structure coefficient above is not purely spatial because it incorporates the effect of competition from the game update rules on graphs, we can look for something corresponding to σ in our model. An analogous condition for our density-based model is found by looking at whether the change in cooperator frequency around $p=1/2$ is positive. From the local interaction model (Eq. 1.11), we easily rediscover Eq. 1.12. We find that for a saturated habitat, $\sigma=X_{ii}/X_{ij}$ (see 1.7.3. Appendix C) or, equivalently, $\sigma=C_{ii}/C_{ij}$ (where $i \neq j$). This result parallels the finding of evolutionary set theory (*83*), which allows for overlapping interaction kernels between individuals and a form of dynamic graph but which, nevertheless, assumes a constant population size. In evolutionary set theory as in the local interaction model, σ is purely spatial. This novel analogy between spatial game and the local interaction model indicates that, given fully specified payoff functions in a saturated habitat, clustering within morph and segregation from the other morph will generally favour within-morph cooperation.

In spatial games with non-constant population size, the effect of space cannot be captured by a single coefficient (e.g. Lion 2009). In 1.7.4. Appendix D, we demonstrate how the dynamic formulation in such a spatial game model of cooperation (*60*) corresponds to our model. It is interesting that locally at each game step, the spatial game involves linear payoffs. However, the rules of the game, including the possibility of empty space, result effectively in nonlinear (quadratic) payoff functions.

We have used the local interaction model to derive results that parallel those in existing evolutionary games. Both non-spatial and spatial reciprocity can be viewed from a game

perspective as similarly augmenting payoffs to favour cooperation. These directly correspond to changes in payoff function asymmetry and changes in local densities.

1.5.2. Multilevel selection theory

Various models of the evolution of cooperation have been built from the group or multilevel selection perspective. The key postulate is the existence of higher levels of organisation in which interactions among individuals occur. We will interpret the concepts of group selection and the contextual analysis - a multilevel selection analysis - using our model.

We refer to group selection as a special case of multilevel selection where only two biotic levels exist: individuals and non-overlapping groups. The most widely cited modern group selection model is the structured deme model (Wilson 1977, Szathmáry & Maynard Smith 1997, Loreau 2010), where interaction occurs within localized "trait groups" (or simply groups) but reproduction and natal dispersal are within the larger deme. The structured deme model captures the conflict between the relative fitness of individuals within groups and the relative fitness of groups. Its status as a special case under our model is explored in 1.7.5. Appendix E. In essence, group selection postulates that a set of group characters (denoted Z_u) affects the individual u belonging to that group. We show that Z_u is the local density x_{u1} within groups of 2 morphs, where the interaction kernel defines a uniform interaction probability within individual u's group. Wilson's (1977) popular model assumed that payoff functions are symmetric. The group selection metric of spatial variance that describes cooperator clustering can be translated into average local densities – see 1.7.5. Appendix E.

A more general method for partitioning selection into lower- and higher-level selections (or into within- and between-group selections) is the contextual analysis, a method borrowed from sociology (*31*) and is related to Price's (1970) equation. Contextual analysis breaks down the causes of evolution into individual-level selection (the selection coefficient associated with the variance in individual characters) and higher-level selection (the selection coefficient associated with the (contextual) covariance between the individual character and a higher-level character) (1.7.6. Appendix F). Most simply and perhaps most satisfyingly, a higher-level character can be considered anything that cannot be predicted by the variance in individual character alone (*54*).

We can analyze a two-morph version of the local interaction model using the contextual analysis. For clarity, we only consider payoff functions that are linear but asymmetric between two morphs. Further, only a_{11} and a_{21} are non-zero (only morph 1 affects others' fitness). Thus, fitness is just as we defined in Eq. 1.5. The change in the average individual character is written in Eq. 1.7.

We can partition the right-hand side of Eq. 1.7 into levels of selection according to the variance and contextual covariance terms. In term [1] of Eq. 1.7, $r_1 - r_2$, or intrinsic growth difference, is an individual-level selection coefficient because it is associated with the variance in individual character. This variance can be predicted by observing the individual character alone.

On the other hand, the covariance term [2] in Eq. 1.7 cannot be predicted by the individual character alone. Term [2] states that even if two morphs respond identically to the same biotic environment, one morph can experience positive selection if it tends to experience a higher local density. The portion of the payoff function that the two

morphs share (a_{21}) constitutes the corresponding higher-level selection coefficient. Term [2] encapsulates the traditional group selection mechanism as introduced at the beginning of this section.

Term [3] in Eq. 1.7, the payoff function asymmetry, is more complex. Its covariance can be partitioned as shown in 1.7.6. Appendix F:

$$X_{\bullet 1}\,\mathrm{var}\left(z_u\right)+\left(1-z\right)\mathrm{cov}\left(x_{u1},z_u\right) \tag{1.13}$$

$X_{\bullet 1}$ is the average local density of morph 1 around any individual. By substituting Eq. 1.13 into Eq. 1.7 and grouping terms by variance and covariance, we obtain the following equation for evolutionary change:

$$\frac{dz}{dt}=\left[\left(r_1-r_2\right)+\boxed{\left(a_{11}-a_{21}\right)X_{\bullet 1}}\right]\mathrm{var}\left(z_u\right)+\left[a_{21}+\boxed{\left(a_{11}-a_{21}\right)\left(1-z\right)}\right]\mathrm{cov}\left(x_{u1},z_u\right) \tag{1.14}$$

Eq. 1.14 says that payoff function asymmetry affects both levels of selection (see boxed terms).

Since the individual-level selection term (Eq. 1.14) contains the average local density $X_{\bullet 1}$, it cannot be predicted by the individual characters alone. On the other hand, $X_{\bullet 1}$ is independent of the individual character at a given time. We may call (a_{11}–a_{21})$X_{\bullet 1}$ an interaction between individual and higher-level selections, since in a dynamic sense higher-level characters do affect $X_{\bullet 1}$. It is not entirely surprising that there is not a one-to-one mapping between mechanisms and levels of selection, as there are many possible selection mechanisms, while our use of contextual analysis only identifies two levels. This multilevel selection partitioning of spatial and non-spatial effects is a novel contribution.

To summarize, group selection theory emphasizes the importance of spatial group formation in the evolution of cooperation. Multilevel selection more generally

identifies intrinsic growth differences as individual-level selection, and the difference in morphs' experienced average local densities as higher-level selection (in particular as traditional group selection). On the other hand, payoff function asymmetry straddles two levels of selection, suggesting that biotic levels are not cleanly segregated under the local interaction perspective.

1.5.3. Inclusive fitness theory

Inclusive fitness theory, including kin selection mechanisms (*13*), is individual-centred. It includes fitness effects on others as part of the actor's fitness, weighted by relatedness (hence the term inclusive fitness). This individual-centred formulation necessitates identifying cost to self (direct fitness effect) and benefit to others (indirect fitness effect). We will show how these features, as well as Wright's *F* statistics (*87*), relate to the local interaction model, thereby reinforcing known but often convoluted links between inclusive fitness theory, spatial population genetics, and spatial ecology in a novel way.

Inclusive fitness can be derived from standard population genetics (1.7.7. Appendix G). For a two-morph population in which individuals affect interacting partners equally within an interaction scale, we arrive at the following equation describing changes in morph 1 frequency:

$$\frac{dp}{dt} = p(1-p)\left(r_1 + R_1 X_{1\bullet} b_{1\rightarrow\bullet} - r_2 - R_2 X_{2\bullet} b_{2\rightarrow\bullet}\right) \tag{1.15}$$

$b_{1\rightarrow\bullet}$ is the benefit given by a morph 1 individual to a partner on each encounter without discrimination. The total benefit given by an individual of morph 1 to its neighbours is then $X_{1\bullet}\, b_{1\rightarrow\bullet}$. The difference between the intrinsic growth rates, $r_1 - r_2$, emerges as the

intrinsic cost to morph 1. This difference is also known as a direct fitness effect. The right hand side of Eq. 1.15 can be called the inclusive fitness of morph 1. There are two relatedness terms, R_1 and R_2, which are dimensionless ratios of global frequency and local densities (1.7.7. Appendix G):

$$R_1 = \frac{X_{11}/X_{1\bullet} - p}{1-p} \qquad R_2 = \frac{X_{21}/X_{2\bullet} - p}{-p} \tag{1.16}$$

Relatedness can be interpreted as describing interaction neighbourhoods. If there are more morph 1 individuals in a morph 1 neighbourhood ($X_{11}/X_{1\bullet}$) than globally (p), R_1 is positive. An associated positive benefit $b_{1\rightarrow\bullet}$ would then contribute positively to morph 1's relative inclusive fitness. If there are fewer morph 1 individuals in a morph 2 neighbourhood ($X_{21}/X_{2\bullet}$) than globally (p), R_2 is positive. But any associated positive benefit $b_{2\rightarrow\bullet}$counts against morph 1's relative inclusive fitness, because then the fitness of morph 2 is raised more than that of morph 1. Such relatedness metrics capture the spatial kin selection mechanism. From our derivation (1.7.7. Appendix G), we find that the benefit given by j is the same as the payoff (or linear payoff function) that any individual gets when encountering morph j: $b_{j\rightarrow\bullet} = a_{\bullet j}$. For a 2-morph population, the equality implies the following constraints: $a_{11} = a_{21}$, $a_{22} = a_{12}$, i.e., payoff function symmetry.

Relatedness has been linked to Wright's F statistics, which are based on probabilities of identity. Probabilities of identity are also known as pair densities when they are not conditional on the individuals' morphs (*26*). In Wright's island model, (*32*, *88*), the probability of fixation of cooperation is determined by F_{ST} in place of relatedness. This substitution hinges on the assumption of weak selection, such that we only have to consider the change in frequency near p=1/2. With the additional

restriction that within-morph clustering is unconditional ($C_{11} = C_{22}$), we show in 1.7.8 Appendix H that F_{ST} is identical to R_1. This equality links the theory of evolution of cooperation based on local densities to the classic subdivided population literature and coalescence theory (*88*).

In inclusive fitness theory, payoff function asymmetry surfaces in the forms of kin and kind discriminations (*56*) and the green beard effect (*89*). These are non-spatial mechanisms whereby benefits are given discriminately towards an individual's own morph. We call these collectively helping by discrimination. Through discriminated helping, the fitness of each morph is affected differently given the same type of encounter, thus it is a scenario of payoff function asymmetry. Rather than expressing helping by discrimination in term of payoff function (or cost and benefit), inclusive fitness theory expresses discrimination through high relatedness (*89*). In other words, in the case of payoff function asymmetry, relatedness is a compound of spatial and non-spatial mechanisms.

To see how we may modify inclusive fitness to decipher spatial and non-spatial mechanisms, we will consider both plastic cost and discriminated benefit (1.7.7. Appendix G). A plastic cost (c_{ij}) is one that is only incurred by an actor of morph *i* when morph *j* is encountered. A discriminated benefit from a morph *i* individual ($b_{i\to j}$) is one that is only received by a partner of morph *j*. In 1.7.7. Appendix G, we show that by specifying the target morph that receives a certain benefit, Eq. 1.15 becomes:

$$(1.17)\quad \frac{dp}{dt} = p(1-p)\left(r_1 + \left(b_{1\to 1} - c_{11}\right)X_{11} + \left(b_{2\to 1} - c_{12}\right)X_{12} - r_2 - \left(b_{1\to 2} - c_{21}\right)X_{21} + \left(b_{2\to 2} - c_{22}\right)X_{22}\right)$$

It can be shown (1.7.7. Appendix G) that Eq.1.17 is equivalent to the spatial Lotka-Volterra Eq. 1.10 – a case of the local interaction model, through the following identity:

$$b_{j \to i} - c_{ij} = a_{ij} \tag{1.18}$$

This equality completes the correspondence between the payoff function terms of inclusive fitness theory, the local interaction model (Eq. 1.5), evolutionary game (Eq. 1.8), and multilevel selection (Eq. 1.14).

1.6. Discussion

We began our investigation by proposing local densities X_{ij} (Eq. 1.1) as the central metrics describing the spatial structure of cooperative populations, incorporating within-morph (subscripted *ii*) and between-morph (subscripted *ij*) clustering and segregations. Using the appropriate interaction kernel, local densities capture interaction potentials. Clustering coefficients C_{ij} (Eq. 1.2), which are ratios of local densities over global densities, prove to be useful numbers to consider: when they are above one, they indicate clustering. Using the local interaction model based on local densities in conjunction with Price's equation, we identified three selection mechanisms in a novel way (Eq. 1.7). These include selections due to intrinsic growth rate difference, to spatial effects, and to payoff function asymmetry – or how different morphs are differently affected by interactions.

Using analyses based on local densities, we uncovered some new connections between evolutionary game theory, multilevel selection theory, and inclusive fitness theory. In evolutionary game theory, assuming habitat saturation, the recently developed structure coefficient σ (*24*) (Eq. 1.12) can be written as a composite of local densities or clustering coefficients: $\sigma = X_{ii}/X_{ij} = C_{ii}/C_{ij}$. In multilevel selection theory, higher level selection corresponds to the selection potential as represented by $\mathrm{cov}(x_{u1},z_u)$, or the covariance between the local density of the helper morph as experienced by individual *u* and the morph *z* of that individual (Eq. 1.14). In inclusive fitness theory, assuming no kin discrimination and a sole helper morph 1, relatedness is a function of local densities: $R_1=(X_{11}/X_{1\cdot})/(1-p)$ (Eq. 1.16). Finally, the fitness effect coefficients found in the different theories can be summarized as payoff function by the

relationship $b_{j\to i} - c_{ij} = a_{ij}$ (Eq. 1.18). Such an expression can also capture non-spatial kin discrimination, as discrimination is a form of payoff function asymmetry (where different morphs i gain differential payoffs from the same interacting partner j).

Local densities can be viewed as a technical means (in the forms of pair densities or probabilities of identity) to obtaining existing composite metrics such as structure coefficient, higher level selection potential and relatedness. However, they can also be viewed as major variables of interest, on par with population density and morph frequency, all of which are interlocked in eco-evolutionary feedbacks. Local densities are ecologically intuitive metrics describing different kinds of clustering, and they clearly partition spatial versus non-spatial effects in the evolution of cooperation. They are measurable quantities in continuous or discrete space and graphs, can incorporate nuanced modeling of interaction kernels or scales, and allow for fully emergent demographic dynamics without pre-defined limits. Through local densities, we have further strengthened the increasingly apparent links between spatial ecology and evolutionary theories (*30*). We hope to have highlighted the value of the common vocabularies that biologists use to formalize cooperation.

The local interaction model is not a replacement of current theories. Rather, it brings unity and focus to the spatial aspect of existing evolutionary theories of cooperation. In favour of clarifying spatial metrics used to construct evolutionary equations, important aspects were left out. For example, there are different ways to evaluate the ultimate evolutionary success of cooperators or a cooperative trait, including evolutionary stability (*4*), fixation probability, and inclusive fitness effect (*64*). In our work, we have mostly discussed the changes in cooperator frequency (p) or cooperative character (z), except when we utilize fixation probability in comparing our

model with the structure coefficient (σ) and F statistics (F_{ST}). Since change in frequency and character are only indicative of evolutionary directions at a given state, before accounting for mutation, we maintain generality but without specifying how to obtain long-term evolutionary trajectories. As well, there are different ways to derive the changes in spatial interaction patterns through identity by descent and family structure (*13*), life history and demography (*32*), and update rules and graph topologies (*26*), among others - which we did not elaborate on. The measure of evolutionary success and the mechanistic understanding on pattern formation are crucial, but in principle they can be expressed through models based on local densities.

We have demonstrated that local densities are general and common spatial metrics across major theories of the evolution of cooperation. For both empirical and theoretical investigations, local densities are technically precise and intuitive vocabularies that can sharpen our understanding of the role of space in maintaining cooperation.

1.7. Appendices

1.7.1. Appendix A. Simulation

To illustrate how local densities and clustering coefficients develop, we simulate a complex public good game. Individuals are either cooperators, who produce the public good at a cost, or defectors, who can benefit from the public good but do not produce it. We place individuals in a 75x75 spatial grid, with each square being larger than a single individual. Multiple individuals can exist in a square. Thus, while space is discrete, it is not restricted like lattice models where only one individual can occupy a square or node, and instead resembles continuous space in that local densities have no upper limit.

Each individual begins with a random health state, orientation, and memory of previous local density within its own square. At each simulation time step, an individual can divide, produce and consume public good, or die, all probabilistically depending on its health state. An individual moves in either its current orientation or tumbles randomly onto an adjacent square with probabilities that depend on its memory of the previous local density and on the current local density, so as to emulate chemotaxis. The public good diffuses into all four adjacent squares at rates that depend on the individual density of those squares, and is lost to the environment through leaching, which is also mediated by the individual density. Note that even though the public good and individuals can only move to adjacent squares at each time step, they do so at different rates. A list of parameter values is shown in Table 1.A.1. The simulation time step is much shorter than that of an average individual generation (~50 time steps), thus approximates continuous time dynamics.

Table 1.A.1. Simulation parameters and values.

parameter	value	parameter	value
background mortality	0.0003	quorum sensing: rate of exponential decrease in movement probability per individual over quorum	0.2
maximum health-dependent mortality rate	0.0035	minimum health to produce public good	0.015
metabolic cost	1e-6	maximum public good production	0.005
minimum health for division at capacity	0.7	cost to produce maximum dose of public good	0.0005
maximum division probability	0.075	public good acquisition rate	0.0025
carrying capacity within square	20	rate of conversion from public good to health	5
quorum: local density above which movement rate decreases exponentially	9	public good saturation level	1
minimum health for moving	0.1	maximum public good horizontal diffusion rate	0.1
maximum movement probability	0.075	amount of public good leaching	0.001
movement cost	0.002	rate of exponential decrease in public good diffusion due to individual density	0.1
tumbling probability under positive individual density gradient	0.25		

Local densities and clustering coefficients are measured as defined in the main text, using the interaction kernel 2 (Fig. 1.1).

1.7.2. Appendix B. Spatial game derivation

To obtain a simple spatial game formulation, we begin with a spatial version of the Lotka-Volterra equation (*90*, *91*).

$$\frac{dX_i}{X_i dt} = r_i + \sum_{j=1}^{2} a_{ij} X_{ij} \quad (1.B.1)$$

This is clearly a case of the local interaction model with average local densities on the right hand side associated with the linear payoff function coefficient a_{ij}. This equation can be transformed into a frequency-based equation by differentiating X_i / X with respect to time:

$$\frac{dp_i}{dt} = \frac{d}{dt}\left(\frac{X_i}{X}\right) = \frac{dX_i / dt}{X} - \frac{X_i dX / dt}{X^2} \tag{1.B.2}$$

Using Eq. 1.B.1 as the expression for change in density, Eq. 1.B.2 becomes:

$$\frac{dp_i}{dt} = \frac{X_i}{X}\left(r_i + \sum_{j=1}^{2} a_{ij} X_{ij}\right) - \frac{X_i}{X^2}\sum_{k=1}^{2} X_k \left(r_k + \sum_{l=1}^{2} a_{kl} X_{kl}\right) \tag{1.B.3}$$

By replacing density with frequency terms, we finally arrive at:

$$\frac{dp_i}{dt} = p_i\left(r_i + \sum_{j=1}^{2} XC_{ij} a_{ij} p_j - \sum_{k=1}^{2} p_k \left(r_k + \sum_{l=1}^{2} XC_{kl} a_{kl} p_l\right)\right) \tag{1.B.4}$$

The linear payoff function coefficient a_{ij} is multiplied by the clustering coefficient C_{ij}. To convert Eq. 1.B.4 into a non-spatial formulation, one only needs to set $C_{ij} = 1$. The result can be readily recognized as the evolutionary game replicator equation (*92*). This is a slightly different and more straightforward translation between ecological (density-tracking) and evolutionary (frequency-tracking) dynamics than what is already published (*93*). Since our game formulation is derived from a case of the local interaction model, we conclude that payoffs a_{ij} in game theory are the coefficients of linear payoff functions in the local interaction model. Furthermore, since the clustering coefficients are only constant multipliers of the original payoff terms, the spatial game will follow evolutionary dynamics that is equivalent to the non-spatial game (specified by the replicator equation) with the payoff terms $C_{ij}a_{ij}$.

1.7.3. Appendix C. Games on graphs

Games on saturated static graphs has been an area of intense study recently. Major results from this body of work has been summarized in (*24*) through a graph structure parameter called structure coefficient (σ). Structure coefficient is a function of

number of nodes (individuals), degree (number of links between individuals), other topological attributes of how individuals are arranged, and update rules. The nodes themselves do not move, but they influence the state of linked nodes.

The appropriate selection condition for such a game in the limits of low mutation rate and weak selection is that the fixation probability of morph 1 must be greater than that of morph 2 (*24*). The condition states that the morph 1 frequency should be, on average, more than ½. Equivalently, we can ask whether the change in morph 1 frequency (Eq. 1.B.4) is greater than zero when the morph 1 frequency is ½ (or $X_1 = X_2$). We readily obtain:

(1.C.1) $$a_{11}X_{11} + a_{12}X_{12} > a_{21}X_{21} + a_{22}X_{22}$$

When morph 1 frequency is ½, we have $X_{12} = X_{21}$ (since $X_1X_{12}=X_2X_{21}$ by conservation of total number of intramorph interactions, and $X_1 = X_2$). So we can divide both sides of the above equation by X_{12} to isolate a_{12} and a_{21}. Further, in a saturated habitat, every individual always has the same number of neighbours, $X_{11} + X_{12} = X_{21} + X_{22} = X$, so $X_{11} = X_{22}$. Eq. 1.C.1 then becomes:

(1.C.2) $$\sigma a_{11} + a_{12} > a_{21} + \sigma a_{22}$$

where $\sigma = X_{ii}/X_{ij}$ for any $i \neq j$ when $X_1 = X_2$. At the same time, since $X_{11} = X_{22}$ due to habitat saturation, we recover the implicit restriction that $C_{11} = C_{22}$ for such a game. Thus, $\sigma = C_{ii}/C_{ij}$ for any $i \neq j$ when $X_1 = X_2$. Eq. 1.C.2 is the same as the result of (*24*). In another word, structure coefficient is the ratio of intramorph over intermorph average local densities, or equivalently, the ratio of intramorph over intermorph clustering coefficients.

1.7.4. Appendix D. Complex spatial game

We demonstrate how lattice/graph models of spatial game, as exemplified by Van Baalen et al.'s (1998) spatial game model of cooperation is a subset of the local interaction model. Pair densities in lattice/graph models are the discrete analogues of average local densities. In particular, the interaction kernel of a lattice/graph model is determined by unweighted links between nodes that can either be occupied by an individual or is empty (but can also be influenced by update rules, as noted by Grafen and Archetti (2008) and (*24*). We use the symbol X_{ij} for both pair density and average local density.

The changes in local densities can be tracked using pair approximation (*33*), analogous to the moment approximation in continuous space (*67*). Knowing that morph 1 is the cooperator and morph 2 is the defector, Eq. 1.D.1 (adapted from Van Baalen et al., 1998) expresses the change in frequency of morph i as a function of the average local densities (or pair densities) X_{i1}, X_{i0} (local density of empty space around morph i) and the structural parameter Y (number of possible spaces around each node). For every available neighbouring empty site, β is a basic intrinsic growth rate that manifests, $b_{i\rightarrow\bullet}$ is the fitness benefit that a morph i individual gives to each present neighbour, and c_i is the cost of being morph i.

$$\frac{dp_i}{dt} = p_i\left(r_i + \left(\beta + b_{i\rightarrow\bullet}\frac{X_{i1}}{Y} - c_i\right)X_{i0}\right) \quad (1.D.1)$$

This frequency-tracking equation can be converted to a density-tracking equation (by writing $p_i = X_i / X$, and $X_{i0} = Y - X_{i1} - X_{i2}$) and then rearranged by local density terms to reveal the payoff parameters:

$$\frac{dX_i}{X_i dt} = r_i + Y(\beta - c_i) + \left(b_{1\to\bullet} - (\beta - c_i)\right) X_{i1} - (\beta - c_i) X_{i2} - \frac{b_{1\to\bullet}}{Y} X_{i1} X_{i2} - \frac{b_{1\to\bullet}}{Y} X_{i1}^2 \quad (1.D.2)$$

We see that the intrinsic growth rate is actually not r_i alone, as the original model suggested, but $r_i + Y(\beta - c_i)$ – i.e. there is an intrinsic cost to being morph 1. The payoff is also nonlinear (quadratic), as there are terms associated with X_{i1}^2 and $X_{i1}X_{i2}$; and asymmetric, as the term c_i appears in the local density dependent terms, making the payoff function morph-dependent.

1.7.5. Appendix E. Structured deme model

According to Wilson (1977), individuals interact with equal probability within local trait groups to which their fitness mostly responds, but their maximal movement range at some point in their life cycle defines a deme. Assuming that the deme is saturated, the composition of trait groups that are more fit (produce more progenies) take up more of the deme over time. The fitness of a group is determined by its composition, or proportion of cooperator (say morph 1) versus defector (morph 2). Wilson (1977) showed that if there is between-group variance in their composition, the change in morph density is a function not of morph frequency in a deme, but of "subjective morph frequency". This is the global frequency plus some function of the between-group variance σ^2. In trait groups where undirected helping is proportional to the number of cooperators within group, the dynamic equations, which we have converted from a change in frequency to a change in density form, are (from Wilson 1977):

$$\frac{dX_1}{X_1 dt} = b_{1\to\bullet}\left(N_d\left(p_1 + \frac{\sigma^2}{p_1}\right) - 1\right) - c_1$$
$$\frac{dX_2}{X_2 dt} = b_{1\to\bullet} N_d\left(p_1 - \frac{\sigma^2}{p_2}\right) \quad \text{(1.E.1)}$$

$b_{i\to\bullet}$ is the fitness benefit that a morph i individual gives to each present neighbour, N_d is the group size, $-c_1$ is the intrinsic growth of morph 1, and p_i is the global frequency of morph i. Within group, it is assumed *a priori* there is no assortment, so without between-group variance, we can see that morph 1 (cooperators) density will grow slower than that of morph 2, even if there is a net increase for both morphs due to cooperators helping. In another word, within-group, cooperators are selected against, even though they enhance the absolute fitness of everyone in the group.

If we take $b_{i\to\bullet}$ to be the linear payoff function to average local densities in Eq. 1.E.1, as is custom in the local interaction model, the average local densities are:

$$X_{ii} = N_d\left(p_i + \frac{\sigma^2}{p_i}\right) - 1$$
$$X_{ij} = N_d\left(p_j - \frac{\sigma^2}{p_i}\right) \quad \text{(1.E.2)}$$

X_{ij} is understood as the average number of morph j individuals around a morph i individual, with the interaction kernel being uniform within the range of a trait group and zero everywhere else. From Eq. 1.E.2, we can solve for the spatial variance:

$$\sigma^2 = \frac{X_i\left(\left(X_{ii}+1\right) - X_i\right)}{N_d^2} = \frac{X_i\left(X_j - X_{ij}\right)}{N_d^2} \quad \text{(1.E.3)}$$

As may be expected, the spatial variance is inversely proportional to group size squared and proportional to the difference within group between the actual number of ij pairs ($X_i X_{ij}$) and number of ij pairs expected in the non-spatial scenario ($X_i X_j$).

1.7.6. Appendix F. Contextual analysis

Contextual analysis (*31*) postulates that individual fitness can be written as follows:

(1.F.1) $$w_u = \beta_z z_u + \beta_Z Z_u$$

where β_z is the selection coefficient for the individual character, β_Z is the selection coefficient for the higher level character, and Z_u is the higher level character that the individual experiences. Then, by plugging Eq. 1.F.1 into Eq. 1.4, we obtain:

(1.F.2) $$\frac{dz}{dt} = \beta_z \operatorname{var}(z_u) + \beta_Z \operatorname{cov}(Z_u, z_u)$$

where the first term in the right hand side is the individual level selection, and the second term is the higher level selection. The most familiar form of var(z_u) is the genetic variance in a population, for the case where the individual u refers to a gene. An example of cov(Z_u,z_u) is the association between a particular gene variation (allele) and the type of group that the allele finds itself in (whether the group contains more of its own morph or of other morphs).

More generally, we can use Eq. 1.6 as a basis to analyze levels of selection for a more complicated payoff function Eq. 1.5. The first two terms in Eq. 1.6 are straightforward to analyze – with the first belonging to individual-level selection, and the second belonging to higher-level selection. On the other hand, the third term (Eq. 1.F.3), referring to payoff function asymmetry, does not neatly fit into one level of selection.

(1.F.3) $$(a_{11} - a_{21}) \operatorname{cov}(z_u x_{u1}, z_u)$$

We can break down the covariance term as follows:

$$\begin{aligned}\operatorname{cov}(z_u x_{u1}, z_u) &= E\left[z_u^2 x_{u1}\right] - zE\left[z_u x_{u1}\right] \\ &= \operatorname{cov}\left(x_{u1}, z_u^2\right) + E\left[z_u^2\right] X_{\bullet 1} - z\left(\operatorname{cov}(x_{u1}, z_u) + z X_{\bullet 1}\right) \\ &= X_{\bullet 1} \operatorname{var}(z_u) + \operatorname{cov}\left(x_{u1}, z_u^2\right) - z \operatorname{cov}(x_{u1}, z_u)\end{aligned}$$

(1.F.4)

Note that $X_{\bullet 1}$ is the average local density of morph 1 around any individual. Since $z_u{}^2 = z_u$ (z_u is either 1 or 0 for each individual), the above equation simplifies to:

$$X_{\bullet 1} \operatorname{var}(z_u) + (1 - z) \operatorname{cov}(x_{u1}, z_u)$$

(1.F.5)

Thus, payoff function asymmetry ($a_{11} - a_{21}$) contributes to both individual level selection (associated with var(z_u)) and higher-level selection (associated with cov(x_{u1},z_u)).

1.7.7. Appendix G. Inclusive fitness derivation

A one-locus population genetics model that accounts for interaction effects is constructed as follows. The fitness (birth minus death probabilities) of an individual u is the sum of its intrinsic growth probability, expected benefits received from each of all other individuals v ($b_{v \to u}$) and all expected costs exerted upon encounter with v (the plastic cost c_{uv}) in a small temporal increment Δt, taken over an ensemble of realizations of the same configuration:

$$w_u = r_u + \sum_{v \neq u} \left(b_{v \to u} - c_{uv}\right)$$

(1.G.1)

The expected changes in the number of morph i individuals (N_i) and of all individuals (N) at a given time are:

$$\frac{\Delta N_i}{\Delta t} = \sum_{u=1}^{N} z_u w_u \qquad \frac{\Delta N}{\Delta t} = \sum_{u=1}^{N} w_u$$

(1.G.2)

z_u is the character value of individual u (where we assign z_u=1 for individuals u belonging to morph i). For instance, if we want to track the change in morph 1 frequency, we can assign morph 1 the character value of 1, and morph 2 the character value of 0. The change in the morph i frequency p_i is then:

$$\frac{\Delta p_i}{\Delta t} = \frac{\Delta}{\Delta t}\left(\frac{N_i}{N}\right) = \frac{\Delta N_i / \Delta t}{N + \Delta N} - \frac{N_i \Delta N / \Delta t}{N(N + \Delta N)} \tag{1.G.3}$$

Putting these all together, we obtain:

$$\begin{aligned}\frac{\Delta p_i}{\Delta t} &= \frac{1}{N+\Delta N}\sum_{u=1}^{N}\left(z_u\left(r_u + \sum_{v\neq u}\left(b_{v\to u} - c_{uv}\right)\right)\right) - p_i \frac{1}{N+\Delta N}\sum_{u=1}^{N}\left(r_u + \sum_{v\neq u}\left(b_{v\to u} - c_{uv}\right)\right) \\ &= \frac{1}{N+\Delta N}\sum_{u=1}^{N}\left(z_u - p_i\right)\left(r_u + \sum_{v\neq u}\left(b_{v\to u} - c_{uv}\right)\right)\end{aligned} \tag{1.G.4}$$

The population structure of this formulation can be understood as being defined for all interacting partners exhaustively (embedded in the summations); similarly, the payoff function to that structure is tallied on an individual basis. In a population with N individuals, there will be N intrinsic growth terms, and $N(N-1)$ cost and benefit terms.

To get to an inclusive fitness formulation, we switch the index of the benefit term between pairs from $b_{v\to u}$ (benefit from neighbour v to focal individual u) *to* $b_{u\to v}$ (benefit from focal individual u to neighbour v).

$$\begin{aligned}\frac{\Delta p_i}{\Delta t} &= \frac{1}{N+\Delta N}\left(\sum_{u=1}^{N}\left(z_u - p_i\right)\left(r_u - \sum_{v\neq u} c_{uv}\right) + \sum_{u=1}^{N}\left(z_u - p_i\right)\sum_{v\neq u}\left(\frac{z_v - p_i}{z_u - p_i} b_{u\to v}\right)\right) \\ &= \frac{1}{N+\Delta N}\left(\sum_{u=1}^{N}\left(z_u - p_i\right)\left(r_u + \sum_{v\neq u}\left(\frac{z_v - p_i}{z_u - p_i} b_{u\to v} - c_{uv}\right)\right)\right)\end{aligned} \tag{1.G.5}$$

The term $(z_v - p_i)/(z_u - p_i)$ is a correlation coefficient called relatedness, defined for every pair of individuals. The result is similar to that of Grafen (2006).

We must reduce the number of terms for a tractable inclusive fitness model that is comparable to the local interaction model. We take the limit of $\Delta t \to 0$ in Eq. 1.G.5, where

$N+\Delta N \approx N$, to arrive at a continuous-time analogue for the change in morph frequency. For a 2-morph population, we associate cost, benefit, and relatedness terms with morph, such that the indices now refer to the morph instead of the individual. We now assume that all individuals of a morph provide the same fitness effect ($b_{i\to\bullet}$) to each interacting neighbour without discrimination in the small time interval dt. As well, we assume no plastic cost. Then, from Eq. 1.G.5 we get:

(1.G.6) $$\frac{dp}{dt} = p(1-p)\left(r_1 + X_{1\bullet}R_1 b_{1\to\bullet} - r_2 + X_{2\bullet}R_2 b_{2\to\bullet}\right)$$

where the relatedness terms are:

(1.G.7) $$R_1 = \frac{X_{11}/X_{1\bullet} - p}{1-p} \qquad R_2 = \frac{X_{21}/X_{2\bullet} - p}{-p}$$

The $\Sigma_{v\neq u}$... summations from Eq. 1.G.5 are replaced in Eq 1.G.6 by $X_{i\bullet}$ (average total local density around morph i) because both represent the average sum of effects on neighbours by one individual. $(1/N)\Sigma^{Ni}$... is replaced by p_i times the average of the term in the summation.

Alternatively, we can retain the possibility of helping with discrimination and plastic cost in Eq. 1.G.5. We obtain:

(1.G.8) $$\frac{dp}{dt} = p(1-p)\begin{pmatrix} r_1 + X_{11}\left(R_{11}b_{1\to1} - c_{11}\right) + X_{12}\left(R_{12}b_{1\to2} - c_{12}\right) \\ -r_2 - X_{21}\left(R_{21}b_{2\to1} - c_{21}\right) - X_{22}\left(R_{22}b_{2\to2} - c_{22}\right) \end{pmatrix}$$

By modeling discriminated helping explicitly, we know exactly the relatedness terms *a priori*:

(1.G.9) $$R_{11} = 1, R_{i12} = \frac{-p_1}{1-p_1}, R_{21} = \frac{1-p_1}{-p_1}, R_{22} = 1$$

We can further simplify the expression of Eq. 1.G.8 by plugging in Eq. 1.G.9. We also use the fact that $pX_{12} = (1-p)X_{21}$ by conservation of total number of inter-morph interactions to obtain:

$$\frac{dp}{dt} = p(1-p)\begin{pmatrix} r_1 + X_{11}(b_{1\to1} - c_{11}) + X_{12}(b_{2\to1} - c_{12}) \\ -r_2 - X_{21}(b_{1\to2} - c_{21}) - X_{22}(b_{2\to2} - c_{22}) \end{pmatrix} \quad (1.G.10)$$

With some simple derivation steps, one can see this expression is identical to the spatial Lotka-Volterra Eq. 1.B.1 and the spatial game Eq. 1.B.4, both of which are cases of the local interaction model. The following relationship connects the inclusive fitness derivation with the other formulations:

$$b_{j\to i} - c_{ij} = a_{ij} \quad (1.G.11)$$

1.7.8. Appendix H. *F* Statistics

Relatedness has been linked to Wright's *F* statistics, which is the ratio of gene correlation within groups with respect to genes between groups, with group usually meaning a spatial area, as in a deme (*22*):

$$F_{ST} = \frac{Q_w - Q_b}{1 - Q_b} \quad (1.H.1)$$

Q_w is the probability of identity by morph within groups, whereas Q_b is the probability of identity by morph between random groups. Probabilities of identity are also known as pair densities when they are not conditional on the individuals' morphs (*26*). These probabilities can be written in term of local densities as:

$$\begin{aligned} Q_w &= pE[x_{11}/x_{1\bullet}] + (1-p)E[x_{22}/x_{2\bullet}] \\ Q_b &= p^2 + (1-p)^2 \end{aligned} \quad (1.H.2)$$

In Wright's island model, (*32*, *88*), the probability of fixation of cooperation is determined by F_{ST} in place of relatedness. This hinges on the assumption of weak selection, such that we only have to consider the change in frequency near $p=1/2$. If we assume habitat saturation in all groups, then the local density of any morph-pair cannot exceed X, and the clustering coefficients $C_{11}=C_{22}=C$, leading to the following:

$$E\left[x_{11}/x_{1\bullet}\right]=X_{11}/X=Cp$$
$$E\left[x_{22}/x_{2\bullet}\right]=X_{22}/X=C\left(1-p\right) \quad \text{(1.H.3)}$$

where necessarily Cp is less than or equal to 1. This implies that C cannot be a constant in such a spatially constrained population. In a population where individuals are sparsely distributed across their habitat, it is possible that C stays near constant through all states. Alternatively we can take C to be the within-morph clustering during invasion or at co-existence equilibrium – depending on whether we want to ask about the invasibility or the stability of a phenotype.

Using Eq. 1.H.1, Eq. 1.H.2, Eq. 1.H.3, we obtain the relationship between F_{ST} and C:

$$F_{ST}=\frac{(C-1)Q_b}{1-Q_b}=\frac{(C-1)\left(\frac{1}{2p}-1+p\right)}{1-p} \quad \text{(1.H.4)}$$

Note that the relatedness term R_1 can now be written as:

$$R_1=\frac{(C-1)p}{1-p} \quad \text{(1.H.5)}$$

We observe that F_{ST} and R_1 only take on the same value when $p=1/2$, which is expected when selection is weak. Precisely, this is when Q_b equals p.

1.7.9. Appendix I. Derivation of the local interaction model

Eq. 1.1 provides the motivation for computing local densities in real empirical systems where the spatial measurement resolution is not infinitely fine-scaled. This discrete-space conceptualization also serves as a basis to construct the continuous-time Eq. 1.3, describing the dynamics of local interactions, using a limiting process following the spatial moment literature (*65*, *95*). To begin its derivation, we repeat the definition of local density X_{ij}, assume that all focal individuals u of morph i weigh their neighbours by the same function ϕ_{ij}, and note that the expectation of x_{uj} across all u that are morph i is the same as the expectation of the average local density in cell location y, $X_{ij}(y)$, across all y:

(1.I.1)
$$X_{ij}=\mathrm{E}[x_{uj}]=\frac{1}{N_i}\sum_{u\in i}\sum_{v\in j}\phi_{uj}(y_v-y_u)=\frac{1}{N_i}\sum_{u\in i}\sum_{v\in j}\phi_{ij}(y_v-y_u)$$
$$=\mathrm{E}[X_{ij}(y)]=\sum_{q\in\Omega}\phi_{ij}(y-q)\mathrm{E}[N_i(y)N_j(q)]$$

q is the location of potential morph j neighbors, and Ω is the habitat space, which is a countable but infinite set of discrete cells. The expectation $\mathrm{E}[N_i(y)N_j(q)]$ is taken over all cells y. So line 1 of Eq. 1.I.1 uses individuals u as focal points (with focal location y_u and neighbour location y_v), while line 2 uses space y as focal points (with focal location y and neighbor location q); these are equivalent Lagrangian and Eulerian perspectives. We define the spatial covariance between morph i and j at distance y-q as:

(1.I.2)
$$\mathrm{Cov}_{ij}(y-z)=\mathrm{E}[N_i(y)N_j(z)]-\mathrm{E}[N_i]\mathrm{E}[N_j]$$

where the first expectation over all focal cells y and the second expectation over all cells. As a simple example, we assume that the interaction effect is linear and can be expressed as a_{ij}. Over an ensemble of realizations of the same system configuration, we

take Δt to be small enough for only one birth or death event to occur. Then, the expected change in the number of morph i individuals (N_i) in Δt is:

(1.I.3)
$$\frac{\mathrm{E}\left[\Delta N_i(y)\right]}{\Delta t}=\mathrm{E}\left[r_i N_i(y)+\sum_{j=1}^{S} a_{ij}\sum_{q\in\Omega}\phi_{uj}(y\text{-}q)\mathrm{E}[N_i(y)N_j(q)]\right]$$
$$=r_i\mathrm{E}[N_i]+\sum_{j=1}^{S} a_{ij}\left(\frac{1}{h}\mathrm{E}[N_i]\mathrm{E}[N_j]+\sum_{q\in\Omega} h\phi_{uj}(y\text{-}q)\frac{1}{h}\mathrm{Cov}_{ij}(y\text{-}q)\right)$$

where h is the area of a cell. Thus, $\mathrm{E}[N_i]/h$ is the expected global density of morph i across all cells. We invoked the Eulerian form of Eq. 1.I.1 to express local densities and Eq. 1.I.2 to go from line 1 to 2 of Eq. 1.I.3. We assume that the distribution of individuals is stationary to the second order and isotropic (*65*), such that the distribution is fully described by global densities and $Cov_{ij}(y\text{-}q)$. Thus, we can move the focal cell y to the origin and rewrite $Cov_{ij}(y\text{-}q)$ as $Cov_{ij}(q)$. In the limit that the cell size h is infinitely small, the point global density of morph i is $X_i=\lim_{h\to o}N_i/h$ and $cov_{ij}=\lim_{h\to o}Cov_{ij}/h^2$. We obtain the continuous-time, continuous-space analog of Eq. 1.I.3 by dividing the equation by h:

(1.I.4)
$$\frac{dX_i}{X_i dt}=r_i+\sum_{j=1}^{S} a_{ij}\left(X_j+\frac{1}{X_i}\int_{\Omega}\phi_{uj}(q)cov_{ij}(q)dq\right)$$

The bracketed term in Eq. 1.I.4 is the continuous-space analog of local density as defined in Eq. 1.1, which is a combination of the first and second spatial moments (X_j and cov_{ij}). Eq. 1.3 in the main text is an abbreviation of Eq. 1.I.4. We did not assume that birth is associated with seed dispersal as was done for plant interactions in the original spatial moment derivation (*65*); rather, we assume that movement can take place at any time, which is realistic for organisms such as bacteria. Note that movement does not affect morph densities directly because it is simply a spatial redistribution of individuals, but it affects local densities through changing cov_{ij} (*95*). As well, cov_{ij} will

be a function of higher moments (densities of triplets and so on) through birth and death processes, so Eq. 1.I.4 and Eq. 1.3 do not constitute a closed set of equations. However, they do sufficiently establish local densities as the variables of interest in this chapter.

Chapter 2. The influence of spatial clustering on the evolution of cooperation

Edward W. Tekwa, Michel Loreau, Andrew Gonzalez

2.1. Prelude

Under the influence of community ecologists at McGill, I became increasingly convinced that the evolution of cooperation should be primarily interesting because of its potential effects on the population, in particular on demographic dynamics. In contrast, many evolutionary theories have concentrated on the change in gene frequency, or the change in the population's distribution of cooperative phenotypes due to selection (*96*); spatial ecology and demographic dynamics are traditionally reduced to effective population size (*22*), so that we can concentrate on the selection and drift of phenotypes in relative isolation. But the evolution of cooperative behaviour influences, and is influenced by, spatial and demographic dynamics. A spatial public-good model, based on first principles of individual behaviours with emergent evolutionary and demographic dynamics, would potentially lead to novel spatial patterns and effects, in comparison to previous models.

The initial idea for this chapter was to simulate the evolution of public good producers versus defectors in different habitat patchiness treatments, which shadows the experiments with *Pseudomonas aeruginosa*'s siderophore production in Chapter 3. To allow for fully emergent demographic dynamics, the conventional individual-based simulations on lattice or network (*23*, *26*, *30*, *33*) would not suffice. These models assume that each node can only be occupied by one individual. Thus, I settled on

dividing the habitat into a grid of squares, which led to a pixelated version of any geometric shape. Each square can contain any number of individuals, such that both local and global densities fully emerge from individual interactions and movement tendencies. Thus, this simulation space is a discrete approximation of continuous space. The first version included an explicit layer of a resource, with highly nonlinear interactions with the individuals. This generated the illustration of local densities and clustering coefficients in Chapter 1. However, we eventually found it too difficult to analyze, so we simplified the local dynamics, eliminated the resource, and reduced the number of habitat patchiness treatments, such that we could analytically derive eco-evolutionary changes in relations to clustering. This simplification proved crucial in clarifying a principle of public goods cooperation: that cooperation only reduces competition, which is one simple way through which realistic demographic dynamics emerge. The result is a formulation of cooperator-defector dynamics that is not much different from the classic Lotka-Volterra equations (*90*, *91*), but which allows for complex clustering patterns.

The concept of local densities was developed in the context of interpreting existing theories in Chapter 1, but is first functionalized here in Chapter 2, in terms of using it to discover new theoretical predictions, and to analyze data from individual-based simulations. The application of local densities to experimental data will have to wait until the appropriate experimental device is built (Chapter 3) and the relevant data is processed (Chapter 4), which turn out to confirm the major predictions from Chapter 2.

2.2. Abstract

Spatial clustering between individuals is known to promote the evolution of cooperative behaviours, such as the production of a public good that benefits the population at large. However, existing models often limit the feedback between evolutionary, spatial, and demographic dynamics, which limits understanding of the effects clustering can have on cooperation. We develop a spatial public-good model with cooperators and defectors, where cooperation reduces competition and leads to emergent demographic dynamics. Through clustering coefficients, we explore the partial effects of different aspects of cluster formation on cooperator frequency and population density. Both mathematical analysis and individual-based simulations show that, counterintuitively, cooperator clustering decreases cooperator frequency, but this is countered by the opposing effect of defector clustering. These effects occur because cooperator clustering develops differently than defector clustering, a decoupling that is not observed in demographically implicit models with weak selection. The model suggests that spatial effects may run counter to the conventional intuition, that clustering generally promotes cooperation, when behaviours impact demography.

Keywords: evolution of cooperation, spatial clustering, competition, demography, public good, kin competition

2.3. Introduction

Spatial clustering is widely known to promote the evolution of cooperation (*13*, *20–22*, *24*, *26*, *30*), which includes public good or common-resource production (*9*, *36*, *97*). These behaviours are among the most striking phenomena in nature, including bacterial siderophore production (*46*) and mound or nest construction (*98*). These are clearly different cooperative behaviours in terms of complexity, but the effects are essentially the same: individuals come together and confer benefits on each other. An important demographic consequence of such cooperation may be an increase in sustained population densities (*8*, *9*).

Currently, most evolutionary models on cooperation do not explicitly address demographic consequences, or changes in population density (*36*, *99*). Even in multilevel selection models where cooperation enhances group fitness, groups periodically compete for a fixed number of possible sites, such that the total population size remains externally constrained (*54*, *100*). Recent research has recognized that demographic dynamics can alter spatial dynamics and cooperative character evolution by introducing empty space into the habitat (*37*, *38*, *101*), but we still lack a simple and demographically realistic public-good cooperation model that is fully defined from first principles through individual behavior, without top-down demographic limits. Moreover, we need a model that allows us to study the direct effects of complex cluster formations on eco-evolutionary outcomes.

To address the gap in the literature, we analyse a simple public-good model involving cooperators and defectors. The principles are that all individuals compete locally, but cooperation alleviates local competition. Using clustering coefficients, a

normalized form of local densities (*33*, *35*, *60*), we derive the partial effects of cooperator, defector, and between-morph clustering on cooperator frequency and total population density (the eco-evolutionary outcomes). However, these derivations do not address how clustering patterns emerge. As a case study, we use individual-based spatial simulations to explore how individual movement rates and habitat patchiness – which are major drivers of spatial pattern formation (*102–104*)– affect cluster formation, and whether such clustering patterns affect cooperator frequency and population density as predicted.

Our major finding is an apparent paradox, that cooperator clustering acts to decrease both cooperator frequency and population density, which appears contrary to previous findings that cooperator clustering should favour cooperation. In individual-based simulations, we show that this paradox exists because cooperator clustering develops differently from defector clustering, a pattern that is not considered in demographically implicit models that assume weak selection. Eco-evolutionary dynamics are determined by the net effect of different clustering aspects, which emerge from individual movement rates, growth rates, and habitat features. Under specific conditions, the net effect of increased clustering can favour cooperation, recovering the result of traditional theories as only one possibility. Our spatial public-good model is an eco-evolutionary model of cooperation that fills a gap at the intersection of evolutionary biology, spatial ecology, and demography.

2.4. Spatial public-good model

We first define our model based on the principles of local competition and cooperation between individuals. Then, we provide an analytical description of its global dynamics, and derive through partial derivatives how different aspects of spatial clustering affect cooperator frequency (P^*) and total population density (X^*). These predictions form hypotheses that are tested with simulations in the next section.

2.4.1. Local interactions

Our model system consists of haploid cooperators that enhance the local carrying capacity (the number of individuals that coexist in a local area) – or the local density - at their own cost, and defectors that avoid the cost but exploit neighbouring cooperators. Cooperators thus contribute to a public good (*36*, *46*), which can increase local density, but whose evolution in a spatial and demographically explicit context remains unclear. Since cooperators and defectors can be phenotypically quite different, the following formulation does not assume weak selection. Symbol definitions are provided in Table 2.1.

Table 2.1. Symbol definitions.

Symbol	Definition	Symbol	Definition
a	benefit	X	total population density
k	competitive effect	x_i	morph i density at a location
r_i	intrinsic growth rate of morph i	x_{ij}	local density of j around i at a location
C_{ij}	clustering coefficient between i and j	X_i	global density of morph i
$\hat{C}_{ij}$	standardized clustering coefficient	X_{ij}	average local density of j around i
n_i	number of morph i individuals	z	cell location
P	cooperator frequency		

In a habitat divided into cells, the local dynamics of cooperator and defector densities (x_c, x_d) at cell z (without movement) can be written as:

$$dx_c(z)/dt = x_c(r_c + ax_{cc}(z) - kx_{c\cdot}(z))$$
$$dx_d(z)/dt = x_d(r_d + ax_{dc}(z) - kx_{d\cdot}(z)) \quad (2.1)$$

Cooperators and defectors grow at intrinsic rates r_c and r_d, respectively; the latter is assumed to be higher than the former, the difference (r_d-r_c) being the cost of cooperation. The growth rate of each individual decreases by k per neighbouring individual in its cell. In addition, its growth rate is supplemented by a per neighbouring cooperator. We assume linear interaction effects and $k>a$, such that the population is intrinsically limited. The local density of each neighbouring morph j, around an individual of morph i, is x_{ij}. The local density of all neighbours around morph i is $x_{i\cdot}$ (=x_{ii}+x_{ij}). Note that the within-morph density x_{ii} excludes self-interaction (*67*, *105*), such that phenotypic effects influencing the self are entirely captured by the intrinsic growth rate r.

Existing models that address demography and cooperation employ nonlinear interaction effects (*70*, *71*) (i.e. an Allee effect), which are appropriate to explore extinction but not population density – they only change population persistence probabilities at low densities, and do not change the upper population carrying capacity. On the other hand, through linear additivity, we are able to synthesize traditional cooperation (a) (*76*) and competition (k) (*90*, *91*) in a simple manner that allows public-good cooperation to influence population density at the same time.

2.4.2. Analytical predictions

The global dynamics of a system defined locally by Eq. 2.1 can be written in a similar form, but with local densities being replaced by the average local densities across the system following the spatial moment literature at the limit of infinitely small cells (*33*, *65*, *95*). The average local densities are X_{ij} = E[$x_{ij}(z)$] over all cells z. An average local density X_{ij} differs from its global density counterpart X_j - the average number of morph j individuals per cell across the entire habitat - when the system is not well mixed. For simplicity we assume that the spatial distribution of individuals is second-order stationary and isotropic, such that $x_{ij}(z)$ is the same everywhere (*65*).

We normalize average local densities by dividing X_{ij} by the global density X_j. We call the resulting metrics clustering coefficients C_{ij}, which lead to the expressions for the dynamics of global cooperator and defector densities (X_c, X_d) (Eq. 2.2, see 2.8.1 Appendix A). Eq. 2.2 is a simple modification of the spatial Lotka-Volterra model (*65*, *90*, *91*).

(2.2)
$$dX_c / dt = X_c(r_c + (a-k)C_{cc}X_c - kC_{cd}X_d)$$
$$dX_d / dt = X_d(r_d + (a-k)C_{cd}X_c - kC_{dd}X_d)$$

Clustering coefficients are theoretically desirable for several reasons. We note that C_{cd}=C_{dc} due to conservation of the number of between-morph pairs (X_cX_{cd}= X_dX_{dc}, see 2.8.1 Appendix A). Thus, we can analyze the correlations between local spatial patterns and eco-evolutionary outcomes with only three clustering coefficients (C_{cc}, C_{cd}, C_{dd}). The clustering coefficient C_{ij} is easy to interpret: when it is greater than one, there is higher than random clustering between morphs i and j; when it is less than one, there is segregation. Local densities increase with global densities even in the absence of spatial patterns due to an increase in overall number of neighbours; clustering

coefficients are normalized local densities that capture clustering levels after removing this trivial correlation.

Clustering coefficients are in reality dynamic variables. However, for the following equilibrium analyses, we will treat them as constants measured at their equilibria C^*_{ij} (with * denoting equilibrium states for all variables). This is an important limitation that prevents a full exploration of the model's dynamics but is done in the spirit of similar model assumptions, such as constant population size in many models that can explore the effect of population size on the evolution of cooperation (*23*, *26*). Solving Eq. 2.2, we obtain the equilibrium cooperator and defector densities:

$$X_c^* = \frac{r_c C_{dd}^* - r_d C_{cd}^*}{(k-a)(C_{cc}^* C_{dd}^* - C_{cd}^{*2})}$$
$$X_d^* = \frac{r_d C_{cc}^* - r_c C_{cd}^*}{k(C_{cc}^* C_{dd}^* - C_{cd}^{*2})} \tag{2.3}$$

These densities are valid under the following conditions for coexistence (obtained by requiring numerators in Eq. 2.3 to be positive), with the left inequality ensuring cooperator persistence, and the right ensuring defector persistence:

$$\frac{C_{dd}^*}{C_{cd}^*} > \frac{r_d}{r_c} > \frac{C_{cd}^*}{C_{cc}^*} \tag{2.4}$$

Based on Eq. 2.3, we obtain partial derivatives for how clustering coefficients are related to cooperator frequency (P^*) and total population density ($X^*=X^*_c + X^*_d$), assuming coexistence (Eq. 2.5). The partial derivatives indicate the effects of clustering aspects when they are externally perturbed; they do not imply causation, however, because clustering dynamics are really coupled to evolutionary and demographic changes.

$$\frac{\partial P^*}{\partial C^*_{cc}} = -\frac{k(k-a)r_d(r_c C^*_{dd} - r_d C^*_{cd})}{((k-a)r_d C^*_{cc} + kr_c C^*_{dd} - ((k-a)r_c + kr_d)C^*_{cd})^2}$$

$$\frac{\partial P^*}{\partial C^*_{dd}} = \frac{k(k-a)r_c(r_d C^*_{cc} - r_c C^*_{cd})}{((k-a)r_d C^*_{cc} + kr_c C^*_{dd} - ((k-a)r_c + kr_d)C^*_{cd})^2}$$

$$\frac{\partial P^*}{\partial C^*_{cd}} = -\frac{k(k-a)(r_d C^*_{cc} - r_c C^*_{dd})}{((k-a)r_d C^*_{cc} + kr_c C^*_{dd} - ((k-a)r_c + kr_d)C^*_{cd})^2}$$

$$\frac{\partial X^*}{\partial C^*_{cc}} = -\frac{(kC^*_{dd} - (k-a)C^*_{cd})(r_c C^*_{dd} - r_d C^*_{cd})}{k(k-a)(C^*_{cc}C^*_{dd} - C^{*2}_{cd})^2}$$

$$\frac{\partial X^*}{\partial C^*_{dd}} = -\frac{((k-a)C^*_{cc} - kC^*_{cd})(r_d C^*_{cc} - r_c C^*_{cd})}{k(k-a)(C^*_{cc}C^*_{dd} - C^{*2}_{cd})^2}$$

$$\frac{\partial X^*}{\partial C^*_{cd}} = \frac{2C^*_{cd}((k-a)r_d C^*_{cc} + kr_c C^*_{dd}) - (C^*_{cc}C^*_{dd} + C^{*2}_{cd})((k-a)r_c + kr_d)}{k(k-a)(C^*_{cc}C^*_{dd} - C^{*2}_{cd})^2} \quad (2.5)$$

All partial derivative denominators are positive, so clustering effect directions are determined solely by the numerators. We see that clustering effects are nonlinear, with effect directions that can change depending on the current clustering levels.

Assuming that Ineq. 2.4 holds, we obtain the following clustering effect directions:

$$\begin{aligned}
&\partial P^* / \partial C^*_{cc} < 0 \\
&\partial P^* / \partial C^*_{dd} > 0 \\
&\partial P^* / \partial C^*_{cd} < 0 \quad \textit{if} \quad C^*_{cc} / C^*_{dd} > r_c / r_d \\
&\partial X^* / \partial C^*_{cc} < 0 \\
&\partial X^* / \partial C^*_{dd} < 0 \quad \textit{if} \quad C^*_{cc} / C^*_{cd} > k / (k-a) \\
&\partial X^* / \partial C^*_{cd} > 0 \quad \textit{if} \quad 2C^*_{cd}((k-a)r_d C^*_{cc} + kr_c C^*_{dd}) \\
&\qquad\qquad > (C^*_{cc}C^*_{dd} + C^{*2}_{cd})((k-a)r_c + kr_d)
\end{aligned} \quad (2.6)$$

The Ineq. 2.6 leads to the following three predictions:

1. Prediction I on population density: within-morph clustering ($\partial X^*/\partial C^*_{cc}$ and $\partial X^*/\partial C^*_{dd}$) likely decrease population density. For $\partial X^*/\partial C^*_{dd}<0$, it is sufficient that $C^*_{cc} > C^*_{cd}$, which in a saturated habitat is achieved even under a random binomial

distribution (*21*). As we will see in the simulations, in unsaturated habitats where there is no attraction mechanisms between morphs, we also find that $C^*_{cc} > C^*_{cd}$. This prediction complements results from spatial ecology (without cooperation) (*103*, *106*) in that clustering can be understood as a lack of dispersal, which is detrimental to population density and raises global extinction risk. On the other hand, the effect of between-morph clustering on population density ($\partial X^*/\partial C^*_{cd}$) depends on exact parameter values and the clustering coefficients themselves, so our model does not make a clear-cut prediction on this issue.

2. Prediction II on cooperator frequency: cooperator clustering ($\partial P^*/\partial C^*_{cc}$) and between-morph ($\partial P^*/\partial C^*_{cd}$) clustering likely decrease cooperator frequency, while defector clustering ($\partial P^*/\partial C^*_{dd}$) increases cooperator frequency. These results are surprising at first sight, since clustering has been implicated to favour cooperation in previous models that assume constant population size (*24*, *25*). However, as $\partial P^*/\partial C^*_{cc}$ holds all other clustering aspects constant, the partial derivative is understandably negative to reflect the fact that cooperators are ultimately net competitors among themselves, and their increased clustering without a proportional increase in defector clustering would put themselves at a comparative disadvantage.

3. Prediction III on the net effect of within-morph clustering: cooperators can be better adapted to within-morph clustering than defectors. This can be quantified as a positive net effect of within-morph clustering on cooperator frequency:

$$\frac{\partial P^*}{\partial C^*_{cc}} + \frac{\partial P^*}{\partial C^*_{dd}} = \frac{k(k-a)(r_c r_d (C^*_{cc} - C^*_{dd}) + (r_d^2 - r_c^2) C^*_{cd})}{((k-a) r_d C^*_{cc} + k r_c C^*_{dd} - ((k-a) r_c + k r_d) C^*_{cd})^2} > 0 \tag{2.7}$$

When $C^*_{cc} \geq C^*_{dd}$, increased within-morph clustering favours cooperators. In addition to offering a conditional prediction, Ineq. 2.7 explains how the paradoxical result of

prediction II can be reconciled with previous theoretical findings. When $C^*_{cc}=C^*_{dd}$, which necessarily holds under the common habitat saturation and weak selection assumptions (*83*) (see 2.8.2 Appendix B), increased within-morph clustering (holding between-morph clustering constant) does favour cooperation, in line with traditional theories.

So far, we have discussed clustering effects, but have not investigated how clustering emerges. In the next section, we test our three predictions through the simulation of a spatially explicit public good system, where clustering emerges from individual movement and habitat patchiness.

2.5. Individual-based simulations

To implement the simulations, for each cell location z we discretized Eq. 2.1 into 100 updates per observation time T, such that local dynamics are similar to the continuous-time analytical predictions. As a case study, we set r_d=0.1, r_d-r_c=0.01 (cost), a=0.05 (benefit), and k=0.1 (competition), each being an expected change in density per observation time T in each cell of the habitat. Growth was implemented as the sum of binomial random birth and death events for all individuals at each update. Cost, benefit, and competition affected the birth rate, and the death rate was set at 0.1. Variations in these growth parameters do not change the predicted clustering effects that we test. Thus, in our simulations we only studied variations in spatial parameters that directly affect cluster formation.

The cost-free local movement rate was set at 0.2, 0.3 or 0.6 crossings between cells per observation time. The movement direction was random - unless the chosen direction was a boundary, in which case the individual stayed. A schematic of the process can be found in 2.8.3 Appendix C. For each of the 3 movement rate treatments, 40 simulation replicates were run in a continuous habitat and a patchy habitat of similar sizes (1296 and 1481 cells). The habitats were obtained from pixelating the icons in the Fig. 2.2 x-axis on a cell grid. The continuous and patchy habitats represent patchiness treatments. We expect that a decrease in movement rate and an increase in patchiness would increase within-morph clustering and decrease between-morph clustering.

Our simulations differ from birth-death processes of many spatial network games (*23*) because here each cell's occupancy is not limited to one or zero individual, and individuals can move at any time except at birth (whereas most game updates only allow

movement at birth). Effectively, we model spatial competition explicitly through *k* and the movement rate, rather than through a limited number of update rules that are known to implicitly add spatial competition at certain scales (*81*).

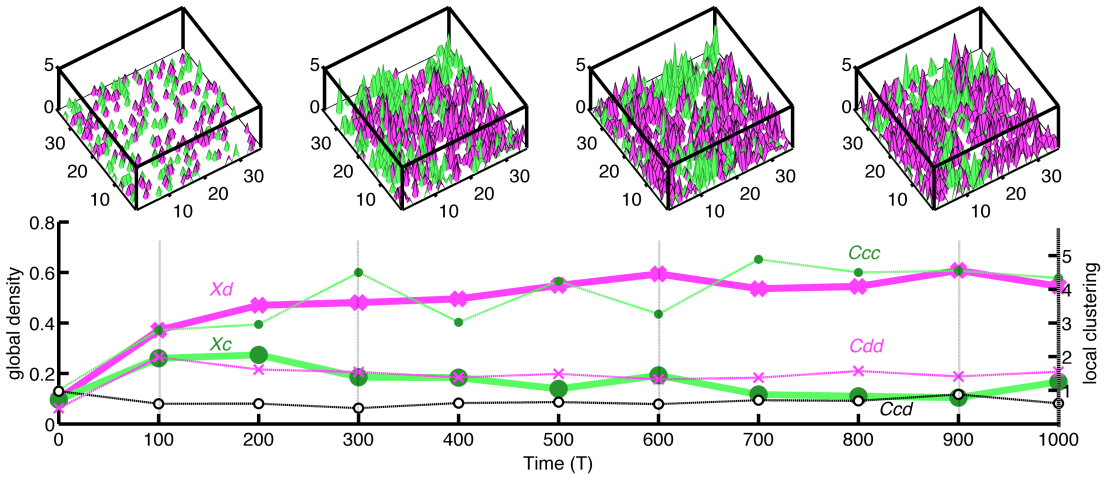

Figure 2.1. Four snapshots from a simulation in a continuous habitat with a movement rate of 0.3. Green (light) indicates locations where cooperator clusters dominate, and magenta (dark) indicates where defector clusters dominate. Global densities of cooperators (X_c) and defectors (X_d) are plotted as thick lines (scaled to the left axis), while local clustering coefficients (cooperator clustering C_{cc}, between-morph clustering C_{cd}, and defector clustering C_{dd}) are plotted as thin lines (scaled to the right axis).

In a representative simulation replicate, we observed the coexistence of cooperators and defectors, and fluctuations in clustering pattern (Fig. 2.1). Both global densities and clustering coefficients approached equilibria by around T=600. Since we will be comparing simulation outcomes with theoretical equilibrium predictions, in the follow analyses, we used global densities and clustering coefficients obtained from the averages of T600 to 1000 in the simulations. The within-morph clustering coefficients were bias-corrected ($C^*_{ii}=(n_i/(n_i-1))X^*_{ii}/X^*_i$ where n_i is the absolute number of morph *i* individuals and -1 corrects for the fact that local densities do not include self-interaction).

We first explore how movement rate and habitat structure affect clustering outcomes below. We then evaluate whether clustering effects in the simulations match the analytical predictions.

2.5.1. Pattern formation

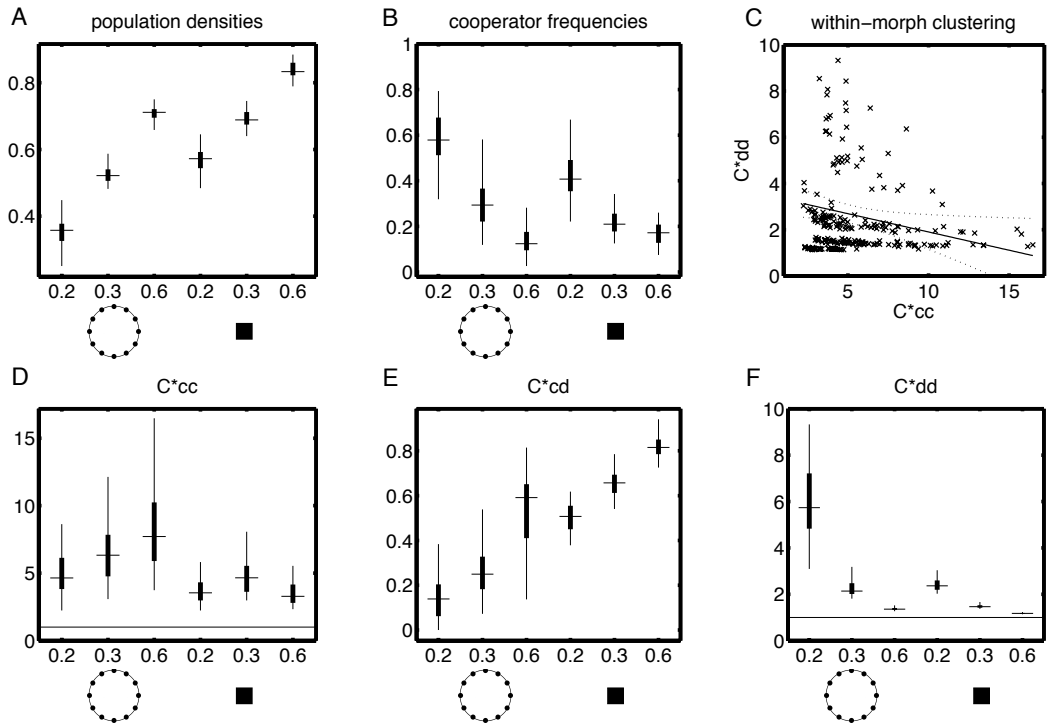

Figure 2.2. *A, B, D-F:* Boxplots of simulation outcomes for 40 replicates in each of 6 treatments, averaged over time T600-1000. Population densities refer to the global sum of cooperators and defectors. The treatments included three movement rates in two habitats (patchy and continuous, cartoons in x-axis). The boxes occupy the 25% and 75% percentiles, and the whiskers span all data excluding outliers. *C*: The correlation between cooperator clustering and defector clustering was negative (regression slope=-0.16, S.E.=0.072, $t_{2,236}$=-2.21, p=0.028, R^2=0.020).

In surveying cooperator frequency P^* and total population density X^*, we found substantial variations across movement and habitat treatments (Fig. 2.2A, B). Concomitantly, we found substantial variation in the clustering coefficients (Fig. 2.2D-F), and according to analysis of variance (ANOVA), movement rate, habitat type, and their interactions were important drivers of these coefficients (Table 2.1). The patchy

habitat increased C^*_{cc} and C^*_{dd}, and decreased C^*_{cd} compared with the continuous habitat (Table 2.2). Increased movement rates significantly increased C^*_{cc} in the patchy habitat but not in the continuous habitat, increased C^*_{cd} in both the patchy and continuous habitats, and decreased C^*_{dd} (Table 2.3). These results are for the most part intuitive. With patchiness, dispersal is hampered, leading to higher within-morph clustering and lower between-morph clustering. At high movement rates, all types of clustering in the absence of selection should decrease. The positive relationship between movement rate and C^*_{cc} in the patchy habitat was unexpected. There, the increased exploitation by defectors with high movement rates appeared to competitively exclude lone cooperators, leaving only denser cooperator clusters viable and resulting in high C^*_{cc} values.

C^*_{cc} and C^*_{dd} developed differently (Fig. 2.2D, F), a fact that allows us to tease apart their partial effects in the next section. In fact, C^*_{cc} and C^*_{dd} were weakly negatively correlated (Fig. 2.2C). This weak correlation is surprising, since in weak selection models without demographic dynamics, $C^*_{cc}=C^*_{dd}$ (they are positively correlated, eg. (*21*, *107*)). Thus, our model shows that one cannot generally talk about clustering without further specifications.

2.5.2. Clustering effects

Using multivariate linear regressions, we determined how clustering coefficients (the predictors) affected cooperator frequency and population density in terms of effect signs. Clustering coefficients $\hat{C}_{ij}$ were standardized (C^*_{ij} divided by their standard deviations) for effect comparisons. We found that clustering coefficients explained

much of the variation in cooperator frequency and population density (R^2=0.91, 0.88, Fig. 2.3), and were the most parsimonious predictors when compared to movement rates and habitat patchiness according to Akaike Information Criterion (AIC) (*108*) (see caption in Fig. 2.3). Thus, we can be confident that clustering coefficients captured the relevant spatial features, including both stochastic and deterministic features, in our eco-evolutionary system.

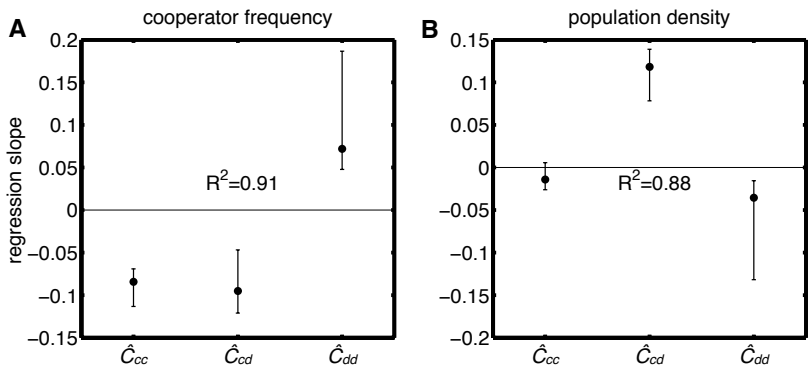

Figure 2.3. Multivariate linear regression slopes of standardized clustering coefficients $\hat{C}_{ij}$ on cooperator frequency and population density. 95% confidence intervals for the overall slope estimates were obtained from bootstrapped regressions (2000x). R^2 values are fractions of variances in cooperator frequency (A) and population density (B) explained by the predictors. The clustering model had an AIC value of -1193. In comparison, a model with habitat type and movement rate as predictors produced R^2 values of 0.73 for cooperator frequencies, 0.95 for population densities, and an AIC value of -1106. From bootstrapping, the net effect of $\hat{C}_{cc}$ and $\hat{C}_{dd}$ on cooperator frequencies was positive for all cases (p<0.0005) except when the movement rate was 0.2 in the patchy habitat, where the net effect was negative (p=0.0770).

Within-morph clustering ($\hat{C}_{cc}$ and $\hat{C}_{dd}$) decreased population density (Fig. 2.3B), although only the $\hat{C}_{dd}$ effect was significantly negative. These results agree with the analytical prediction I. Cooperator and between-morph clustering ($\hat{C}_{cc}$ and $\hat{C}_{cd}$) decreased cooperator frequency, while defector clustering $\hat{C}_{dd}$ increased cooperator frequency (Fig. 2.3A), in agreement with the analytical prediction II. Interestingly, Fig. 2.2A, D, and E appear to indicate that cooperator clustering may be positively correlated with population density, while defector clustering may be negatively correlated with

population density across movement treatments, contrary to the regression analyses in Fig. 2.3A. The discrepancy may be attributed to the fact that within-movement treatment clustering variations appear to be much more important than between-movement treatment clustering variations.

The net effect of cooperator and defector clustering on cooperator frequency was positive for the cases of m=0.3 (patchy habitat only) and 0.6 ($p<0.0005$) where $C^*_{cc} \geq C^*_{dd}$. However, the net effect was marginally negative for m=0.2 (continuous habitat, $p=0.0770$) where C^*_{cc} were smaller than C^*_{dd} (Fig. 2.2 and 2.3). These results confirm the analytical prediction III, which identifies the correct clustering conditions where cooperators should be better adapted to increased within-morph clustering than defectors.

2.6. Discussion

We showed analytically and through individual-based simulations that cooperator clustering is directly detrimental to the global cooperator frequency, but the net effect of within-morph clustering can be positive. Although the result seems paradoxical in the context of the existing literature, they can be reconciled. We will discuss the features of our model, and how the results compare with previous findings.

The spatial public-good model differs from others because cooperator clustering is decoupled from defector clustering due to movement and habitat patchiness (Fig. 2.2C-F). In traditional weak selection models without demographic dynamics (*21*, *26*, *36*, *83*), such a decoupling is not observed (i.e. $C^*_{cc}=C^*_{dd}$ in these models). In contrast, our public-good model is built from the first principles of individual cooperation and competition, which lead to fully emergent demographic dynamics without top-down population limits, and consequently to complex cluster formations. We quantified cooperator, defector, and between-morph clustering through clustering coefficients (Eq. 2.2), which are more precise than the traditional compound metrics of relatedness (*13*), structure coefficient (*24*), and inbreeding coefficient (F_{ST}) (*32*) where different clustering aspects are coupled through spatially limiting assumptions such as externally imposed population density limits. The quantification of different clustering types led to the paradoxical result, that cooperator clustering decreases cooperator frequency.

Our analyses on clustering effects highlighted a paradox, but also identified a solution to it, which nicely relates our results to traditional theories. The paradox was analytically derived in predictions I and II through the partial derivatives $\partial X^*/\partial C^*_{cc}$ and $\partial P^*/\partial C^*_{cc}$, which are the direct effects of cooperator clustering on total population

density and cooperator frequency. These partial derivatives are always negative in our model regardless of parameter values (Eq. 2.6), facts that were corroborated by the individual-based simulation results (Fig. 2.3). We can interpret these results by recalling that in the public-good model, the per-capita competitive effect (k) is always greater than the cooperative effect (a) (Eq. 2.1); coupled with the fact that the partial derivatives hold all other clustering aspects constant, it makes sense that cooperator clustering on its own decreases both population density and cooperator frequency. The partial derivative $\partial P^*/\partial C^*_{cc}$ can be considered a novel quantification of kin competition (*55*, *109*, *110*). In contrast, when we consider cooperator and defector clustering in concert, we found that the net within-morph clustering effect can be positive for cooperator frequency (Ineq. 2.7) given the condition $C^*_{cc} \geq C^*_{dd}$ (prediction III). Individual-based simulations confirmed this conditional result (Fig. 2.3). We also note that the condition $C^*_{cc} \geq C^*_{dd}$ is satisfied by the assumptions of no demographic dynamics and weak selection in traditional theories, where $C^*_{cc} = C^*_{dd}$. Thus, we have identified the specific conditions that allow clustering to favour cooperation, which is the main finding in traditional theories (*13*, *20–22*, *24*, *26*, *30*).

Not only did our results clarify that within-morph clustering only favours cooperation under certain conditions, our individual based simulations revealed that such scenarios might not even occur due to complex spatial dynamics. In theory, increased within-morph clustering may increase cooperator frequency; in reality, within-morph clustering is not cohesive, in that cooperator and defector clustering do not change in unison. Across our simulation movement and patchiness treatments, cooperator and defector clustering break cohesion by exhibiting a negative correlation (Fig. 2.2C). This highlights the importance of modeling and measuring different

clustering aspects, and incorporating demographic dynamics in the evolution of cooperation when there is a potentially large phenotypic difference between morphs.

Admittedly, short of deriving clustering from first principles of movement and growth (which has proven challenging even in simpler systems (*23*, *24*, *26*, *65*)), we lack a thorough understanding of how different clustering aspects develop in concert. Nevertheless, this shortcoming did not prevent us from taking some useful steps towards understanding clustering effects. The measurements and analyses of clustering in different morphs can be applied to empirical research, especially with social microbes (*111*), whose phenotypes can be reliably tracked in space over generations in microfluidic experimental devices (*112*). By taking advantage of haploid inheritance and isolating morph differences to a particular spatial public good production, microbial experiments can reveal how clustering patterns emerge and affect eco-evolutionary dynamics. Similar experiments may also be applied to humans in a game theoretic context (*113*, *114*), where clustering coefficients can emerge in a social network space to reveal effects on individual choices and total good contributions. We believe that the spatial public-good model, with its foundation in demography, may be a productive springboard for future research on the evolution of cooperation.

2.7. Tables

Table 2.1. ANOVA statistics for the effects of habitat patchiness, movement rate, and their interaction on clustering coefficients.

predictor	response	statistics	*p*
habitat	C_{cc}	$F_{1,234}$=74.69	8.765e-16
movement	C_{cc}	$F_{1,234}$=8.121	0.0048
habitat*movement	C_{cc}	$F_{1,234}$=25.12	1.065e-6
habitat	C_{cd}	$F_{1,234}$=546.77	3.686e-63
movement	C_{cd}	$F_{1,234}$=397.88	2.190e-52
habitat*movement	C_{cd}	$F_{1,234}$=8.14	0.0047
habitat	C_{dd}	$F_{1,236}$=29.60	1.327e-7
movement	C_{dd}	$F_{1,236}$=50.98	1.148e-11
habitat*movement	C_{dd}	$F_{1,236}$=19.27	1.717e-5

Table 2.2. T-tests for the mean differences between clustering coefficient values in patchy versus continuous habitats.

predictor	response	statistics	*p*
patchy vs. continuous	C_{cc}	difference=0.930, *SE*=0.05748, t_{236}=8.09	3.118e-14
patchy vs. continuous	C_{cd}	*difference*=-1.362, *SE*=0.04748, t_{236}=-14.34	5.753e-34
patchy vs. continuous	C_{dd}	*difference*=0.5926, *SE*=0.06177, t_{238}=4.80	2.853e-6

Table 2.3. Linear regression statistics for the effects of movement rates in different habitats on clustering coefficients.

predictor	response	statistics	*p*
movement (patchy)	C_{cc}	*slope*=2.534, *SE*=0.5437, t_{116}=4.66	8.492e-6
movement (continuous)	C_{cc}	*slope*=-0.6639, *SE*=0.3403, t_{118}=-1.951	0.05345
movement (patchy)	C_{cd}	*slope*=3.891, *SE*=0.3129, t_{116}=12.43	4.479e-23
movement (continuous)	C_{cd}	*slope*=2.919, *SE*=0.1414, t_{118}=20.64	5.728e-41
movement (patchy)	C_{dd}	*slope*=-3.694, *SE*=0.6371, t_{118}=-5.797	5.741e-8
movement (continuous)	C_{dd}	*slope*=-0.8812, *SE*=0.06789, t_{118}=-12.98	1.772e-24

2.8. Appendices

2.8.1. Appendix A. Derivation of public-good model

The local growth dynamics of cooperator (x_c) and defector densities (x_d) in cell z are:

$$dx_c(z)/dt = x_c(r_c + ax_{cc}(z) - kx_{c\cdot}(z))$$
$$dx_d(z)/dt = x_d(r_d + ax_{dc}(z) - kx_{d\cdot}(z)) \quad (2.A.1)$$

In Eq. 2.A.1, individuals interact with all other cooperators (x_{ic}) and compete with all other neighbours ($x_{i\cdot}=x_{ii}+x_{ij}$). To move from a description of local dynamics to global dynamics in space, we can think of both cases as consequences of the same individual behavioral parameters (r, a, k), but with the individual now experiencing not all other individuals, but the neighbours in an interaction cell on average. We further assume second-order spatial stationarity and anisotropy, such that we can replace x_{ij}, the local density of j around i at cell z, with X_{ij}, the average local density of j around i across all cells:

$$dX_c/dt = X_c(r_c + aX_{cc} - kX_{c\cdot})$$
$$dX_d/dt = X_d(r_d + aX_{dc} - kX_{d\cdot}) \quad (2.A.2)$$

Using the fact that $X_{i\cdot}=X_{ii}+X_{ij}$, we can rearrange terms to obtain:

$$dX_c/dt = X_c(r_c + (a-k)X_{cc} - kX_{cd}) \quad (2.A.3)$$
$$dX_d/dt = X_d(r_d + (a-k)X_{dc} - kX_{dd})$$

Finally, we define clustering coefficients $C_{ij}=X_{ij}/X_j$. Note that $X_{ij}X_i=X_{ji}X_j$, because the average numbers of ij pairs from either the i or j perspective is the same. By substitution, $C_{ij}X_jX_j=C_{ji}X_iX_j$, thus $C_{ij}=C_{ji}$. Substituting in C_{ii} and C_{ij}, Eq. 2.A.3 becomes:

$$dX_c/dt = X_c(r_c + (a-k)C_{cc}X_c - kC_{cd}X_d) \quad (2.A.4)$$
$$dX_d/dt = X_d(r_d + (a-k)C_{cd}X_c - kC_{dd}X_d)$$

2.8.2. Appendix B. Clustering in saturated habitats

In saturated habitats, there is a constant total population density X. Thus, all individuals experience the same total local density, which is also X

(2.B.1) $$X_{cc} + X_{cd} = X_{dc} + X_{dd} = X$$

With weak selection (when two morphs are phenotypically very close), we expect that the cooperator frequency is ½. Thus, $X_{cd} = X_{dc}$ (since $X_c X_{cd} = X_d X_{dc}$ by conservation of total number of intramorph interactions, and $X_c = X_d$). This leads to $X_{cc} = X_{dd}$, and $C_{cc} = C_{dd}$.

2.8.3. Appendix C. Model discretization

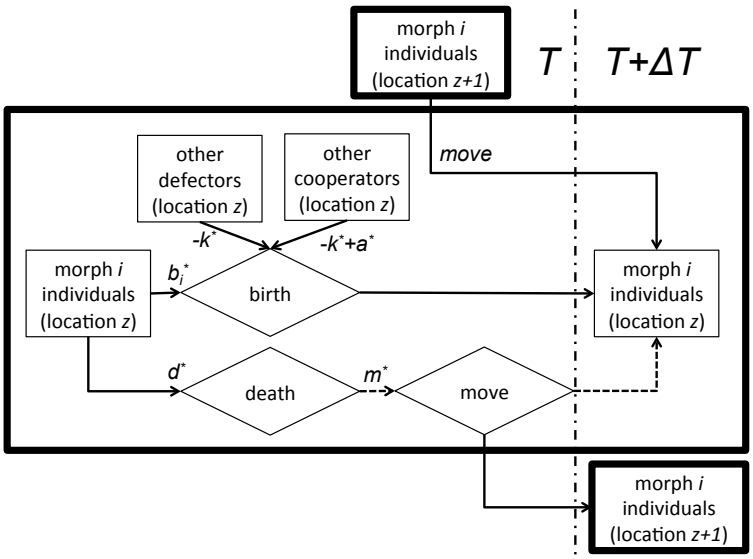

Figure 2.C.1. Simulation process chart for each location *z* in a habitat. Thick boxes indicate distinct locations (*z*+1 is any neighbouring location of *z*). Thin boxes are state variables, and diamonds are events. Connectors flowing out are modifiers to the rates (binomial probabilities) that the events they point to occur. Rates are subscripted * to indicate that they are 1/100 of the model parameters as part of the discretization procedure. Solid connectors out of events indicate that the process continues if the events occured, whereas dashed connectors indicate the process continues if the events did not occur. Each update uses state variables from time *T* to project their values at *T*+*ΔT*.

The simulation model is a discretization of the local interaction model of Eq. 2.2. At each time step, cooperation and competition from neighbours in a cell affects birth probabilities, while death and movement events occur at constant probabilities according to model parameters. The simulation process is illustrated in Fig. 2.C.1.

Chapter 3. Patchiness in a microhabitat chip affects evolutionary dynamics of bacterial cooperation

Edward W. Tekwa, Dao Nguyen, David Juncker, Michel Loreau, Andrew Gonzalez

Lab on a Chip 15 (2015) 3723-3729

3.1. Prelude

Andy, Michel and I first envisioned a microfluidic device that would allow fragmentation experiments on community assembly. I was on board because my engineering experience prepared me to build one. Naturally, I co-opted the device to study the evolution of cooperation. The objective is to study the effect of habitat edge-to-area ratio, or patchiness in short (*43*), on the evolution of cooperation. These patchiness treatments correspond to those tested in the simulations of Chapter 2.

Microbes are excellent experimental organisms because of simple haploid inheritance and fast generation time (*115*). They also comprise the majority of life on Earth (*116*), and exhibit primitive cooperative characters (*117*) that are on the verge of major evolutionary transitions (*2*). In addition, microbes are medically relevant for humans (*118*). We chose the bacteria *Pseudomonas aeruginosa* for our experiment, following recent works on cooperation (*46*, *119*), because this opportunistic pathogen undergoes within-host evolution in naturally patchy environments. In the patchy respiratory tract of cystic fibrosis patients, *P. aeruginosa* often mutates into loss-of-function defectors, in terms of producing a variety of public goods (*44*, *120*).

A naturalist strives to observe her study organisms in their varied habitats. While I couldn't directly observe *P. aeruginosa* as a contemporary cell in their natural habitats, I spent many hours staring at them under the microscope, as a photojournalist would in a safari. The rates at which the bacteria move and divide are astounding, and depending on the environment, one observes complex self-organized patterns. For example, when I inoculated *P. aeruginosa* under agar, the bacteria employed their type IV pili (*121*) and twitched into new territories following the leads of a few leaders (Figure 3). But my actual experimental conditions are more aqueous, where the bacteria employ flagella for swimming instead. There, the bacteria exhibit more dispersion, but still self-organize into non-trivial patterns in response to spatial constraints and as functions of movement and growth.

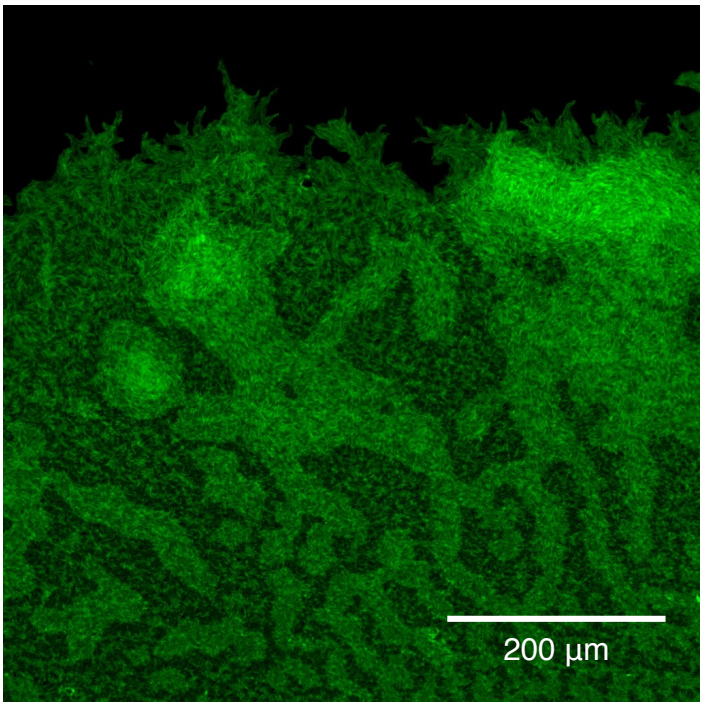

Figure 3. *Pseudomonas aeruginosa* (PAO1 pvdA mutants expressing green fluorescent protein) 20 hours after stab inoculation into the bottom of a 1% agar with a 20% succinate minimal media (*122*).

Pertinent to the subject of cooperation is the bigger question, why are bacteria still unicellular? There seems to be a variety of reasons, ranging from high evolutionary rate (*123*), adaptation to diverse habitats (*116*), and chance (*124*). The most compelling reason to me is that bacteria have retained an extraordinary ability to disperse (*125*), such that in spite of living much of their lives in aggregates (*126*), they do not, over long time frames, retain the spatial structure necessary for the evolution of elaborate cooperation. None of these explanations are ultimate, of course, and perhaps there isn't one. Sadly, my research does not directly address such long-term evolutionary factors – and what can one expect in experiments that last 18 hours? Such a short time frame is relevant, however, because loss-of-function defector mutants are frequent and recurrent threats to the maintenance of cooperation. In this respect, the current chapter is important because it explores a spatial factor that may contribute to the coexistence of cooperators and defectors (*127*), which then bides time for longer evolutionary processes, such as drift and mutation, to construct more elaborate cooperative traits. The experiment also generates clustering data, which is left for further analyses in Chapter 4.

3.2. Abstract

Localized interactions are predicted to favour the evolution of cooperation amongst individuals within a population. One important factor that can localize interactions is habitat patchiness. We hypothesize that habitats with greater patchiness (greater edge-to-area ratio) can facilitate the maintenance of cooperation. This outcome is believed to be particularly relevant in pathogenic microbes that can inhabit patchy habitats such as the human respiratory tract. To test this hypothesis in a simple but spatially controlled setting, we designed a transparent microhabitat device (MHD) with multiple patchiness treatments at the 100-micron scale. The MHD is a closed system that sustains bacterial replication and survival for up to 18 hours, and allows spatial patterns and eco-evolutionary dynamics to be observed undisturbed. Using the opportunistic pathogen *Pseudomonas aeruginosa*, we tracked the growth of wild-type cooperators, which produce the public good pyoverdin, in competition with mutant defectors or cheaters that use, but do not produce, pyoverdin. We found that while defectors on average outnumbered cooperators in all habitats, habitat patchiness significantly alleviated the ecological pressure against cooperation due to defection, leading to coexistence. Our results confirmed that habitat-level spatial heterogeneity can be important for cooperation. The MHD enables novel experiments, allows multiple parameters to be precisely varied and studied simultaneously, and will help uncover dynamical features of spatial ecology and the evolution of pathogens.

Keywords: evolution of cooperation, habitat patchiness, *Pseudomonas aeruginosa*, public good, microfluidic device, pathogen, coexistence

3.3. Introduction

The evolution of cooperation has driven the rise of biological complexity (*2*, *13*). But, because cooperation is costly, it is not necessarily evolutionarily viable unless the benefit of cooperation tends to be directed toward cooperators. The non-uniform spatial distribution of individuals is one of the most important factors favouring the evolution of cooperation (*21*, *22*, *24–26*, *30*, *128*, *129*). As individuals become more clustered, the benefit of cooperation can be preferentially bestowed on cooperators, making cooperation viable, either in the traditional evolutionary sense — the frequency of cooperators is greater than for defectors (*96*)— or in an ecological sense —localized interactions are stabilizing and lead to coexistence (*65*, *127*, *130*).

Spatial patchiness, or the ratio of edge-to-area (*43*), characterizes the habitats of most organisms (*131*), including bacteria (*132*). It appears that patchiness can facilitate cooperation in bacteria (*133*), likely because interactions become localized. Common bacteria such as *Pseudomonas aeruginosa* are opportunistic pathogens that live in the soil (*134*) and water (*135*), and can colonize various parts of the patchy human respiratory tract (*29*). The wild-type bacteria are cooperators that produce the siderophore pyoverdin, a diffusible extracellular iron-chelator responsible for bacterial iron uptake and growth (*42*) that is a form of public good. The production of a public good (*8*, *9*), by definition, implies an individual behaviour that benefits the public or the wider population, so cooperation can have an important ecological effect. Interestingly, loss-of-function mutants, or defectors, often arise in the human host environment over time (*44*, *45*, *120*). Thus, the evolutionary race between cooperators and defectors in patchy habitats is an important case for both general

eco-evolutionary theory (*40*, *46*, *133*, *136*) and the study of infectious diseases (*41*, *118*).

The traditional approach of emulating habitat structure and localized interaction has been through serial transfers of liquid subpopulations (*46*, *119*). This approach imposed cyclical bottlenecks on population size (*137*, *138*) during transfers, and did not allow populations to form natural aggregates, since growth occurred in a relatively large-volume of well-mixed liquid. Larger beaker (*139*) and flow cell experiments (*126*) allowed for endogenous spatial pattern formation, but at much larger spatial scales where whole-population census is generally not feasible.

Various microfluidic devices (*39*, *40*, *140–144*) have been developed to emulate patchy microbial habitats, which afford the capacity to track individuals in space and time while minimizing sample volumes. These devices allowed detailed investigations of microbial movement, pattern formation, and interaction (*112*). In particular, it was observed that in comparison to well-mixed test tube cultures, a microhabitat favoured the maintenance of cooperation (*133*). However, these devices did not contain a systematic variation in habitat patchiness, and required substantial setup time. Building on these past innovations, we introduce a microhabitat device (MHD) that is simple to fabricate and operate, reusable, and systematically varies habitat patchiness.

The MHD is a reusable poly(dimethyl)siloxane (PDMS) device that contains 9 habitats with varying patchiness. Patchiness was achieved by fragmenting habitats at 100-micron scales. We used simplicity and functionality as guiding principles (*145*) to focus on acquiring accurate individual-level spatiotemporal data for entire habitats. The PDMS elastomer layer seals with an optical cover slip to create an

enclosed environment for bacteria to spatially self-organize with minimal disturbance. We investigate whether three habitat patchiness treatments affect the evolution of pyoverdin (*146*, *147*) producers, and therefore the growth and equilibrium densities of cooperators and defectors in *P. aeruginosa*. The wild-type cooperators and mutant defectors were genetically engineered to emit green or red fluorescence, so that their population size and spatial location can be accurately quantified by confocal microscopy.

We performed monoculture and mixed culture experiments to ascertain whether habitat patchiness affects maximum growth rates and equilibrium densities of these populations. We found that while defectors outnumbered cooperators in all habitats, and are thus more likely to achieve dominance, patchiness contributed to the ecological coexistence of cooperators and defectors.

3.4. Methods

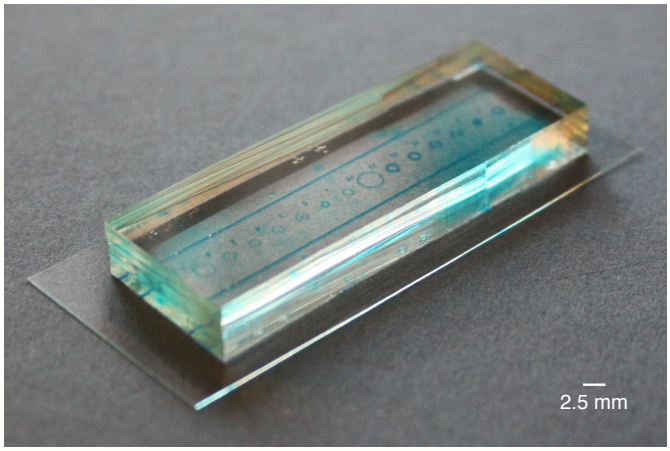

Figure 3.1. The microfluidic device contains 14 habitats and 9 variations (some are duplicated). Habitats are dyed blue for visualization. The elastomer (PDMS) layer is pressed onto a 60 mm x 24 mm glass cover slip after inoculation to create a sealed device. The confocal microscope acquires images through the thin cover slip.

The MHD (Fig. 3.1) contains 9 treatments of habitat patchiness, with each habitat ranging from 1404 μm to 2671 μm in diameter, and 10 or 20 μm in depth. Each habitat takes the shape of a ring or a network of patches, representing a range of continuous and patchy treatments (see Fig. 3.2 and 3.8 Supplementary Fig. 3.S.1 for specifications). Here we focus on three treatments (Fig. 3.2), which are 10 μm deep and 0.4241 mm^2 in the main habitat area. At this depth, all bacteria are confined to a thin layer, which facilitates image acquisition. Habitat 1 represents the most continuous case, whereas habitat 2 represents an intermediary between the continuous and patchy cases. A central pillar is necessary in these habitats to prevent collapse due to aspect ratio constraints (*148*). In habitat 3, 24x100 μm^2 corridors are introduced between 12 circular patches (210 μm diameter) to represent the patchy case (area including corridors is 0.4529 mm^2). The edge-to-area ratios of the habitats are 0.0108, 0.0153, and 0.0223 μm^{-1}, which represent an approximately linear increase in patchiness (*43*).

Compared to the size of *P. aeruginosa* (~1 μm diameter), the 100-micron scale patchiness treatments in the three habitats are large. On the other hand, an individual bacterium can theoretically traverse 100 μm in several seconds (*149*), but slows down considerably in aggregates when spatially confined (*150*). We expect that the chosen scale of patchiness treatments can affect eco-evolutionary dynamics. During experiments, the three habitats were run in parallel. Other habitat treatments are shown in the Supplementary Fig. 3.S.1, but were not used in the experiments reported here because of time constraints in image acquisition.

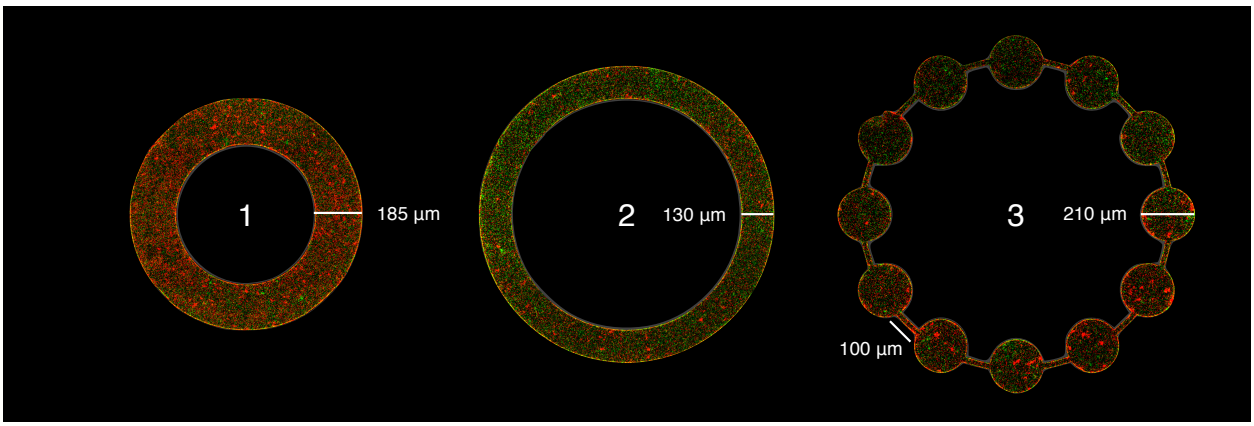

Figure 3.2. Three habitat patchiness treatments. The habitats are inoculated with green cooperators and red defectors. Images shown are taken at T=10 (about 10 hours after inoculation). The habitats are 10 μm deep and have diameters of 915, 1165 and 1405 μm. The corridors are 24 μm wide.

A silicon mold with two spin-coated layers (to accommodate both 10 and 20 μm depth features) was produced using photolithography (McGill Nanotools Microfab). Polydimethylsiloxane (Sylgard 184 PDMS, Dow Corning) was poured onto the mold, cured, and detached to yield MHD replicates that are about 5 mm thick, and baked at 100°C for at least 24 hours. To make the PDMS MHD hydrophilic, it was soaked in 0.01N HCl at 80°C for one hour, then plasma treated (modified after (*39*)). Finally, the MHD was autoclaved, and stayed in the sterilized water at room temperature until the

experiment began. The MHD thus remained saturated with water, which mitigated drying during the experiment.

We used the common *P. aeruginosa* lab strain PAO1 as our wild-type cooperators, and an isogenic *pvdA* transposon mutant (*151*), which is defective in producing the primary iron-chelating siderophore (pyoverdin), as defectors. The cooperator and defector strains were transformed with plasmids that constitutively expressed either the green fluorescent protein GFP (pMRP9-1 (*152*)) or the red mCherry (pMKB1 (*153*)).

In 8 independent experimental replicates for each of 3 culture conditions (cooperator monocultures, defector monocultures, mixed cultures) in the MHD, the expression of GFP or mCherry in cooperators and defectors were alternated to average out fluorescence-dependent growth or measurement biases. Cultures were prepared overnight (16 hours) in LB media with antibiotic (250 μg/ml carbenicillin) at 37°C in a shaker incubator. The overnight bacterial cultures were washed and diluted to an optical density (600nm) of 0.005. The experimental media consisted of casamino acids (5g with 0.005M K_2HPO_4 and 0.001M $MgSO_4$ per litre), 50mM $NaHCO_3$ and 1mg/mL human apo-transferrin to create an iron-limited environment where the cooperators' pyoverdin production should be beneficial (*46*, *146*). 0.7 μL of the diluted culture was pipetted onto each of the habitat locations on the PDMS MHD (Fig. 3.1). The MHD was then carefully pressed onto a cover slip (24x60mm #1.5H, Schott Nexterion), and excess liquid was wiped from the sides. By minimizing the amount of liquid used, the PDMS reversibly sealed to the glass for the duration of the experiment without additional treatment. Three such MHDs were fitted into a 30°C heat chamber (Chamlide TC, Live Cell Instrument) on the inverted robotic stage of a laser scanning confocal microscope

(LSM 700, Zeiss) to allow for parallel experiments (two for monocultures and one for mixed culture). The chamber interior was lined with wet tissue papers and water wells to maintain device moisture. Images covering the relevant habitats were acquired every 57 minutes and 18 seconds (the minimum acquisition time in our case) for 20 time points (Fig. 3.3). After an experiment, the MHD was disassembled and soaked in 70% ethanol, washed, and autoclaved for reuse. Each MHD can be used at least 10 times with no noticeable degradation.

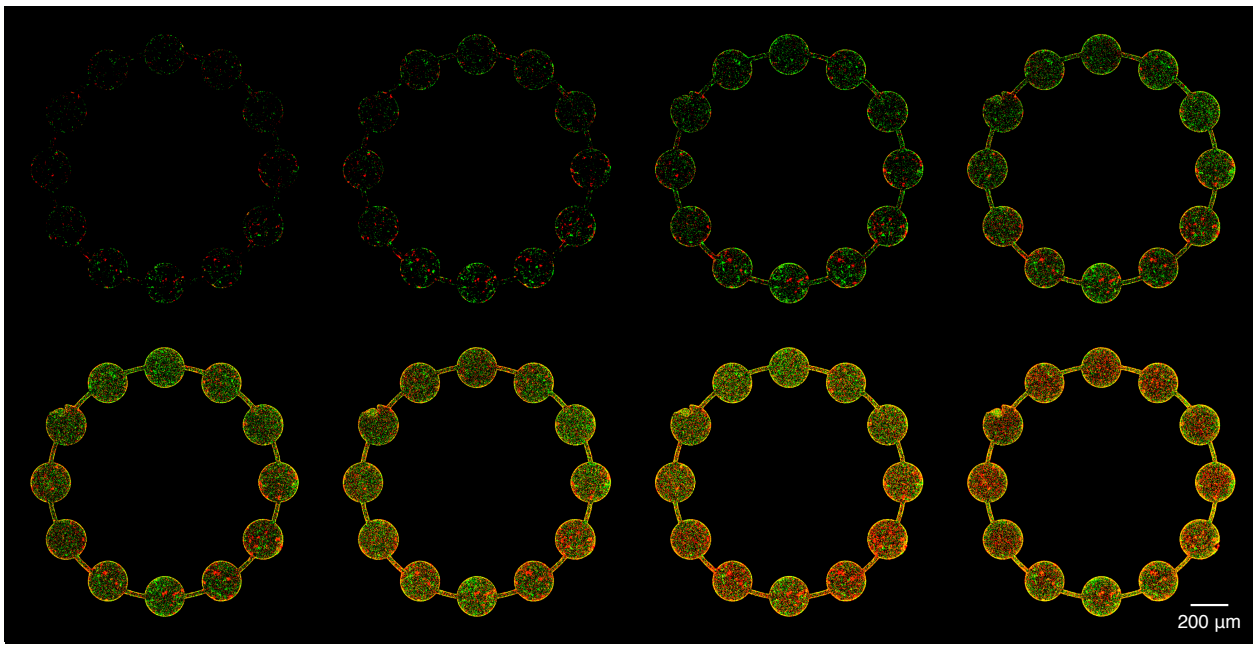

Figure 3.3. Timed images of green cooperators and red defectors in a patchy habitat (T=5 to 12 from top left to bottom right). For all figures, the time interval T is 57 minutes 18 seconds.

The images were cropped to show only habitat and corridor areas (ImageJ 1.49). We then obtained the count and position of each individual bacterium at every time point (Imaris 7.6.0). Some biases were observed in comparing raw GFP and mCherry counts of the same strain in monocultures, and in comparing monocultures to mixed fluorescence cultures of the same strain. These biases were corrected through a calibration procedure (see 3.7.1. Appendix A).

The corrected counts were converted to densities X for each habitat, and the resulting time series were fitted to logistic growth curves using least-squares maximum likelihood (Matlab R2013a, Eq. 3.1):

$$\frac{dX_{i,S}}{X_{i,S}dt} = r_{i,S}(1 - X_{i,S} / K_{i,S}) \tag{3.1}$$

For a replicate of each strain i (cooperator or defector) in each culture condition S (monoculture or mixed culture), we estimated its maximum growth rate r and equilibrium density K. Note that we used the parameter K not as a carrying capacity, which would not make sense in a mixed culture involving both inter- and intraspecific competition and cooperation. Instead, we used K as an estimate of a strain's equilibrium density, since the logistic growth curve describes the trajectories of each strain well regardless of culture type and the length of individual time series (Fig. 3.4).

3.5. Results and discussion

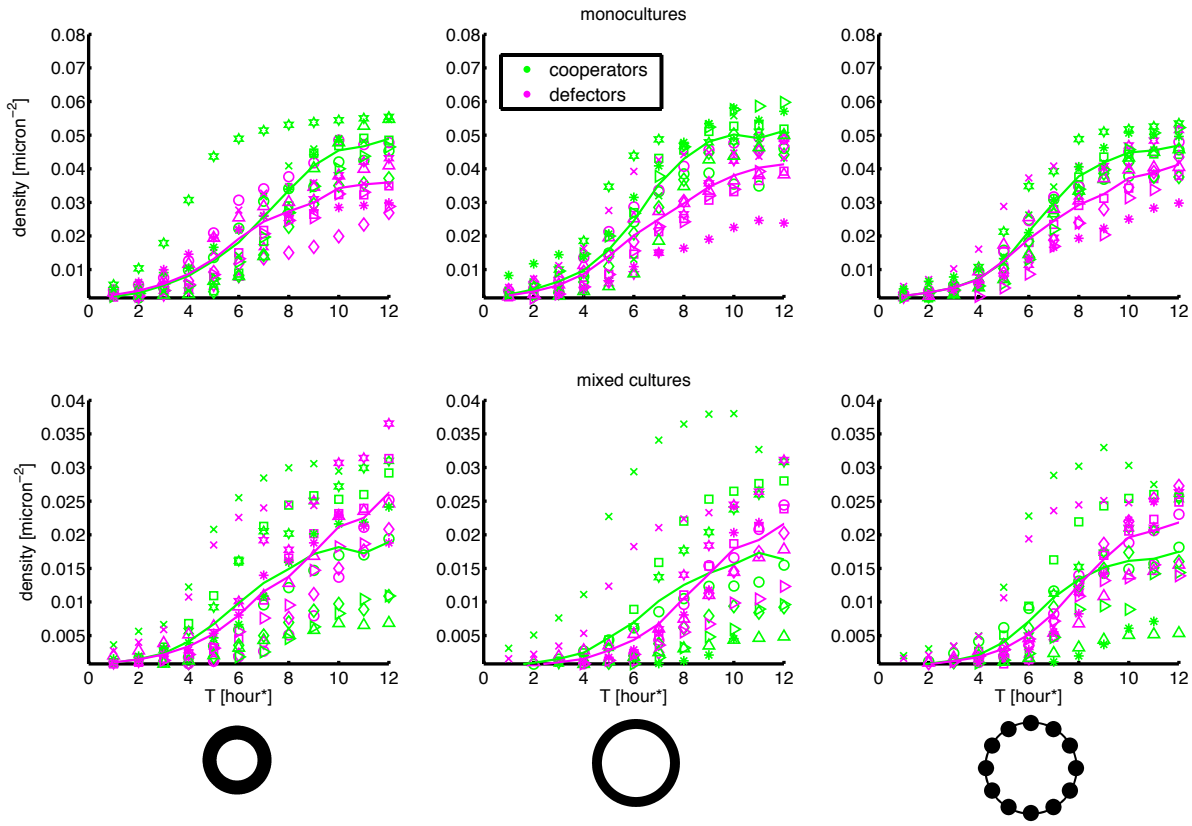

Figure 3.4. Time series of cooperator and defector monocultures, and mixed cultures in three habitat patchiness treatments, as illustrated by icons at the bottom. Densities are expressed as individuals per micron squared. The different markers represent the 8 experimental replicates, and the line plots are averages for each strain at each time point. *Each time interval T is 57 minutes 18 seconds.

In 8 experimental replicates of each habitat and culture types, bacteria replicated and survived for 12 to 18 hours. All cooperator and defector populations demonstrated expected growth kinetics during the experimental time frame, with evidence of lag, log and stationary phases (by 10 hours, Fig. 3.4), characteristics of logistic growth curves. The equilibrium density estimates (*K*) represent strain populations that range from 2367 (cooperators in a mixed culture) to 38170 (cooperators in a monoculture) individuals, or 5.58×10^8 to 9.00×10^9 individuals per mL.

We found that the maximum growth rate r (Supplementary Fig. 3.S.2) was not significantly different in all cases according to ANOVA ($F_{3,87}$=2.18, p=0.096 for strain and culture type effect, $F_{1,87}$=0.09, p=0.77 for patchiness effect, and $F_{3,87}$=0.23, p=0.88 for interaction effect).

In monocultures, the equilibrium density K (Supplementary Fig. 3.S.3) was significantly greater for cooperators than for defectors (ANOVA F1,44=21.73, p=2.93x10-5), but was not significantly different across patchiness treatments (F1,44=0.06, p=0.81); the interaction between strain and patchiness was not statistically significant either (F1,44=3.19, p=0.081). In other words, cooperation enhanced population densities regardless of habitat patchiness. In mixed cultures, K was significantly lower for cooperators than for defectors (F1,43=8.25, p=0.0063), but was not significantly different, both in terms of patchiness (F1,43=0.0024, p=0.96) and in terms of the interaction between strain and patchiness (F1,44=0.047, p=0.83). Thus, defectors outnumbered cooperators in all habitats, a result that was also found in well-mixed test tube cultures (see 3.7.2 Appendix B). This illustrates the cooperation dilemma (*7*, *9*, *36*), where uniform cooperation provides the best outcome for the population, but is an evolutionarily inferior strategy.

We can further investigate the cooperation dilemma from an ecological perspective through the differences between monocultures and mixed cultures. Judging from monoculture equilibrium densities alone (K_{mono}), one may expect cooperators to be evolutionarily dominant over defectors (since $K_{mono,C} > K_{mono,D}$). If each strain grows in mixed cultures as if in monoculture, then the ratio $2K_{mix}/K_{mono}$ for each strain should be one (*154*). The actual ratios, computed from bootstrapping, turned out to differ from one (box plots in Fig. 3.5). For cooperators, $2K_{mix,C}/K_{mono,C}$ was less than one in all

habitats, indicating that when evolutionarily challenged by defectors, they did not grow as well. Conversely, for defectors, $2K_{mix,D}/K_{mono,D}$ was greater than one in all habitats, meaning that they benefited from cooperators.

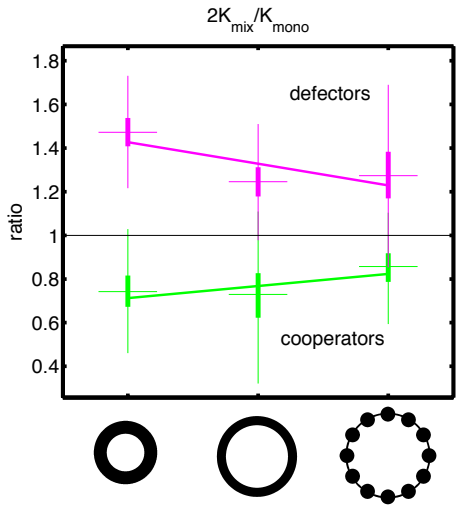

Figure 3.5. The ratios of equilibrium densities (K) in mixed cultures (x2) over monocultures as estimated from bootstrapping for three habitats. If the interaction between cooperators and defectors has no effect on their equilibrium densities, the ratio should be 1. In the box plots, horizontal bars indicate medians, thick vertical bars (boxes) indicate 25th and 75th percentiles, and thin vertical bars indicate minima and maxima excluding outliers. From bootstrapped linear regressions, patchiness significantly increases the ratio for cooperators (green regression line, p=0.0075), but marginally decreases the ratio for defectors (magenta regression line, p=0.16).

The habitat patchiness effects on the $2K_{mix}/K_{mono}$ ratios can be quantified as the slopes of bootstrapped linear regressions. By repeating the regression on the ratio computed from the resampling of K_{mix} and K_{mono} values with replacement 2000 times, we obtained the median regression slopes (lines in Fig. 3.5), and obtained distributions of regression slopes with which to calculate the following p values. We found that patchiness does not affect the $2K_{mix,D}/K_{mono,D}$ ratio for defectors (p=0.16). On the other hand, patchiness significantly increased the $2K_{mix,C}/K_{mono,C}$ ratio for cooperators (p=0.0075). These trends suggest that with increased patchiness, the ecological pressure against the pyoverdin public-good cooperation, stemming from the challenge by defectors, is alleviated. Moreover, as patchiness increases, the ratios $2K_{mix,C}/K_{mono,C}$

and $2K_{mix,D}/K_{mono,D}$ appear to approach one, so patchiness leads competing strains to grow as if in isolation. This effect is known in ecology as a spatial stabilizing effect, in that patchiness isolates strains such that they increasingly compete within strains rather than between strains, leading to coexistence regardless of how competitive each strain is relative to the other (*65*, *127*, *130*).

Our experiment generated the first empirical evidence that a gradual increase in habitat patchiness, occurring at a scale much larger than the individual, can affect the ecology of cooperation, and the coexistence of cooperators and defectors in bacteria. These results complement a previous microfluidic experiment (*133*), which demonstrated the coexistence of bacterial cooperators and defectors in one microhabitat. The results are comparable to traditional test tube experiments, which by controlling serial transfer patterns, showed that spatial restrictions and artificially localized interactions can favour the evolution of cooperation (*46*, *119*, *137*, *138*). Our MHD also provides an alternative to beaker (*139*) and flow cell experiments (*126*), which study cooperative aggregates and biofilms at much larger spatial scales where whole-population census is generally not feasible.

We have overcome important challenges that are crucial for the use of microscale habitat devices in evolutionary biology (*145*). In creating a sealed device that can run multiple replicates without pumps for 12-18 hours, we have enabled high-throughput spatial experiments with minimal setup time and cost. The runtime is an improvement over previous PDMS microhabitat devices (*140*, *141*), and is much simpler to operate than devices requiring active nutrient flow (*39*, *40*, *142*, *143*). Many aspects of the generated data, such as individual positions, population spatial distributions, and movement patterns can be further investigated, and would lead to a

more comprehensive understanding of patchiness and individual-level clustering effects (*35*, *155*) than what our current analyses yielded. It is also possible to recover bacteria from the MHD at the end of experiments to detect *de novo* mutations through sequencing (*143*).

Some limitations exist with the MHD. Because of aspect ratio requirements with PDMS chambers (*148*), it is not possible to create patches and habitats of any dimension. The enclosed system afforded by our design is simple and exhibits the familiar logistic growth of bacteria (Fig. 3.4). However, without serial transfer of bacteria into fresh medium, the system limits the possible duration of the experiment for the following reasons. PDMS facilitates gas exchange, but gradually absorbs liquid at the same time (*156*). The sealed system also prevents nutrients from being replenished. Lastly, the number of different strains or species in mixed culture experiments that can be tracked is limited by the available fluorescent proteins (eg. GFP, mCherry) that can be visualized concurrently by fluorescence microscopy.

3.6. Conclusions

We demonstrated that a simple and reusable microfluidic device can provide insights into the eco-evolutionary dynamics of *Pseudomoas aeruginosa*, a medically important pathogen. In the first microbial cooperation experiment with multiple spatial habitat treatments, we observed that mutant defectors are evolutionarily more competitive than wild-type cooperators that produce siderophores. However, the ecological pressure against cooperation due to defection is alleviated in increasingly patchy habitats, leading to continued coexistence (Fig. 3.5). The trends suggest that at patchiness levels higher than those we tested, competing strains may grow as if in isolation – a hypothesis that merits further investigations.

The results suggest that pathogenic bacteria in patchy habitats, such as the respiratory tract (*29*), may be more cooperative in exploiting nutrient resources in comparison to a continuous habitat like a conventional test tube. Nevertheless, defectors, or loss-of-function mutants, can be expected to arise and co-exist with wild-type cooperators, as has been observed in patients with cystic fibrosis (*44*, *45*, *120*). The simple device design and operation should facilitate its uptake in ecological, evolutionary, and medical research, leading to novel experiments that complement existing studies on microbes in spatially complex environments (*46*, *126*, *133*, *143*, *157*). Specifically, future experiments using our microhabitat device can address how habitat patch size and corridor topology affect demography (*103*, *158*, *159*) and cooperation (*23*, *24*), and how nutrient availability (*160*) interacts with patchiness to affect microbial community dynamics (*48*).

2109 ## 3.7. Appendices

2110 ### 3.7.1. Appendix A. Fluorescent count calibration

2111 To estimate and correct for fluorescence-related biases in individual counts, 8
2112 independent control experiments are conducted, each of which involves a GFP
2113 monoculture, a mCherry monoculture, and a GFP/mCherry mixed culture with cooperators
2114 and defectors seeded at half of the monoculture density. First, the Imaris spot detection
2115 parameters Threshold (T) and Quality (Q) are varied for each of GFP and mCherry, and the
2116 counts for each strain is recorded. Treating the counts as functions of T and Q, we search
2117 for the T and Q settings that minimize the differences between GFP and mCherry counts,
2118 and between monoculture and mixed culture counts. Finally, the remaining biases are
2119 corrected by multiplying experimental counts with correction factors. The final T and Q
2120 settings for GFP are 3.83 and 0.5, and for mCherry are 4 and 2. The correction factor for
2121 mixed culture relative to monoculture counts is 0.64. The correction factor for GFP relative
2122 to mCherry counts is 1.11. Using these settings and corrections, the resulting GFP-to-
2123 mCherry count ratio is 1 (S.E. 0.074), and the monoculture-to-mixed culture ratio is 1 (S.E.
2124 0.065) across the calibration dataset.

2125

2126 ### 3.7.2. Appendix B. Test tube experiment

2127 As a control with no spatial structure, we grew mixed cultures of wild-type
2128 cooperators and mutant defectors in 1mL of media (identical to experiments in MHD) in
2129 conventional deep-well plates. After 10 hours in a 30°C shaker incubator, the cultures
2130 were diluted and grown on carbenicillin (for cooperators) and tetracycline (for defectors)

agar plates for cell count. Defectors outnumbered cooperators (cooperator frequency mean=0.451, SE=0.0097, t_2=-8.80, p=0.013).

3.8. Supplementary figures

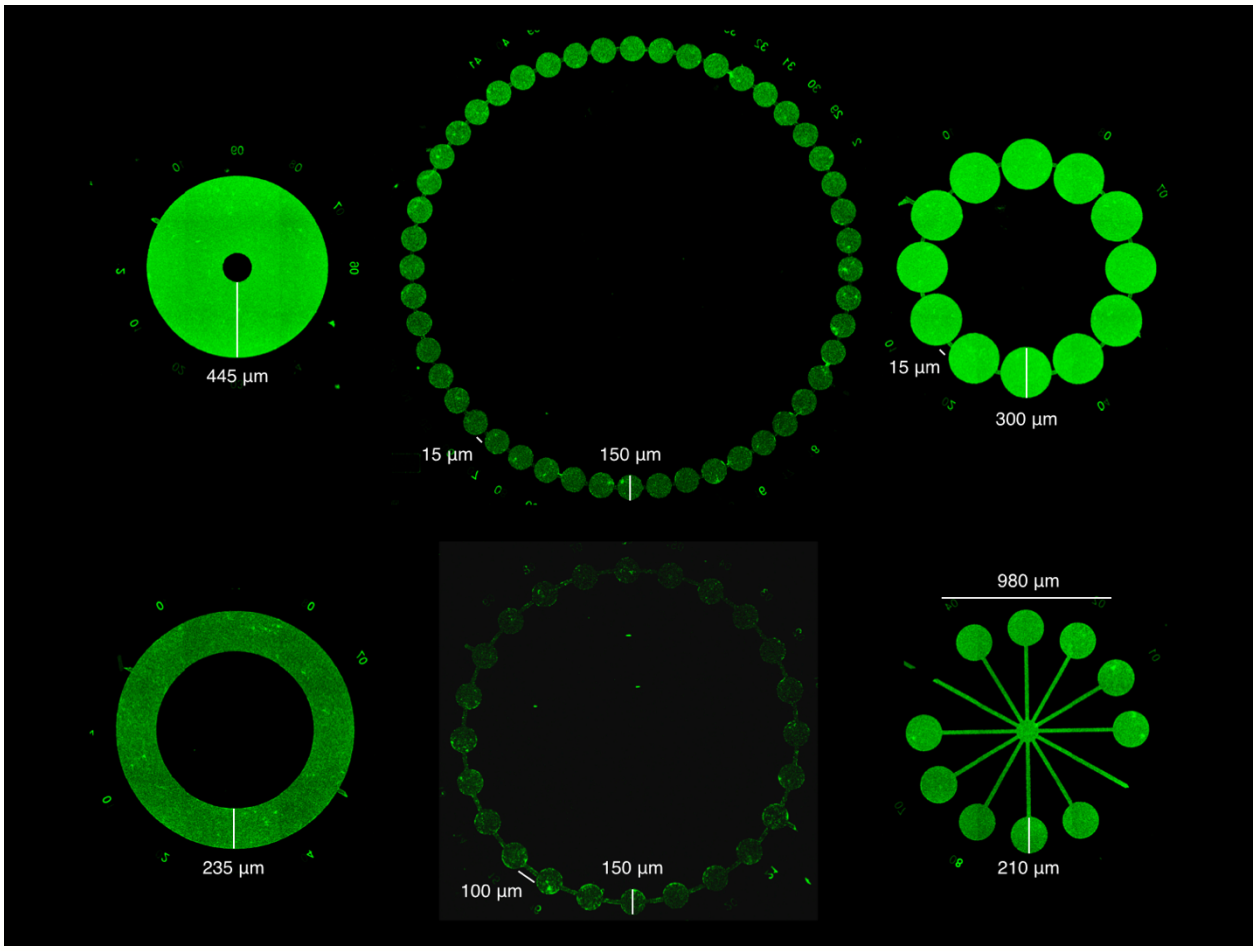

Figure 3.S.1. Addtional habitat variations. The habitats are inoculated with green cooperators and are imaged at T=8. Clockwise from the top left corner, the diameters and depths (µm) are: 1050x20, 2670x20, 1500x20, 1405x10, 2060x10, 1380x20. All corridors are 24 µm wide.

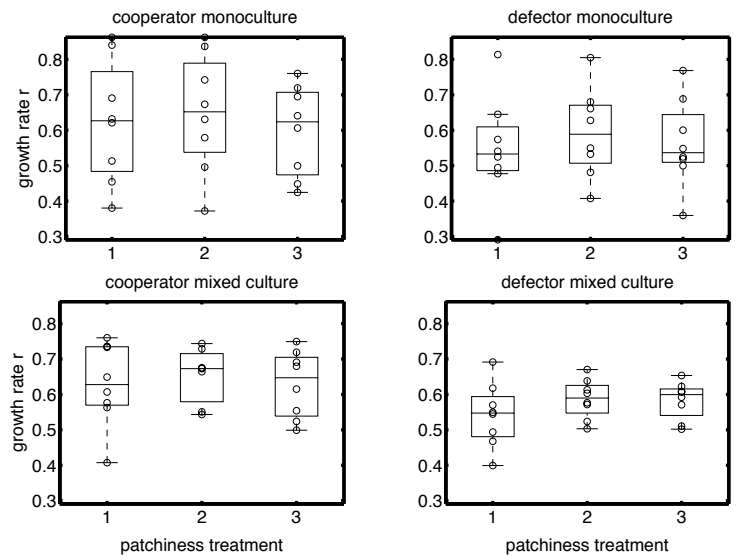

Figure 3.S.2. Maximum growth rate *r* estimates for cooperators and defectors in monocultures and mixed cultures as functions of habitat connectivity treatments. According to ANOVA, *r* is not significantly different in terms of strain and culture type (*p*=0.096), patchiness treatment (*p*=0.77), or their interaction (*p*=0.88).

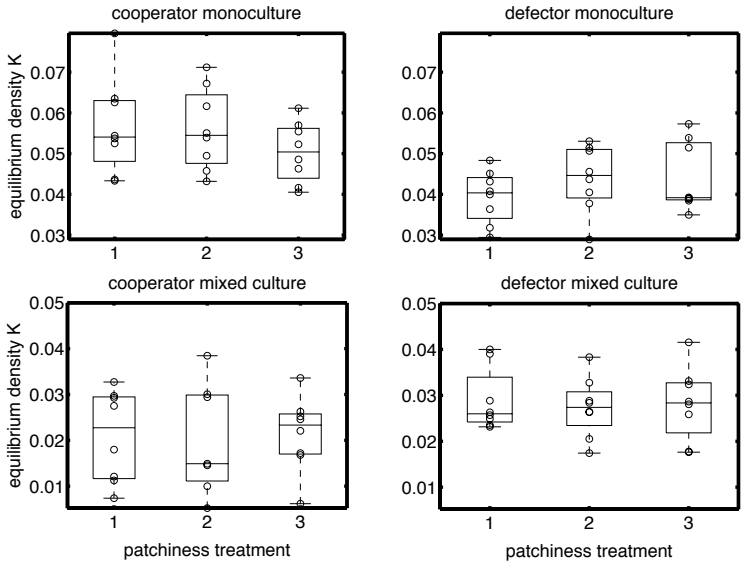

Figure 3.S.3. Equilibrium density *K* estimates for cooperators and defectors in monocultures and mixed cultures as functions of habitat connectivity treatments. According to ANOVA, in monocultures, *K* is significantly higher for cooperators than for defectors (*p*=2.9e-05), but is not significantly different in terms of patchiness treatments (*p*=0.81) and the interaction between strain and patchiness (*p*=0.081). In mixed cultures, *K* is significantly lower for cooperators than for defectors (*p*=0.0063), but is not significantly different in terms of patchiness treatments (*p*=0.96) and the interaction between strain and patchiness (*p*=0.83).

Chapter 4. Small-scale clustering mediates the evolution of cooperation in a pathogenic bacterium

Edward W. Tekwa, Dao Nguyen, Michel Loreau, Andrew Gonzalez

4.1. Prelude

From Chapter 1 to 2, the concept of local densities was increasingly functionalized. We moved from establishing theoretical importance to making novel predictions about clustering effects. But a major hurdle remains for the empirical deployment of spatial metrics in both spatial ecology and evolutionary biology whenever interaction scale is invoked. That is, how do we determine the appropriate interaction scale in order to obtain the appropriate local densities, or in fact to obtain any evolutionary spatial metrics?

The empirical scale problem can be partly resolved when cooperation and competition scales are experimentally manipulated (*46*), but remains a theoretical construct in models where the intermediary processes facilitating interactions are implicit and emergent (*35*). In our experiment, the intermediary processes are siderophore production, diffusion, consumption, and degradation. Technically, it may be possible to derive the physics of these processes in a particular environment and arrive at the appropriate scale. A more robust approach may be to infer the appropriate scale from the performance of models that assume different scales, but this has so far been unexplored. The individual-level resolution of our experimental data (Chapter 3), coupled with the theoretical model and predictions from Chapter 2, provides an excellent opportunity to further functionalize local densities. In particular, it is an

opportunity to test a surprising prediction: that cooperator clustering decreases both cooperator frequency and population density. We include a new and simple derivation of this result using Price's Equation, following its use in Chapter 1.

This chapter can be thought of as a synopsis of the entire thesis. Or, the other chapters can be considered as footnotes to this paper, which brings novel metrics (at least for the evolution of cooperation), theories, and experiments together.

4.2. Abstract

The production of a public good is a costly cooperative trait that benefits neighbours and is an eco-evolutionary dilemma because individuals can defect and receive the benefits without paying the costs. While spatial clustering between individuals can strongly influence the evolution of this cooperative trait, it is unknown how clustering emerges and what the fitness effects of clustering in an undisturbed system are. Using a microhabitat device with two *Pseudomonas aeruginosa* strains—siderophore-producing cooperators and defectors (cheats)—we measured emergent clustering patterns and their effects at different scales. We found that cooperator clustering counterintuitively decreased cooperator frequency in the population. This arose because cooperator clustering and defector clustering developed differently because of strong selection and demographic dynamics. This result is corroborated by the selection analysis of an analytical model that incorporates both cooperation and competition. Clustering of individuals at the 5-μm scale explains the eco-evolutionary outcomes much better than larger scale habitat constraints. The study suggests that microbial interactions at a very small scale can mediate the costs and benefits of cooperation. Complex and emergent spatial patterns may be the key to understanding the maintenance of cooperation in natural populations.

Keywords: evolution of cooperation, public goods, scale, Pseudomonas aeruginosa, strong selection, microhabitat device

4.3. Introduction

The evolution of cooperation is responsible for the rise and maintenance of biotic complexity (*2*). Even apparently simple bacteria exhibit cooperative behaviours, such as the production of locally diffusive public goods (*117*) that benefit the greater population and thus do not qualify as zero-sum games. For pathogens such as *Pseudomonas aeruginosa*, public-good cooperation can lead to increased virulence, simply because public good enhances population growth (*41*). An important determinant of the evolutionary success of cooperation is the spatial pattern of individuals in their habitat. The association between cooperators creates clusters of varying density and size. Theory predicts that clustering promotes cooperation within the population under weak selection or in zero-sum games (*13*, *21–26*) but can actually hinder cooperation under strong selection and coupled demographic dynamics. These contrasting hypotheses form an open empirical question that can only be answered by adequately studying the emergence of clustering. Theoretically, while the positive effect of clustering on cooperation has often been established, we begin by giving a new account of why this may not be generally true.

Consider a dimorphic population of cooperators (c) and defectors (d). All neighbours impose a competitive cost k, while cooperator neighbours bestow an additional benefit a to a focal individual, and $k>a$ so that realistic demographic dynamics emerge. This can describe public-good cooperation, such as bacterial siderophore production (*46*) and mound or nest construction (*98*), where cooperation alleviates competition. Let the cooperative character value of an individual be $z=1$ if it is

a cooperator, and z=0 if it is a defector. The density-dependent fitness (growth rate) w of individuals with character z is given by:

$$w(z=1) = r_c - (k-a)C_{cc}X_c - kC_{cd}X_d$$
$$w(z=0) = r_d - (k-a)C_{dc}X_c - kC_{dd}X_d \quad (4.1)$$

X_i is the global density of morph i, r_i is the intrinsic growth rate of morph i, and C_{ij} is the clustering coefficient between morphs i and j. $C_{ij}>1$ indicates clustering when compared to the well-mixed, non-spatial case, and $C_{ij}X_j$ yields X_{ij}, the local density of j around i. Local density (*35*) is the demographically explicit version of pair density or conditional probability of identity, which are used to model space in evolutionary games (*24*, *26*) and inclusive fitness in graphs (*23*) or subdivided populations (*22*). We analyse the selection pressure that each clustering coefficient exerts on cooperation using Price's Equation (*63*, *74*), which states that the change in the average character Z of a population is $dZ/dt = \mathrm{cov}(w, z)$. With some derivations (see Methods 4.5.1), we obtain:

$$dZ/dt = \mathrm{var}(z)((r_c - r_d) - (k - a)X_cC_{cc} + kX_dC_{dd} - ((k - a)X_c - kX_d)C_{cd}) \quad (4.2)$$

Eq. 4.2 states that the evolution of the cooperative trait Z is determined by the variance in the individual characters z in the population, multiplied by the sum of four factors. The sign of each factor indicates whether cooperation is selected for (Z increases) or against (Z decreases). The first factor is $r_c - r_d$, which is the non-spatial intrinsic growth rate difference or the cost of cooperation, also known as individual-level selection (*161*). The second factor is cooperator clustering C_{cc}, multiplied by $-(k - a)X_c$, which is negative. The third factor is defector clustering C_{dd}, multiplied by kX_d, which is positive. The fourth factor is between-morph clustering C_{cd}, multiplied by $(k - a)X_c - kX_d$, whose sign is density dependent and thus cannot be predicted in a straightforward way. In summary, because of the interplay between cooperation and competition,

cooperator clustering should disfavour cooperation, while defector clustering should favour cooperation. If we were to assume weak selection (X_c=X_d=X_i) and no demographic dynamics, we can set C_{cc}=C_{dd}=C_{ii} (*24*, *26*), such that the net effect of within-morph clustering would be positive ($-(k - a)X_iC_{ii} + kX_iC_{ii} = aX_iC_{ii}$). This recovers the traditional hypothesis that clustering promotes cooperation. It remains to be elucidated how clustering arises, whether C_{cc}=C_{dd}, and whether strong or weak selection occurs in empirical systems.

Clustering in bacteria may arise partly as a result of limited movement (*27*), chemotaxis (*28*), biofilm formation (*126*), and spatial constraints in patchy habitats, such as in soil (*162*) or in the human respiratory tract (*29*), that *P. aeruginosa* can colonize. Because these processes occur at tiny spatial scales, the experimental study of bacterial cooperation is deceptively challenging but is an essential first step towards testing theories (*115*, *139*). Microfluidic devices now allow novel tests of theories on microbes (*112*) because they can control spatial habitat structure at the micron scale and allow precise imaging of locations of individuals in the population.

While clustering has been experimentally manipulated to study the evolution of cooperation (*46*, *136*, *163*), it remains unknown how clustering emerges if individuals are left undisturbed, and how clustering patterns affect eco-evolutionary dynamics. Some efforts have been made to measure emergent spatial patterns in a microfluidic experiment (*40*), but so far individual-level resolution data have not been obtained to infer clustering effects on cooperation. A critical and unresolved empirical issue with emergent spatial patterns is to establish the scale at which spatial interactions occur between individuals (*128*, *131*). Even in microfluidic experiments that define structure

at a certain scale, it is not obvious that the cluster patterns relevant to interactions should arise at the same scale.

In light of our predictions our objective was to investigate whether cooperator clustering increases or decreases cooperator frequency in the pathogenic bacterium *P. aeruginosa*. Cooperator and defector strains compete in a microhabitat device, which imposes 100-micron scale patchiness constraints but otherwise allows competing cooperator and defector strains to grow and self-organize undisturbed. Patchiness is expected to lead to higher clustering at that scale, which we may hypothesize, in the absence of further prior information, to be the interaction scale that best explains eco-evolutionary outcomes. We quantify clustering within cooperators, within defectors, and between cooperators and defectors using clustering coefficients at different scales and infer the interaction scale by evaluating how well clustering at each scale explains cooperator frequency and population density. Clustering effects are then obtained from the inferred scale and are used to evaluate the theory.

4.4. Results and Discussions

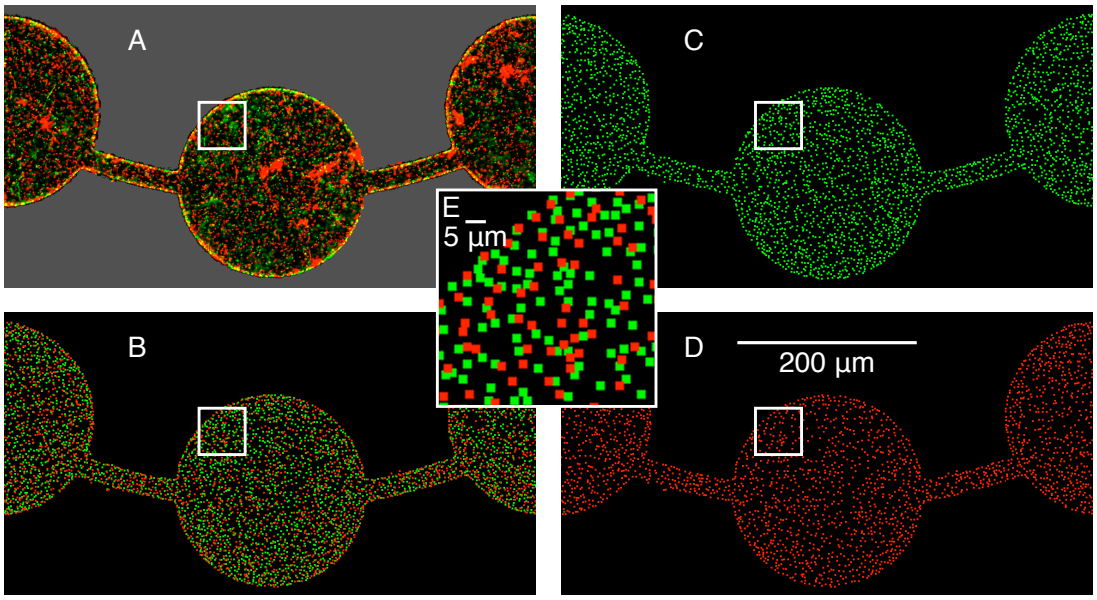

Figure 4.1. A snapshot of cooperator (green/light) and defector (red/dark) distributions in a patchy habitat (T=10). A: fluorescent intensities; B: spot detections for cooperators and defectors using Imaris, C: spot detection for cooperators only; D: spot detection for defectors only; E: zoom-in of cooperator and defector spot detections in the squared area.

In *P. aeruginosa*, the wild type lab strain (PAO1) produces the public good pyoverdin, which is the primary siderophore responsible for iron uptake and growth (*42*). Loss-of-function defectors often arise in infected humans (*44*, *120*), with relatively large phenotypic changes, which represent a recurrent and potentially strong selection pressure against cooperation. We set up a competition between cooperators (density X_c) versus defectors (pvdA mutant, density X_d) in an elastomeric microhabitat device which contains three habitat patchiness treatments (8 replicates each), ranging from a continuous ring to a patchy network, with edge-to-area ratios (*43*) of 0.0108, 0.0153, and 0.0223 μm^{-1} (Fig 2A). Cooperators and defectors were inoculated at approximately equal densities (see Methods 4.5.2). While patchiness was implemented at the 100-micron scale, bacteria are free to form finer-scale clusters in the habitats. We tracked

the bacteria with fluorescent tags (GFP and mCherry) every hour, up to 18 hours (Fig. 4.1; Chapter 3). Cooperator frequency (X_c/X) and total population density ($X=X_c+X_d$) were positively correlated (measured as averages of T10-12 hours, when equilibrium was reached), indicating that pyoverdin production appears to be an effective public good (Fig. 4.2B). The three patchiness treatments did not affect population density and cooperator frequency according to MANCOVA (Fig. 4.2B), so we predicted that smaller scale clustering between the morphs was important (Fig. 4.1E).

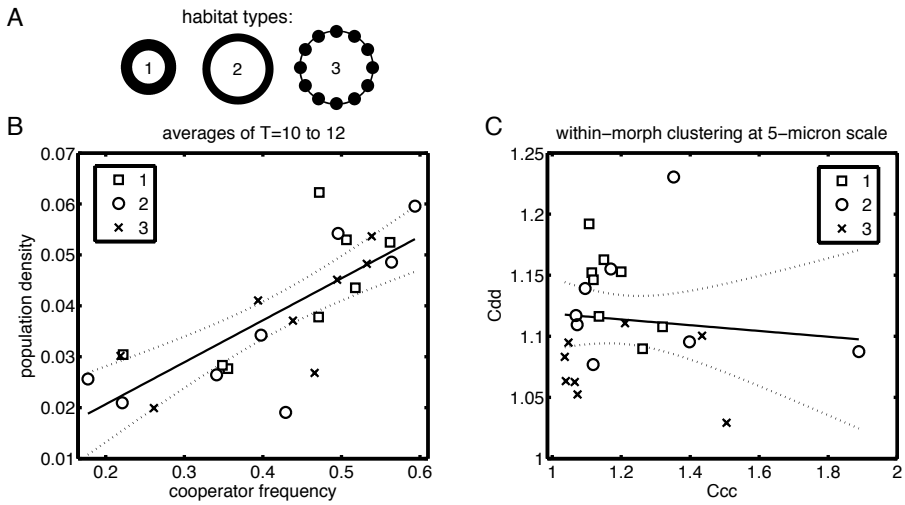

Figure 4.2. A: habitat types. B: cooperator frequencies versus total population densities plotted by habitat type. The relationship between cooperator frequency and population density was positive ($F_{2,22}$=32.6, p=9.59e-6, R^2=0.58). MANOVA shows that habitat type did not significantly affect cooperator frequencies and population densities ($\chi^2(4,n=24)$=0.93, *Wilk's* Λ=0.96, p=0.92). C: within-defector clustering C_{dd} versus within-cooperator clustering C_{cc} measured at the 5 µm scale. Data points were distinguished by their habitat types. The overall slope was not significantly different from zero ($F_{2,22}$=0.23, p=0.64, R^2=0.010).

To quantify clustering at different scales, we use clustering coefficient C_{ij}, which is defined as the clustering between morphs i and j. C_{ij} is the normalized local density (*65*) of morph j around morph i ($C_{ij}=X_{ij}/X_j$, where X_{ij} is the average number of j individuals around an i individual within a radius or scale). The cooperator, defector, and between-morph clustering coefficients (C_{cc}, C_{dd}, C_{cd} as averages of T10-12) were computed at the 5-µm scale. There is no relationship between cooperator and defector

clustering, as the regression slope between C_{cc} and C_{dd} was not significant (Fig. 4.2C). If clustering does turn out to affect eco-evolutionary dynamics, then $C_{cc} \neq C_{dd}$ indicates that the traditional assumptions of weak selection and habitat saturation would not apply.

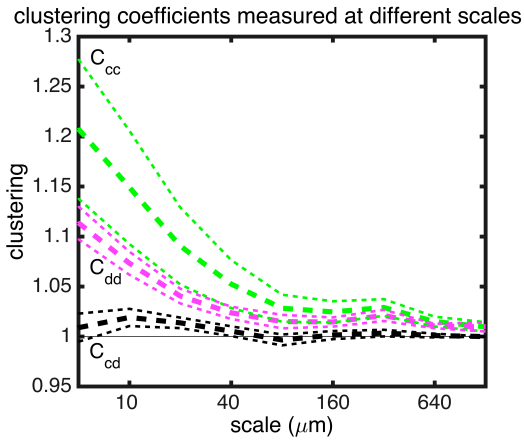

Figure 4.3. Clustering coefficients (C_{cc}, C_{cd}, C_{dd}) measured at different scales (from 5 to 1280 μm). Thick dotted lines are means, and thin dotted lines are standard errors.

We analysed how clustering coefficients changed as functions of the assumed interaction scale, with 9 radii or scales ranging from 5 to 1280 μm (Fig. 4.3). Clustering coefficients between different morph pairs were most pronounced at 5 μm and approached the well-mixed approximation of C_{ij}=1 at 1280 μm, where the large scale averaged out spatial heterogeneities. Cooperators were more clustered than defectors. This can be explained by the following: without clustering, defectors were more competitive than cooperators when they interacted (from test tube well-mixed experiments, Chapter 3), but cooperators grew to higher densities than defectors when on their own (from monoculture experiments in microhabitats, Chapter 3). As a result, only dense cooperator clusters remained, while defectors were viable when dispersed. As well, the fact that between-morph clustering stayed near or above 1 indicates a weak mutual attraction, probably through chemotaxis (*28*).

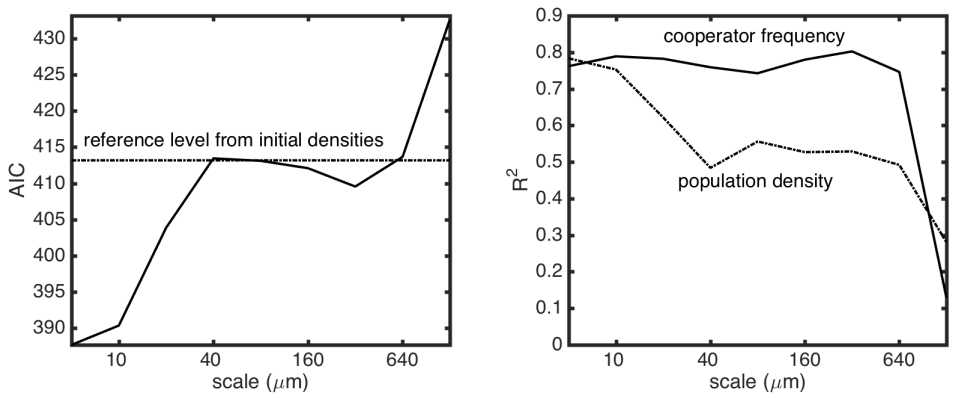

Figure 4.4. AIC and portions of variance in cooperator frequency and total population density explained by clustering coefficients measured at different scales. AIC indicated that the characteristic interaction scale of the bacteria populations was close to 5 μm. The dotted horizontal line (the reference level) represents the AIC obtained from using initial cooperator and defector densities as predictors; AICs below this line indicate clustering scales that explain more than experimental setup variations.

We evaluated how the assumed interaction scale changes the variations in population density and cooperator frequency explained by multivariate linear regressions with clustering coefficients as predictors. This was done by computing the models' Akaike Information Criterion (AIC) (*108*) and R^2 (portion of variance explained) for population density and cooperator frequency (Fig. 4.4). As the 5 μm model exhibited the lowest AIC, with R^2 values of almost 0.8 for both population density and cooperator frequency, we can infer that the most important interactions occurred within 5 μm of each focal bacterium (which is around 2 μm in length). At this scale, the AIC was much lower than the reference AIC obtained from using the inoculation densities as predictors (Fig. 4.4), indicating that clustering provides additional biological insights. We cannot be more precise than to state that the important scale was below 5 μm, since our image analysis algorithm could only partially correct for the undercounting bias below this scale (see Methods 4.5.3).

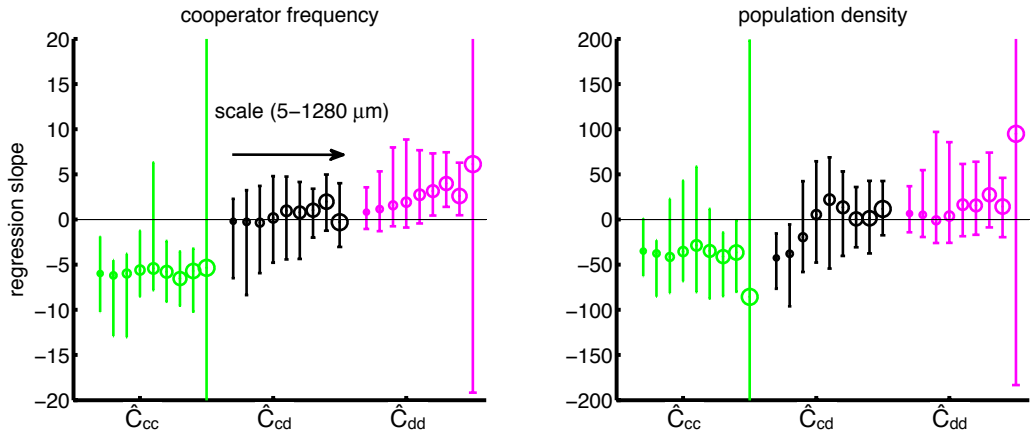

Figure 4.5. Multivariate linear regressions of standardized clustering coefficients ($\hat{C}_{cc}$, $\hat{C}_{cd}$,$\hat{C}_{dd}$) as predictors for cooperator frequency and total population density. For each scale tested (represented by circle size), the 95% confidence intervals of the regression slopes of cooperator frequency and population density on $\hat{C}_{cc}$, $\hat{C}_{cd}$ and $\hat{C}_{dd}$ were obtained from bootstrapping (by repeating regressions on resampled data 2000 times).

To compare clustering effects, we used standardized clustering coefficients (C_{ij} divided by their standard deviations). We found that for scales near 5 μm, cooperator clustering was negatively correlated with population density and cooperator frequency, while defector clustering was marginally positively correlated with cooperator frequency (Fig. 4.5). As well, between-morph clustering was consistently negatively correlated with population density. Compared to most previous findings that suggest clustering to generally promote cooperation (*13*, *21–26*), our results seem counterintuitive. But the clustering effects observed here match the more precise and general predictions of our analytical model, where cooperation only alleviates competition and leads to emergent demographic dynamics. The combination of demographic dynamics and strong selection allows cooperators and defectors to cluster differently in such a way that eco-evolutionary outcomes are determined by net clustering effects, and that clustering does not promote cooperation in all scenarios.

In summary, the study shows that eco-evolutionary dynamics of cooperation and population size can be well explained by clustering patterns at a very small scale, which

is consistent with biophysical studies of molecular diffusions between microbes (*126*, *162*). This scale can be inferred from population data without explicitly modelling the underlying interaction process. Because of strong selection and demographic dynamics, we found that clustering did not generally promote the evolution of cooperation, contrary to most previous findings (*13*, *21–26*) but represents an instance of kin competition (*110*). Our experiment does not invalidate previous studies, however, because they assumed weak selection and no demographic dynamics. The results also complement other cooperation models, where relaxation of demographic limits led to complex eco-evolutionary outcomes (*37*, *38*, *59*, *164*) but where direct clustering effects remained unexplored.

The biological implications for cooperation and virulence in *Pseudomonas aeruginosa* is that large-scale habitat heterogeneities in the respiratory tract (*29*) may not be as important as smaller, near-individual scale cluster formation, at least in the short term. Small-scale surface structure, such as the mucus (*165*), and self-organization due to chemotaxis and biofilm formation may strongly affect cooperative and competitive interactions. Nevertheless, large-scale heterogeneities may still be important, especially for organisms with large interaction scales and merit further empirical studies.

Strong and weak selection together contribute to the evolution of cooperation. Our empirical system exhibited strong selection due to the relatively large phenotypic difference between cooperators and defectors and may represent a common and recurrent evolutionary challenge to cooperation since loss-of-function mutations are frequent, at least in bacteria (*123*). Strong selection determines the maintenance of existing cooperative traits, but constructive, gain-of-function evolution is long believed

to arise from rare mutations with gradual phenotypic changes, resulting in weak selection (*10*, *13*, *166*, *167*). Exciting research can be done with microfluidic technology to reveal how different selection regimes contribute to the evolution of cooperation when different spatial patterns emerge and co-evolve with cooperation (*59*). Our research with pathogenic bacteria could be scaled up to more complex organisms and address how space mediates the maintenance of cooperation when cooperation affects demographic dynamics in complex environments.

4.5. Methods

4.5.1. Derivation of selection factors

Based on Eq. 4.1, we can write the intrinsic growth rate r, clustering to cooperators C_c, and clustering to defector C_d of an individual of character z as:

$$r(z) = r_d - (r_c - r_d)z$$
$$C_c(z) = C_{cd} - (C_{cc} - C_{cd})z$$
$$C_d(z) = C_{dd} - (C_{cd} - C_{dd})z \quad (4.3)$$

These substitutions allow us to write the fitness of an individual as a single expression of the form $w(z)$:

$$w(z) = r_d - (r_c - r_d)z - (k-a)X_c(C_{cd} - (C_{cc} - C_{cd})z) - kX_d(C_{dd} - (C_{cd} - C_{dd})z) \quad (4.4)$$

We then analyse the selection pressure that each clustering coefficient exerts on cooperation using Price's Equation (*63*), which states that the change in the average character of a population is $dZ/dt = \mathrm{cov}(w, z)$. By inserting Eq. 4.4 ($w$) into the covariance equation, we obtain:

$$dZ/dt = (r_c - r_d)\mathrm{var}(z) - (k - a)X_c(C_{cc} - C_{cd})\mathrm{var}(z) - kX_d(C_{cd} - C_{dd})\mathrm{var}(z)$$
$$= \mathrm{var}(z)((r_c - r_d) - (k - a)X_cC_{cc} + kX_dC_{dd} - ((k - a)X_c - kX_d)C_{cd}) \quad (4.5)$$

4.5.2. Device construction and operation

The microhabitat device is built from a silicon mould using photolithography, on which poly(dimethyl)siloxane (PDMS) was poured to about 5 mm in thickness. The elastomer layer contains the three habitat patchiness treatments shown in Fig. 4.2A, which are 10 μm deep and 0.4241 mm² in the main habitat area. For habitat 3, the addition of corridors brings the total area to 0.4529 mm². The edge-to-area ratios of the

habitats are 0.0108, 0.0153, and 0.0223 μm^{-1}. Details on the preparation of the PDMS can be found in Chapter 3.

The wild-type cooperators belong to the common *P. aeruginosa* lab strain PAO1. Isogenic *pvdA* transposon mutants (*151*) defective in producing pyoverdin served as defectors. The cooperator and defector strains were transformed with plasmids that constitutively expressed either the green fluorescent protein GFP (pMRP9-1(*152*)) or the red mCherry (pMKB1(*153*)), which were alternated in each successive experiment.

We diluted 16-hour overnight cultures of the cooperator and defector strains (LB, 37°C shaker incubator) to an O.D. (600nm) of 0.005 in casamino acids (5g with 0.005M K_2HPO_4 and 0.001M $MgSO_4$ per litre), 50mM $NaHCO_3$, and 1mg/mL human apo-transferrin, which create an iron-limited environment to render pyoverdin an effective public good (*46*, *146*). 0.7µL of the mixed culture was pipetted directly onto each habitat, then the PDMS device was sealed onto a glass cover slip (24x60mm #1.5H, Schott Nexterion). The device was placed in a 30°C heat chamber (Chamlide TC, Live Cell Instrument) on the inverted robotic stage of a laser scanning confocal microscope (LSM 700, Zeiss) and was imaged every 57 minutes and 18 seconds, up to 20 hours. Across the 8 replicates, the mean initial density was 0.0013 (S.E. = 5.6e-04) μm^{-2}, and the mean initial cooperator frequency was 0.51 (S.E. = 0.26).

The position of each bacterium was acquired using Imaris spot detection. Corrections of biases for individual counts due to slight differences between GFP and mCherry fluorescences are documented in Chapter 3.

4.5.3. Clustering coefficient measurements and corrections

Because of Imaris' spot detection limitations, bacteria of the same fluorescent colour cannot be reliably distinguished if they are very close together. Thus, raw clustering estimates are biased. The resolution limit was defined by the Threshold settings for each fluorescent colour (3.83μm for GFP, 4μm for mCherry), which were the estimated fluorescent footprint of each bacterium. Bacteria of the same colour closer than 4 μm apart were likely counted as one. This undercounting bias is weaker for between-morph clustering measurements, because the focal bacterium is of a different colour than the neighbours that are being counted. The between-morph clustering may still be underestimated because the neighbours of another colour may be clustered among themselves, but can serve as a lower limit for clustering estimates.

By comparing mono-fluorescent monocultures with mixed-fluorescent "monocultures" (either cooperators or defectors only, 7 replicates), we found that monocultures were undercounted by a factor of 0.6369 on average. Thus, we inferred that a portion M=1-0.6369 came from missed counts within 4 μm of focal individuals. As well, GFP counts on average were greater than mCherry counts by a factor of 1.1098. Let G_G=1/1.1098, and G_M=1, to account for the GFP and mCherry bias. We added $G_i M n_i E[A_4]/A$ to within-morph neighbour counts, where $E[A_4]$ is the expected interaction area with a radius of 4 μm, when non-habitat areas within the radius are subtracted. A is the total habitat area, n_i is the number of morph i individuals, and n_{ii} is the number of morph i neighbours around one focal individual of morph i. We also set the denominator such that C_{ii} approaches 1 as the interaction radius approaches infinity. Thus, the uncorrected raw within-morph clustering coefficient $\tilde{C}_{ii}$ is:

(4.6) $\tilde{C}_{ii} = X_{ii}/X_i = \mathrm{E}[(G_i n_{ii} - 1)/A_f]/((G_i n_i - 1)/A)$

where A_f is the interaction area at the given scale, with non-habitat areas within the scale subtracted. The corrected version C_{ii} is:

$$C_{ii} = \frac{E[(G_i n_{ii} + G_i M n_i A_4 / A - 1)/A_f]}{(G_i n_i + G_i M n_i E[A_4]/A - 1)/A} = \frac{E[(G_i(n_{ii} - 1) + G_i + G_i M n_i A_4 / A - 1)/A_f]}{(G_i n_i + G_i M n_i A_4 / A - 1)/A}$$

$$= \frac{E[(G_i n_{ii} - 1)/A_f] + E[G_i M n_i A_4 / (A A_f)]}{(G_i n_i - 1)/A + G_i M n_i E[A_4]/A^2}$$

$$= \tilde{C}_{ii} \frac{1 - 1/(G_i n_i)}{1 - 1/(G_i n_i) + ME[A_4]/A} + \frac{ME[A_4]/E[A_f]}{(G_i n_i - 1)/(G_i^2 n_i) + ME[A_4]/A} \quad (4.7)$$

While C_{ii} is biologically more meaningful, regression analyses using $\tilde{C}_{ii}$ yielded almost identical model fit and clustering effects across the scales. Because we are uncertain of the cluster coefficient estimates at scales below 5 μm, we did not include them in our presentation. If these were included, it can be shown that the 5-μm scale remains the optimal assumption in term of model fit.

Conclusions

The evolution of cooperation is an enormous topic, spanning the disciplines of evolution, ecology, and economics, among others. Being central to explaining how major evolutionary transitions occurred, and how humans collectives may continue to evolve, the topic is understandably grandiose, emotionally charged, and controversial. One approach to tackling such an imposing research topic is to stay technical, objective, small, and boring. I hope to have achieved the first three in my thesis.

In Chapter 1, I establish the fundamental roles that local densities play as the spatial components of evolutionary game, multilevel selection, and inclusive fitness theories. By showing how local densities compose the metrics of structure coefficient, spatial variance, contextual covariance, relatedness, and inbreeding coefficient, I provide a body of mathematical derivations for how to relate different theories on the evolution of cooperation. But the main innovation here is in applying Price's equation, often thought of as the formalization of Darwinian (*168*) or Fisherian (*166*) natural selection, and alternatively thought of as the trivial chain rule in calculus (*73*), to identify spatial and non-spatial classes of selection mechanisms influencing the evolution of cooperation.

In Chapter 2, I use a demographically-explicit spatial public-good model to show that, given the principle that cooperation only diminishes competition, cooperator clustering decreases cooperator frequency and population density. This counterintuitive finding is made possible by the divergence of cooperator clustering and defector clustering when the cooperator/defector phenotypes are quite different, and when demographic dynamics is possible. We identify strong selection and demographic

dynamics as being responsible for the discrepancy between the clustering effects found here, and the general finding that clustering promotes cooperation in previous models (*13*, *20–22*, *24*, *26*, *30*).

In Chapter 3, I introduce a novel microhabitat device for spatial experiments on the evolution of cooperation with *Pseudomonas aeruginosa*, concentrating on siderophore production as the cooperative trait. We find that while patchiness, or the edge-to-area ratio of a habitat, does not influence cooperator frequency and population density, patchiness contributes to coexistence in that it reduces the population density differences between monocultures and mixed cultures for each strain. This is the first empirical evidence that a gradual change in patchiness can influence the evolution of cooperation.

In Chapter 4, I use clustering coefficients to analyze a.) how clustering influences cooperator frequency and population density in microhabitat experiments with *P. aeruginosa*'s sideorphore production, b.) whether one can infer the interaction scale, and c.) whether the clustering effects turn out to affirm theoretical predictions. We inferred from model evaluation that the important interactions occur below the 5-μm scale, where clustering explains almost 80% of the variations in cooperator frequency and population density. In contrast, patchiness treatment, or the more precise edge-to-area ratio, explains much less. Cooperators and defectors cluster differently, which do not occur in models without strong selection and demographic dynamics. Cooperator clustering is found to significantly decrease cooperator frequency and population density, thus suggests that the bacterial system conforms to the spatial public-good model.

I do not believe that my findings change existing tenants in major ways – cost (intrinsic growth difference) and benefit (payoff), spatial association (clustering), and discrimination (payoff asymmetry, Chapter 1) remain major factors in the evolution of cooperation (*27*). But in finding that spatial associations are more complex than one may have supposed, especially when selection is strong due to large phenotypic differences between cooperators and defectors, and when there is demographic dynamics, we are compelled to revise how we consider space. Broadly, the research leaves us wondering, how might the haploid theories developed here apply to all organisms generally? In the grand scheme of evolution where functional innovations seem to have been attributed solely to the slow accumulation of minute phenotypic changes, what role does defection, by all accounts a phenotypic backward leap, play in thwarting or shaping cooperative traits? How does clustering emerge, and how does it coevolve with cooperation?

By focusing on spatial effects on haploid organisms, I did not touch upon the broader issues on the evolution of cooperation, such as sexual recombination (*13*, *169*), life stages (*32*), resource (*170*), cell differentiation (*171*), and interspecific interactions (*172*). While space is the default arena where all mechanisms play out, clearly the major evolutionary transitions caused by the evolution of cooperation unfolds at many scales simultaneously. Regarding these subjects, all of which have been dealt with in some way, I can only dream that they may all be eventual extensions of the "haploids in space" theories presented in this thesis. In this delusion I suppose I have only partially inherited Hamilton's gene-centric view, as explained by Dawkins (*50*), which saw units above the gene as mere vehicles for the essentially haploid inheritance of individual genes. Whereas the original gene-centric view centered on how genes affect fitness in a

spatially implicit context, the haploids in space concept in my thesis is strictly a geometric study of interacting genes or individuals in spatial environments, where fitness is the sum of local-density independent and dependent components of per-capita growth rate. One can imagine the unwieldy mathematics required to describe the local densities between a million different kinds of individual genes nested in chromosomes, nested in cells, nested in multicellular bodies nested in societies. But for Hamilton, multicellular organisms are the most socially interesting, which kept him away from the allure of trying to model individual genes. For me, unicellular haploids exhibit the dominant mode of life, and this mode, from the perspective of individual cells, is more or less preserved even in multicellular bodies. This is an important perspective, and is probably a viable line of research based on computer simulations, but mathematically and empirically such an overtly reductionist approach may fail to capture the emergent higher scales at which complex aggregates of cells interact in nature. For now, I must confine my findings to the evolution of cooperation in microbes, which optimistically serves as an allegory for how higher organisms may evolve (*66*).

I also only considered the short-term evolution of cooperators in competition with defectors, whose large phenotypic differences bring about strong selection and divergence in cooperator and defector clustering. In contrast, many evolutionary theorists believe that gradual mutational changes and weak selection (*10*, *13*, *82*) are largely responsible for the evolutionary innovations of functional traits. It appears that since loss-of-function mutations leading to defection are common, the strong selection theories developed in my thesis are crucial for the maintenance of already-evolved cooperative traits. On the other hand, gain-of-function mutations should be rare, where weak selection theories can elucidate on how innovative cooperative traits evolve. Both

strong and weak selections can be important for the evolution of cooperation (*173*), and are not incompatible. Work remains to be done to integrate how these different selection events contribute to the grand scheme of evolution.

The research leads to some concrete and intriguing possibilities for future works. While I have established protocols for how to measure and model spatial patterns through local densities and clustering coefficients, there is a limited understanding of how such patterns arise from the synergy of individual behaviour and spatial habitats (Chapter 1). For the mathematically inclined, the obvious next step is to derive how clustering arises in the demographically explicit spatial public-good model (Chapter 2), and extend such models to incorporate the co-evolution of cooperation and clustering (*59*). For empiricists, it is exciting to see that spatial coexistence (Chapter 3), clustering effects, and interaction scales (Chapter 4) can be inferred from spatiotemporal data. These concepts and analyses can be transferred to different organisms and behaviours, so long as phenotypes can be tracked.

Specifically for the study of *P. aeruginosa* siderophore cooperation in the microhabitat device, a decrease in iron availability is expected to increase the importance of cooperation. This follows from the literature on plant facilitation (*160*), where harsh environments can make cooperation more important. Concomitantly, this may set up the possibility that high cooperation level correlates with low population density across systems, even though the underlying public good benefits the local population. This would be reminiscent of the non-unimodal relationship between biodiversity and productivity (*174*), or the negative relationship between urbanization and human fertility (*175*). If we consider urbanization as a form of cooperation,

whereby individuals cooperate to increase local densities, we may find the current research relevant to human demographers (*176*).

As I am writing the last words of my thesis, I am reading Darwin's Descent of Man (*177*). I feel that in comparison, the work presented here has inevitably painted a poor picture of what is interesting about evolution, cooperation, and how they are relevant to organisms in general, and perhaps to humans. I imagine that long ago, Darwin had already anticipated modern multilevel selection, "actions are regarded… as good or bad, solely as they obviously affect the welfare of the tribe – not that of the species"; evolutionary game, "As ye would that men should do to you, do ye to them likewise"; and inclusive fitness, "Even if they [socially beneficial individuals] left no children, the tribe would still include their blood-relations" (*177*). He might have designed these clairvoyant remarks about the current theories on cooperation, but such foresights are not to be found in me. There may be an appearance of designed logic from the first chapter to the last in my thesis, but the false appearance of design came from an organic evolutionary process of trial and error. The thread that binds them – that clustering can have counterintuitive effects – came accidentally, and rather late into my study. But doggedly I go on, cobbling together broken ideas and reinventing memories of past ambitions, in an evolutionary march whose direction remains a mystery.

References

1. W. D. Hamilton, *Narrow Roads of Gene Land, Vol. 1* (W. H. Freeman, New York, 1996).

2. J. Maynard Smith, E. Szathmáry, *The origins of life* (Oxford University Press, Oxford, 1999).

3. W. D. Hamilton, in *Narrow Roads of Gene Land, Volume 1* (W. H. Freeman, New York, 1996), p. 135.

4. J. Maynard Smith, G. R. Price, The logic of animal conflict. *Nature*. **246**, 15–18 (1973).

5. E. O. Wilson, *Sociobiology* (Belknap, Cambridge, MA, 1975).

6. R. L. Trivers, The evolution of reciprocal altruism. *Q. Rev. Biol.* **46**, 35–57 (1971).

7. G. Hardin, The Tragedy of the Commons. *Science (80-.).* **162**, 1243–1248 (1968).

8. M. Olson, *The Logic of Collective Action* (Harvard University Press, Harvard, MA, 1965).

9. E. Ostrom, Collective action and the evolution of social norms. *J. Econ. Perspect.* **14**, 137–158 (2000).

10. C. Darwin, *On the origins of species by means of natural selection* (J. Murray, London, 1859; http://sciencestudies.pbworks.com/f/OoS.pdf).

11. P. Kropotkin, *Mutual Aid* (William Heinemann, London, 1902).

12. L. A. Dugatkin, Strange Bedfellows : A Russian Prince , A Scottish Economist , and the Role of Empathy in Early Theories for the Evolution of Cooperation. *J. Exp. Zool. B. Mol. Dev. Evol.* **320B**, 407–411 (2013).

13. W. D. Hamilton, The genetical evolution of social behaviour. I. *J. Theor. Biol.* **7**, 1–16 (1964).

14. V. C. Wynne-Edwards, Intergroup selection in the evolution of social systems. *Nature*. **200**, 623–626 (1963).

15. R. Axelrod, W. D. Hamilton, The evolution of cooperation. *Science (80-.)*. **211**, 1390–1396 (1981).

16. S. Okasha, Multi-Level Selection, Covariance and Contextual Analysis. *Br. J. Philos. Sci.* **55**, 481–504 (2004).

17. L. Keller, *Levels of selection in evolution* (Princeton University Press, Princeton, NJ, 1999; http://books.google.com/books?hl=en&lr=&id=5b_iEzNFlBUC&oi=fnd&pg=PR9&dq=Levels+of+selection+in+evolution&ots=Hin6kLQJPc&sig=w7DF9ecY-m_Zn4ci-7M1S4bbD4Q).

18. M. A. Nowak, C. E. Tarnita, E. O. Wilson, The evolution of eusociality. *Nature*. **466**, 1057–1062 (2010).

19. P. Abbot *et al.*, *Nature*, in press, doi:10.1038/nature09831.

20. M. A. Nowak, R. M. May, Evolutionary games and spatial chaos. *Nature*. **359**, 826–829 (1992).

21. D. S. Wilson, Structured demes and the evolution of group-advantageous traits. *Am. Nat.* **111**, 157–185 (1977).

22. F. Rousset, *Genetic Structure and Selection in Subdivided Populations* (Princeton University Press, Princeton, NJ, 2004).

23. P. D. Taylor, T. Day, G. Wild, Evolution of cooperation in a finite homogeneous graph. *Nature*. **447**, 469–472 (2007).

24. C. E. Tarnita, H. Ohtsuki, T. Antal, F. Fu, M. A. Nowak, Strategy selection in structured populations. *J. Theor. Biol.* **259**, 570–81 (2009).

25. J. A. Fletcher, M. Doebeli, A simple and general explanation for the evolution of altruism. *Proc. R. Soc. B Biol. Sci.* **276**, 13–9 (2009).

26. F. Débarre, C. Hauert, M. Doebeli, Social evolution in structured populations. *Nat. Commun.* **5**, 3409 (2014).

27. W. D. Hamilton, in *Biosocial Anthropology*, R. Fox, Ed. (Malaby Press, London, 1975; http://scholar.google.com/scholar?hl=en&btnG=Search&q=intitle:Innate+social+aptitude+of+men#1), pp. 133–153.

28. D. B. Dusenbery, Fitness landscapes for effects of shape on chemotaxis and other behaviors of bacteria. *J. Bacteriol.* **180**, 5978–5983 (1998).

29. A. Folkesson *et al.*, Adaptation of Pseudomonas aeruginosa to the cystic fibrosis airway: an evolutionary perspective. *Nat. Rev. Microbiol.* **10**, 841–851 (2012).

30. S. Lion, M. van Baalen, Self-structuring in spatial evolutionary ecology. *Ecol. Lett.* **11**, 277–295 (2008).

31. I. L. Heisler, J. Damuth, A method for analyzing selection in hierarchically structured populations. *Am. Nat.* **130**, 582–602 (1987).

32. L. Lehmann, F. Rousset, How life history and demography promote or inhibit the evolution of helping behaviours. *Philos. Trans. R. Soc. Lond. B. Biol. Sci.* **365**, 2599–2617 (2010).

33. H. Matsuda, N. Ogita, A. Sasaki, K. Sato, Statistical Mechanics of Population. *Prog. Theor. Phys.* **88**, 1035–1049 (1992).

34. F. Rousset, Inbreeding and relatedness coefficients: what do they measure? *Heredity (Edinb).* **88**, 371–380 (2002).

35. S. A. Levin, S. W. Pacala, in *Spatial ecology: the role of space in population dynamics and interspecific interactions*, D. Tilman, P. Kareiva, Eds. (Princeton University Press, Princeton, NJ, 1997), pp. 271–296.

36. T. Killingback, M. Doebeli, C. Hauert, Diversity of cooperation in the tragedy of the commons. *Biol. Theory.* **5**, 3–6 (2010).

37. C. Hauert, J. Y. Wakano, M. Doebeli, Ecological public goods games: cooperation and bifurcation. *Theor. Popul. Biol.* **73**, 257–263 (2008).

38. J. Y. Wakano, M. a Nowak, C. Hauert, Spatial dynamics of ecological public goods. *Proc. Natl. Acad. Sci. U. S. A.* **106**, 7910–7914 (2009).

39. H. Cho *et al.*, Self-organization in high-density bacterial colonies: efficient crowd

control. *PLoS Biol.* **5**, e302 (2007).

40. J. E. Keymer, P. Galajda, G. Lambert, D. Liao, R. H. Austin, Computation of mutual fitness by competing bacteria. *Proc. Natl. Acad. Sci. U. S. A.* **105**, 20269–73 (2008).

41. A. Buckling *et al.*, Siderophore-mediated cooperation and virulence in Pseudomonas aeruginosa. *FEMS Microbiol. Ecol.* **62**, 135–141 (2007).

42. K. Poole, G. A. McKay, Iron acquisition and its control in Pseudomonas aeruginosa: many roads lead to Rome. *Front. Biosci.* **8**, 661–686 (2003).

43. P. A. Marquet *et al.*, in *Patch dynamics*, S. A. Levin, T. M. Powell, J. H. Steele, Eds. (Springer-Verlag, New York, 1993), pp. 277–304.

44. E. E. Smith *et al.*, Genetic adaptation by Pseudomonas aeruginosa to the airways of cystic fibrosis patients. *Proc. Natl. Acad. Sci. U. S. A.* **103**, 8487–8492 (2006).

45. D. Nguyen, P. K. Singh, Evolving stealth: genetic adaptation of Pseudomonas aeruginosa during cystic fibrosis infections. *Proc. Natl. Acad. Sci. U. S. A.* **103**, 8305–8306 (2006).

46. A. S. Griffin, S. A. West, A. Buckling, Cooperation and competition in pathogenic bacteria. *Nature.* **430**, 1024–7 (2004).

47. R. Kümmerli, A. S. Griffin, S. a West, A. Buckling, F. Harrison, Viscous medium promotes cooperation in the pathogenic bacterium Pseudomonas aeruginosa. *Proc. Biol. Sci.* **276**, 3531–3538 (2009).

48. M. a. Leibold *et al.*, The metacommunity concept: a framework for multi-scale community ecology. *Ecol. Lett.* **7**, 601–613 (2004).

49. P. W. Glimcher, *Decisions, Uncertainty, and the Brain: The Science of Neuroeconomics* (MIT Press, Cambridge, MA, 2004).

50. R. Dawkins, *The Selfish Gene* (Oxford University Press, Oxford, UK, 1976).

51. A. Grafen, Optimization of inclusive fitness. *J. Theor. Biol.* **238**, 541–563 (2006).

52. J. A. J. Metz, S. D. Mylius, O. Diekmann, When does evolution optimize. *Evol.*

Ecol. Res. **10**, 629–654 (2008).

53. P. Turchin, Does population ecology have general laws? *Oikos.* **94**, 17–26 (2001).

54. S. Okasha, *Evolution and the Levels of Selection* (Clarendon Press, Oxford, 2006).

55. S. Lion, V. a a Jansen, T. Day, Evolution in structured populations: Beyond the kin versus group debate. *Trends Ecol. Evol.* **26**, 193–201 (2011).

56. J. E. Strassmann, O. M. Gilbert, D. C. Queller, Kin discrimination and cooperation in microbes. *Annu. Rev. Microbiol.* **65**, 349–367 (2011).

57. L. Lehmann, L. Keller, The evolution of cooperation and altruism--a general framework and a classification of models. *J. Evol. Biol.* **19**, 1365–1376 (2006).

58. S. A. West, A. S. Griffin, A. Gardner, Social semantics: altruism, cooperation, mutualism, strong reciprocity and group selection. *J. Evol. Biol.* **20**, 415–432 (2007).

59. F. Rousset, O. Ronce, Inclusive fitness for traits affecting metapopulation demography. *Theor. Popul. Biol.* **65**, 127–141 (2004).

60. M. van Baalen, D. Rand, The Unit of Selection in Viscous Populations and the Evolution of Altruism. *J. Theor. Biol.* **193**, 631–648 (1998).

61. S. W. Pacala, J. A. Silander, Neighborhood models of plant population dynamics. I. Single-species models of annuals. *Am. Nat.* **125**, 385–411 (1985).

62. J. Sapijanskas, C. Potvin, M. Loreau, Beyond shading : Litter production by neighbors contributes to overyielding in tropical trees. *Ecology*. **94**, 941–952 (2013).

63. G. R. Price, Selection and covariance. *Nature*. **227**, 520–521 (1970).

64. C. E. Tarnita, P. D. Taylor, Measures of relative fitness of social behaviors in finite structured population models. *Am. Nat.* **184**, 477–88 (2014).

65. B. M. Bolker, S. W. Pacala, Spatial Moment Equations for Plant Competition: Understanding Spatial Strategies and the Advantages of Short Dispersal. *Am. Nat.* **153**, 575–602 (1999).

66. A. Grafen, in *Behavioural ecology: an evolutionary approach*, J. R. Krebs, N. B. Davies, Eds. (Blackwell Scientific Publications, Oxford, ed. 2nd, 1984; http://xbiblio.ecologia.edu.mx/biblioteca/Cursos/Ecologia/Grafen_Alan.PDF), pp. 62–84.

67. B. M. Bolker, S. W. Pacala, Using Moment Equations to Understand Stochastically Driven Spatial Pattern Formation in Ecological Systems. *Theor. Popul. Biol.* **52**, 179–197 (1997).

68. J. Hofbauer, K. Sigmund, Evolutionary game dynamics. *Bull. Am. Math. Soc.* **40**, 479–520 (2003).

69. R. Durrett, S. Levin, The importance of being discrete (and spatial). *Theor. Popul. Biol.* **46**, 363–394 (1994).

70. W. C. C. Allee, *Animal aggregations: a study in general sociology* (University of Chicago Press, Chicago, 1931; http://www.getcited.org/pub/101601596).

71. F. Courchamp, T. Clutton-Brock, B. Grenfell, Inverse density dependence and the Allee effect. *Trends Ecol. Evol.* **14**, 405–410 (1999).

72. G. R. Price, Extension of covariance selection mathematics. *Ann. Hum. Genet.* **35**, 485–490 (1972).

73. S. C. Walker, Derivation of the continuous-time Price equation (2012), (available at http://stevencarlislewalker.wordpress.com/2012/06/26/derivation-of-the-continuous-time-price-equation/).

74. T. Day, P. D. Taylor, Evolutionary dynamics and stability in discrete and continuous games. *Evol. Ecol. Res.* **5**, 605–613 (2003).

75. J. von Neumann, Zur theorie der gesellschaftsspiele. *Math. Ann.* **100**, 295–320 (1928).

76. M. A. Nowak, *Evolutionary Dynamics* (Harvard University Press, Cambridge, MA, 2006).

77. T. Clutton-Brock, Cooperation between non-kin in animal societies. *Nature.* **462**, 51–58 (2009).

78. R. C. Connor, Cooperation beyond the dyad: on simple models and a complex society. *Philos. Trans. R. Soc. Lond. B. Biol. Sci.* **365**, 2687–97 (2010).

79. C. Taylor, M. A. Nowak, Transforming the dilemma. *Evolution*. **61**, 2281–2292 (2007).

80. M. A. Nowak, Five rules for the evolution of cooperation. *Science*. **314**, 1560–1563 (2006).

81. H. Ohtsuki, C. Hauert, E. Lieberman, M. a Nowak, A simple rule for the evolution of cooperation on graphs and social networks. *Nature*. **441**, 502–5 (2006).

82. B. Allen, M. a. Nowak, U. Dieckmann, Adaptive Dynamics with Interaction Structure. *Am. Nat.* **181**, E139–E163 (2013).

83. C. G. Nathanson, C. E. Tarnita, M. a Nowak, Calculating evolutionary dynamics in structured populations. *PLoS Comput. Biol.* **5**, e1000615 (2009).

84. S. Lion, Relatedness in spatially structured populations with empty sites: An approach based on spatial moment equations. *J. Theor. Biol.* **260**, 121–131 (2009).

85. E. Szathmáry, J. Maynard Smith, From replicators to reproducers: the first major transitions leading to life. *J. Theor. Biol.* **187**, 555–571 (1997).

86. M. Loreau, *From Populations to Ecosystems* (Princeton University Press, Princeton, NJ, 2010).

87. S. Wright, The genetical structure of populations. *Ann. Eugen.* **15**, 323–354 (1949).

88. F. Rousset, S. Billiard, A theoretical basis for measures of kin selection in subdivided populations : ® nite populations and localized dispersal. *J. Evol. Biol.* **13**, 814–825 (2000).

89. A. Gardner, S. a West, Greenbeards. *Evolution*. **64**, 25–38 (2010).

90. A. J. J. Lotka, *Elements of physical biology* (Williams & Wilkins, Baltimore, 1925).

91. V. Volterra, Fluctuations in the abundance of a species considered mathematically. *Nature*. **118**, 558–560 (1926).

92. P. D. Taylor, L. B. Jonker, Evolutionarily stable strategies and game dynamics. *Math. Biosci.* **40**, 145–156 (1978).

93. J. Hofbauer, On the occurrence of limit cycles in the Volterra-Lotka equation. *Nonlinear Anal.* **5**, 1003–1007 (1981).

94. A. Grafen, M. Archetti, Natural selection of altruism in inelastic viscous homogeneous populations. *J. Theor. Biol.* **252** (2008), pp. 694–710.

95. R. Law, U. Dieckmann, A dynamcial system for neighborhoods in plant communities. *Ecology*. **81**, 2137–2148 (2000).

96. S. H. Rice, *Evolutionary Theory* (Sinauer, Sunderland, MA, 2004).

97. F. Dionisio, I. Gordo, The tragedy of the commons, the public goods dilemma, and the meaning of rivalry and excludability in evolutionary biology. *Evol. Ecol. Res.* **8**, 321–332 (2006).

98. B. L. Thorne, Evolution of eusociality in termites. *Annu. Rev. Ecol. Syst.* **28**, 27–54 (1997).

99. S. A. Frank, A general model of the public goods dilemma. *J. Evol. Biol.* **23**, 1245–1250 (2010).

100. E. Sober, D. S. Wilson, *Unto others: The evolution and psychology of unselfish behavior* (Harvard University Press, Cambridge, MA, 1998; http://books.google.com/books?hl=en&lr=&id=ouwg5swAV5oC&oi=fnd&pg=PA1&dq=unto+others:+the+evolution+and+psychology+of+unselfish+behaviour&ots=-Sse7SfQya&sig=W6e2lVb5UfW_BRL2JBg2l5-T_C8).

101. S. Lion, S. Gandon, Habitat saturation and the spatial evolutionary ecology of altruism. *J. Evol. Biol.* **22**, 1487–1502 (2009).

102. R. Nathan *et al.*, A movement ecology paradigm for unifying organismal movement research. *Proc. Natl. Acad. Sci.* **105**, 19052–19059 (2008).

103. A. Gonzalez, J. Lawton, F. Gilbert, T. Blackburn, I. Evans-Freke, Metapopulation dynamics, abundance, and distribution in a microecosystem. *Science (80-.).* **281**,

2045–7 (1998).

104. S. Kondo, T. Miura, Reaction-diffusion model as a framework for understanding biological pattern formation. *Science (80-.).* **329**, 1616–1620 (2010).

105. J. W. Pepper, Relatedness in trait group models of social evolution. *J. Theor. Biol.* **206**, 355–368 (2000).

106. I. Hanski, Single-species metapopulation dynamics: concepts, models and observations. *Biol. J. Linn. Soc.* **42**, 17–38 (1991).

107. C. E. Tarnita, T. Antal, H. Ohtsuki, M. A. Nowak, Evolutionary dynamics in set structured populations. *Proc. Natl. Acad. Sci. U. S. A.* **106**, 8601–8604 (2009).

108. H. Akaike, A new look at the statistical model identification. *Autom. Control. IEEE Trans.* **19**, 716–723 (1974).

109. D. S. Wilson, G. B. Pollock, L. A. Dugatkin, Can altruism evolve in purely viscous populations? *Evol. Ecol.* **6**, 331–341 (1992).

110. P. D. Taylor, Altruism in viscous populations — an inclusive fitness model. *Evol. Ecol.* **6**, 352–356 (1992).

111. J. B. Xavier, Social interaction in synthetic and natural microbial communities. *Mol. Syst. Biol.* **7**, 483 (2011).

112. R. H. Austin, C.-K. Tung, G. Lambert, D. Liao, X. Gong, An introduction to micro-ecology patches. *Chem. Soc. Rev.* **39**, 1049–1059 (2010).

113. E. Fehr, H. Gintis, Human Motivation and Social Cooperation: Experimental and Analytical Foundations. *Annu. Rev. Sociol.* **33**, 43–64 (2007).

114. S. a. Levin, Public goods in relation to competition, cooperation, and spite. *Proc. Natl. Acad. Sci.* **111**, 10838–45 (2014).

115. S. F. Elena, R. E. Lenski, Evolution experiments with microorganisms: the dynamics and genetic bases of adaptation. *Nat. Rev. Genet.* **4**, 457–469 (2003).

116. W. B. Whitman, D. C. Coleman, W. J. Wiebe, Perspective Prokaryotes : The unseen majority. *Proc. Natl. Acad. Sci.* **95**, 6578–6583 (1998).

117. G. Velicer, Social strife in the microbial world. *Trends Microbiol.* **11**, 330–337 (2003).

118. B. Crespi, K. Foster, F. Úbeda, First principles of Hamiltonian medicine. *Philos. Trans. R. Soc. Lond. B. Biol. Sci.* **369**, 20130366 (2014).

119. R. Kümmerli, A. Gardner, S. a West, A. S. Griffin, Limited dispersal, budding dispersal, and cooperation: an experimental study. *Evolution.* **63**, 939–949 (2009).

120. D. De Vos *et al.*, Study of pyoverdine type and production by Pseudomonas aeruginosa isolated from cystic fibrosis patients: Prevalence of type II pyoverdine isolates and accumulation of pyoverdine-negative mutations. *Arch. Microbiol.* **175**, 384–388 (2001).

121. J. S. Mattick, Type IV pili and twitching motility. *Annu. Rev. Microbiol.* **56**, 289–314 (2002).

122. M. a. Meyer, J. M., and Abdallah, The fluorescent pigment of *Pseudomonas fluorescens*: biosynthesis, purification and physicochemical properties. *J Gen Microbiol.* **107**, 319–328 (1978).

123. L. Bromham, Why do species vary in their rate of molecular evolution? *Biol. Lett.* **5**, 401–404 (2009).

124. S. Carroll, Chance and necessity: the evolution of morphological complexity and diversity. *Nature.* **409**, 1102–1109 (2001).

125. W. . Hamilton, T. M. Lenton, Spora and Gaia: how microbes fly with their clouds. *Ethol. Ecol. Evol.* **10**, 1–16 (1998).

126. C. D. Nadell, J. B. Xavier, K. R. Foster, The sociobiology of biofilms. *FEMS Microbiol. Rev.* **33**, 206–224 (2009).

127. P. Chesson, Mechanisms of Maintenance of Species Diversity. *Annu. Rev. Ecol. Syst.* **31**, 343–366 (2000).

128. A. Gardner, S. A. West, Spite and the scale of competition. *J. Evol. Biol.* **17**, 1195–1203 (2004).

129. H. Celiker, J. Gore, Cellular cooperation: Insights from microbes. *Trends Cell Biol.* **23** (2013), pp. 9–15.

130. S. A. Levin, Dispersion and population interactions. *Am. Nat.* **108**, 207–228 (1974).

131. S. a. Levin, The Problem of Pattern and Scale in Ecology: The Robert H. MacArthur Award Lecture. *Ecology*. **73**, 1943 (1992).

132. C. H. Ettema, D. a. Wardle, Spatial soil ecology. *Trends Ecol. Evol.* **17**, 177–183 (2002).

133. F. J. H. Hol *et al.*, Spatial Structure Facilitates Cooperation in a Social Dilemma: Empirical Evidence from a Bacterial Community. *PLoS One*. **8**, e77402 (2013).

134. S. K. Green, M. N. Schroth, J. J. Cho, S. K. Kominos, V. B. Vitanza-jack, Agricultural plants and soil as a reservoir for Pseudomonas aeruginosa. *Appl. Microbiol.* **28**, 987–991 (1974).

135. K. Botzenhart, G. Döring, in *Pseudomonas aeruginosa as an Opportunistic Pathogen* (Springer US, 1993; http://link.springer.com/chapter/10.1007/978-1-4615-3036-7_1), pp. 1–18.

136. J. Smith, J. D. Van Dyken, P. C. Zee, A generalization of Hamilton's rule for the evolution of microbial cooperation. *Science*. **328**, 1700–1703 (2010).

137. M. a. Brockhurst, Population bottlenecks promote cooperation in bacterial biofilms. *PLoS One*. **2**, e634 (2007).

138. J. S. Chuang, O. Rivoire, S. Leibler, Simpson's paradox in a synthetic microbial system. *Science*. **323**, 272–275 (2009).

139. P. B. Rainey, K. Rainey, Evolution of cooperation and conflict in experimental bacterial populations. *Nature*. **425**, 72–74 (2003).

140. S. Park *et al.*, Motion to form a quorum. *Science (80-.).* **301**, 188 (2003).

141. S. Park *et al.*, Influence of topology on bacterial social interaction. *Proc. Natl. Acad. Sci. U. S. A.* **100**, 13910–13915 (2003).

142. A. Groisman *et al.*, A microfluidic chemostat for experiments with bacterial and yeast cells. *Nat. Methods*. **2**, 685–689 (2005).

143. Q. Zhang *et al.*, Acceleration of emergence of bacterial antibiotic resistance in connected microenvironments. *Science (80-.).* **333**, 1764–1767 (2011).

144. A. K. Wessel *et al.*, Oxygen limitation within a bacterial aggregate. *MBio*. **5**, e00992–14 (2014).

145. E. K. Sackmann, A. L. Fulton, D. J. Beebe, The present and future role of microfluidics in biomedical research. *Nature*. **507**, 181–189 (2014).

146. J. M. Meyer, a Neely, a Stintzi, C. Georges, I. a Holder, Pyoverdin is essential for virulence of Pseudomonas aeruginosa. *Infect. Immun*. **64**, 518–523 (1996).

147. S. A. West, A. Buckling, Cooperation, virulence and siderophore production in bacterial parasites. *Proc. Biol. Sci.* **270**, 37–44 (2003).

148. Y. Xia, G. M. Whitesides, Soft Lithography. *Annu. Rev. Mater. Sci.* **28**, 153–184 (1998).

149. T. B. Doyle, A. C. Hawkins, L. L. McCarter, The complex flagellar torque generator of Pseudomonas aeruginosa. *J. Bacteriol.* **186**, 6341–6350 (2004).

150. J. L. Connell *et al.*, Probing prokaryotic social behaviors with bacterial "lobster traps". *MBio*. **1** (2010), doi:10.1128/mBio.00202-10.

151. K. Held, E. Ramage, M. Jacobs, L. Gallagher, C. Manoil, Sequence-verified two-allele transposon mutant library for Pseudomonas aeruginosa PAO1. *J. Bacteriol.* **194**, 6387–6389 (2012).

152. D. G. Davies *et al.*, The involvement of cell-to-cell signals in the development of a bacterial biofilm. *Science*. **280**, 295–298 (1998).

153. M. K. Brannon *et al.*, Pseudomonas aeruginosa Type III secretion system interacts with phagocytes to modulate systemic infection of zebrafish embryos. *Cell. Microbiol.* **11**, 755–768 (2009).

154. B. J. Cardinale *et al.*, Impacts of plant diversity on biomass production increase through time because of species complementarity. *Proc. Natl. Acad. Sci. U. S. A.* **104**, 18123–18128 (2007).

155. S. A. Levin, Self-organization and the emergence of complexity in ecological systems. *Bioscience*. **55**, 1075–1079 (2005).

156. M. W. Toepke, D. J. Beebe, PDMS absorption of small molecules and consequences in microfluidic applications. *Lab Chip*. **6**, 1484–1486 (2006).

157. G. Bell, A. Gonzalez, Adaptation and evolutionary rescue in metapopulations experiencing environmental deterioration. *Science*. **332**, 1327–1330 (2011).

158. I. Hanski, Metapopulation dynamics. *Nature*. **396**, 41–49 (1998).

159. E. I. Damschen *et al.*, The movement ecology and dynamics of plant communities in fragmented landscapes. *Proc. Natl. Acad. Sci. U. S. A.* **105**, 19078–19083 (2008).

160. S. Kéfi, M. van Baalen, M. Rietkerk, M. Loreau, Evolution of local facilitation in arid ecosystems. *Am. Nat.* **172**, E1–17 (2008).

161. E. W. Tekwa, A. Gonzalez, M. Loreau, Local densities connect spatial ecology to game, multilevel selection and inclusive fitness theories of cooperation. *J. Theor. Biol.* **380**, 414–425 (2015).

162. D. Or, B. F. Smets, J. M. Wraith, a. Dechesne, S. P. Friedman, Physical constraints affecting bacterial habitats and activity in unsaturated porous media - a review. *Adv. Water Resour.* **30**, 1505–1527 (2007).

163. J. S. Chuang, O. Rivoire, S. Leibler, Cooperation and Hamilton's rule in a simple synthetic microbial system. *Mol. Syst. Biol.* **6**, 398 (2010).

164. S. Lion, S. Gandon, Life history, habitat saturation and the evolution of fecundity and survival altruism. *Evolution*. **64**, 1594–1606 (2010).

165. T. Bjarnsholt *et al.*, Pseudomonas aeruginosa biofilms in the respiratory tract of cystic fibrosis patients. *Pediatr. Pulmonol.* **44**, 547–558 (2009).

166. R. A. Fisher, *The Genetical Theory of Natural Selection* (Clarendon Press, Oxford, 1930).

167. J. A. J. Metz, S. A. H. Geritz, G. Meszéna, F. J. A. J. A. Jacobs, J. S. S. van

Heerwaarden, in *Stochastic and Spatial Structures of Dynamical Systems*, S. J. van Strien, S. M. Verduyn Lunel, Eds. (North Holland, Amsterdam, 1996; http://citeseerx.ist.psu.edu/viewdoc/download?doi=10.1.1.199.2875&rep=rep1&type=pdf), vol. 45, pp. 183–231.

168. S. A. Frank, The Price Equation, Fisher's Fundamental Theorem, Kin Selection, and Causal Analysis. *Evolution (N. Y).* **51**, 1712 (1997).

169. D. Roze, F. Rousset, The robustness of Hamilton's rule with inbreeding and dominance: kin selection and fixation probabilities under partial sib mating. *Am. Nat.* **164**, 214–231 (2004).

170. C. de Mazancourt, M. W. Schwartz, A resource ratio theory of cooperation. *Ecol. Lett.* **13**, 349–359 (2010).

171. I. Ispolatov, M. Ackermann, M. Doebeli, Division of labour and the evolution of multicellularity. *Proc. Biol. Sci.* **279**, 1768–1776 (2012).

172. T. Clutton-Brock, Breeding together: kin selection and mutualism in cooperative vertebrates. *Science.* **296**, 69–72 (2002).

173. V. A. A. Jansen, in *The Mathematics of Darwin's Legacy*, F. A. C. C. Chalub, J. F. Rodrigues, Eds. (Springer, Basel, 2011; http://link.springer.com/chapter/10.1007/978-3-0348-0122-5_8), pp. 139–157.

174. M. Loreau *et al.*, Biodiversity and ecosystem functioning: current knowledge and future challenges. *Science.* **294**, 804–808 (2001).

175. R. Mace, Reproducing in cities. *Science.* **319**, 764–6 (2008).

176. R. Sear, Evolutionary contributions to the study of human fertility. *Popul. Stud. (NY).* **69**, S39–S55 (2015).

177. C. Darwin, *The Descent of Man, and Selection in Relation to Sex* (Joh Murray, London, 1871).